UNIVERSITY OF MESSINA

DEPARTMENT OF ENGINEERING

PHD IN Materials and Construction Engineering and Chemistry

XXXVI CYCLE

S.S.D ING-IND/22

Economic and Environmental Impact Assessments of Advanced Geopolymeric Materials

ENVISAGE

PH.D. THESIS OF:

HOSSEM BELHAMDI

TUTOR:

PROF. ANNAMARIA VISCO

CO-TUTOR:

DR. MARIA ROSARIA PLUTINO

PROF. ROBERTA SALOMONE

DR. ANA FERNÁNDEZ- JIMÉNEZ

HEAD OF THE PH.D. COURSE:

PROF. PROVERBIO EDOARDO

2021-2024

Table of contents

Acknowledgement

This work has been carried out under the supervision of Prof. Annamaria Visco (University of Messina, Italy). I am deeply grateful for her supervision and support of my research activity and for giving me the opportunity to improve my scientific skills during these years. Her encouragement and dedication have significantly contributed to my professional growth and the enhancement of my scientific skills over the years.

I would like to express my sincere gratitude to my industrial co-tutor Dr. Maria Rosaria Plutino of the ISMN-CNR (Palermo, URT of Messina, Italy). Dr. Maria Rosaria Plutino sincerely deserves to be highly applauded for her guidance, inspiration, advice and direction during all these years of research. I have had the pleasure of learning at her side and under her guidance, allowing me to join her research group dedicated to sustainable and environmentally friendly development, supporting me in all initiatives and encouraging me to participate in all related activities.

I would like to thank my co-tutor Prof. Roberta Salomone from the Department of Economics (University of Messina, Italy) for her guidance on the LCA studies part of this thesis and for pushing me towards developing a greener environment.

I must also express my gratitude and appreciation to my co-tutor, Prof. Anna Fernández, and to all the people I met at the "Institute of Construction Science of Eduardo Torroja (IETcc), Madrid-Spain" for their hospitality, valuable support and advice on the research activity carried out during my stay there, where I had the opportunity to interact with new techniques and approaches. I would like to thank Alfredo Gil, Hector, Paco and Dr. Salma for their help in carrying out the chemical and physical tests at the IETcc.

A very special gratefulness goes to the Programma Operativo Nazionale (PON), Athena Green Solutions Srl and the Institute of Construction Science of Eduardo Torroja (IETcc) of the "Consejo Superior de Investigaciones Científicas" (IETccCSIC). This research was funded by the PON-MIUR "Ricerca e Innovazione 2014-2020" Industrial Doctorate.

I would also like to thank my colleagues in the office and department for their friendship, support, help and the wonderful moments we shared: Dr. Cristina, Dr. Giulia, Dr. Silvia, and Salim.

I would like to extend my deepest and heartfelt gratitude to my parents who are in Algeria, hundreds of kilometers away from Italy, and yet I felt during the last three years that they were always behind me whenever I needed them.

Thank you all for your encouragement!

Abstract

Geopolymers are a promising material with diverse applications in the construction industry, which offers an alternative to traditional cement-based materials. Inorganic-organic hybrid geopolymer, instead, offers more enhanced physical and chemical properties with the incorporation of the functional agents.

Therefore, the aim of this PhD thesis is to propose an innovative and sustainable solution following the global pollution caused by the construction sector and aims to use local precursors to produce best performing green geopolymer and hybrid geopolymer materials. This thesis work was done in collaboration between University of Messina, ATHENA Green Solutions Srl in which raw materials and their characterization were done at Messina university while geopolymer and hybrid geopolymers materials was done at the Instituto de Ciencias de la Construcción 'Eduardo Torroja' (IETCC-CSIC) in Madrid (Spain).

Firstly, a series of experiments were conducted, to synthesize, characterize and evaluate the performance and suitability of various geopolymeric materials to produce base geopolymers. Initially, the geopolymer was made of the combination of different local Sicilian raw materials including Electric Arc Furnace Slag (DS), clay, brick waste (BW), kaolin (K), and slag activated with NaOH solution in combination with alkaline activators liquid (A.A.L) and powder (A.A.P) under different conditions. Based on the different performance evaluation results through mechanical test, X-ray diffraction, Fourier-transform infrared spectroscopy and scanning electron microscopy, we had to further examine the properties of the calcined clay and electric arc furnace slag, and calcined clay and brick waste mixtures activated with (A.A.L) and (A.A.P) as a promising mixture for developing high-performance hybrid geopolymer.

Secondly, through the sol-gel technique, we investigated the effect of incorporating four different organic functional agents: polydimethylsiloxane (PDMS), tetraethyl orthosilicate (TEOS), acrylic resin, and TP56 mixture, on the chemical-physical properties such as water resistance. In which, PDMS, TEOS, acrylic resin, and TP56 added separately the C-Clay and DS_g mixture samples, thereafter only PDMS and TP56 added in the C-Clay and BW mixture samples. The results showed that the hybrid geopolymer based on C-Clay and DS_g incorporated PDMS (H-GP @ PDMS), presented improved compressive strength properties, and surface water resistance. Hence, due to the improved performance, low cost, non-toxicity, and low volatility, we selected this consolidant for chemical-physical characterization with C-Clay @ DS_g. The XRD analysis showed no change in phases with the addition of PDMS. The SEM analysis revealed microcracks in both types of alkaline activators. The porosity and water absorption results showed that the samples activated with A.A.L had increased compared to those activated

with A.A.P due to the increased pores. The contact angle measurement indicated that GP-P is hydrophilic (rapid water absorption) while H-GP-P @ PDMS is highly hydrophobic (resistant to water absorption). Hybrid geopolymer made with A.A.L (H-GP-L @ PDMS) is less hydrophobic than hybrid geopolymer made with A.A.P (H-GP-P @ PDMS), which is consistent with contact angle results.

Future research should be directed to conduct a life cycle assessment and life cycle cost to compare the environmental and economic impacts of geopolymers against traditional materials. The results are expected to contribute to demonstrating the feasibility of geopolymers as an alternative to conventional materials.

Publications list

1- **H. Belhamdi**, S. Sfameni, G. Rando, A. Visco, A. Fernández Jiménez, M.R. Plutino, **2024**, *Inorganics*, submitted.

2- **H. Belhamdi**, S. Sfameni, G. Rando, A. Visco, A. Fernández Jiménez, M.R. Plutino, **2024**, *Materials*, submitted.

3- B. Kouini, **H. Belhamdi**, A. Hachaichi, A.N. El Houda Sid. *IOP Publishing*, pp. 2-1 (**2023**). https://doi.org/10.1088/978-0-7503-5177-5ch2

4- A. Visco, C. Scolaro, M. Facchin, S. Brahimi, **H. Belhamdi**, V. Gatto, V. Beghetto. *Polymers*, 14 (**2022**) 13, 2752. https://doi.org/10.3390/polym14132752

5- **H. Belhamdi**, B. Kouini, A. Grasso, C. Scolaro, A. Sili, A. Visco. *Journal of Applied Polymer Science*, 139 (**2022**) 23, 52313. https://doi.org/10.1002/app.52313

6- F. Giacobello, I. Ielo, **H. Belhamdi**, M. R. Plutino. *Materials*, 15 (**2022**) 5, 1725. https://doi.org/10.3390/ma15051725

7- B. Kouini and **H. Belhamdi**. *Cham: Springer International Publishing*, pp. 149-177 (**2021**). https://doi.org/10.1088/978-0-7503-5177-5ch2

Conference Proceedings

1- A. Visco, A. Grasso, C. Scolaro, **H. Belhamdi**, A. Sili. *Macromolecular Symposia*, 404 (**2022**) 1, 2100294. https://doi.org/10.1002/masy.202100294

2- A. Visco, C. Scolaro, **H. Bellhamdi**, A. Grasso. *Macromolecular Symposia*. 404 (**2022**), 404, 2100330. https://doi.org/10.1002/masy.202100330

Nomenclature & Abbreviation

Abbreviations

CO_2 - Carbon Dioxide

SiO_2 - Silicon Dioxide

Al_2O_3 - Alumina

Fe_2O_3 - Iron Oxide

CaO - Calcium Oxide

MgO - Magnesium Oxide

Na_2O - Sodium Oxide

K_2O - Potassium Oxide

SO_3 - Sulfur Trioxide

NH_3 - Ammonia

N_2O - Nitrous Oxide

NOx - Nitrogen Oxides

SO_2 - Sulfur Dioxide

Zn - Zinc

BW - Brick Waste

C-Clay - Calcined Clay

K - Kaolin

MK_T - Thermally Treated Kaolin

DS - Electric Arc Furnace Slag

DS_g - Electric Arc Furnace Slag Grounded

EAF - Electric Arc Furnace

GGBFS - Ground Granulated Blast Furnace Slag

A.A.L - Alkaline Activator Liquid

A.A.P - Alkaline Activator Powder

H-GP - Hybrid Geopolymer

PDMS – Polydimethylsiloxane

TEOS - Tetraethyl Orthosilicate

TP56 - Mixture of PDMS, ethoxysilane, and n-octylamine

CDW - Construction and Demolition Waste

CO_2-eq - Carbon Dioxide Equivalent

CML - Center for Environmental Studies

CTUh - Comparative Toxic Unit for humans

CTUe - Comparative Toxic Unit for ecosystems

ECO - Environmental Conception

EPS - Expanded Polystyrene

GWP - Global Warming Potential

HH - Human Health

HP - Human Toxicity Potential

IPCC - Intergovernmental Panel on Climate Change

ISO - International Organization for Standardization

LCA - Life Cycle Assessment

LCI - Life Cycle Inventory

MFA - Material Flow Analysis

ODP - Ozone Depletion Potential

OPC - Ordinary Portland Cement

PM - Particulate Matter

POF - Photochemical Ozone Formation

REPA - Resource and Environmental Profile Analysis

RUF - Resource Utilization, Fossil

RUM - Resource Utilization, Minerals and Metals

SH - Sodium Hydroxide

SFA - Substance Flow Analysis

SWOT - Strengths, Weaknesses, Opportunities, Threats

UNEP - United Nations Environment Programme

USEtox - United States Environmental Protection Agency's Toxicity Model

WP - Water Pollution

Experimental Techniques

TGA/DTG - Differential Thermal Gravimetric

DSC - Differential Scanning Calorimetry

FTIR - Fourier-Transform Infrared Spectroscopy

SEM - Scanning Electron Microscopy

XRD - X-ray Diffraction

WA- Water absorption

LOI - Loss on Ignition

PSD - Laser Diffraction Particle Size Analysis

CA- Contact angle measurement

List of Figures

Chapter 01

Chapter 02

Chapter 03

Chapter 04

Chapter 06

List of tables

Chapter 01

Chapter 02

Chapter 03

Chapter 04

Chapter 06

CHAPTER 1

INTRODUCTION

Chapter 1 provides a comprehensive overview of geopolymeric materials, focusing on their composition and properties. The primary aim is to highlight the main characteristics of geopolymers, compare them with Ordinary Portland Cement (OPC) concrete, and justify their use in eco-construction due to their environmental and economic advantages. The discussion covers various sources of raw materials, such as clay and kaolin, and details the alkaline activation solutions like sodium hydroxide and sodium silicate that are crucial for geopolymer synthesis. Additionally, the chapter explores hybrid and sustainable functional geopolymeric materials, examining the incorporation of secondary raw materials, including Electric Arc Furnace Slag, brick waste, and volcanic rock (slag). It also delves into the role of functional additives, such as sol-gel based, polymeric based, and nanofillers, in enhancing the properties of geopolymers. The applications and advantages of geopolymer concrete are discussed. The chapter sets the stage for the subsequent detailed analysis and development of geopolymer materials presented in the thesis.

1.1. Overview of geopolymeric materials

The term "geopolymer" was coined in the 1970 s by the scientist and French engineer Joseph Davidovits [1] and refers to a class of solid materials synthesized through the reaction of an aluminosilicate powder with an alkaline solution. A “geopolymer” generically identifies an amorphous alkaline aluminosilicate and is also commonly referred to "inorganic polymers", "alkali-activited cement", "geocement", "alkali-activited cement", “ceramics with alkaline bond”, “hydroceramics”, etc [2, 3]. Moreover, geopolymer materials are considered as a third-generation cement, following lime and Ordinary Portland Cement (OPC).

According to Provis and Deventer [4], the discovery of alkali-activated materials is attributed to Purdon (1940), who succeeded in producing a building material by alkali-activating a calcium-rich slag. However, Shi and al [5] credit this discovery to Kuhl, a German chemist and cement engineer, in the 1930s. A Kuhl patent filed in 1908 is recognized as the first documented use of alkali-activated aluminosilicate precursors to create an alternative material to Ordinary Portland Cement (OPC)[6].

In the 1950s, Victor Glukhovsky and later Pavel Krivenko developed alkali-activated systems containing hydrated calcium silicate (C-S-H) and aluminosilicates in Ukraine. These systems were used to construct a large building in Russia. Glukhovsky proposed that the geological process of transforming certain volcanic rocks into zeolites takes place that take place during the formation of sedimentary rocks at low temperatures and pressures, could be modeled and applied in cementitious system[6].

Glukhovsky was also the first to study binders used in ancient Roman and Egyptian constructions. He concluded that these binders were composed of aluminosilicate calcium hydrates similar to those in Portland cement, as well as crystalline phases of analcite, a natural rock that contributed to their durability. Based on this research, Glukhovsky developed a new type of binder—called "soil-cement", named for its resemblance to bedrock and its cementitious properties. Soil-cement was created from crushed aluminosilicate mixed with alkaline-rich industrial waste[7].

---

[1] Davidovits J. Geopolymers and geopolymeric materials. *J Therm Anal*. **1989**;35(2):429-441.
[2] Singh B, Ishwarya G, Gupta M, Bhattacharyya SK. Geopolymer concrete: A review of some recent developments. *Constr Build Mater*. **2015**;85:78-90.
[3] Provis JL. Alkali-activated materials. *Cem Concr Res*. **2018**;114:40-48.
[4] Provis JL, Deventer JSJ Van. *Geopolymers: Structures, Processing, Properties and Industrial Applications*. Elsevier Ltd; **2009**.
[5] Shi C, Jiménez AF, Palomo A. New cements for the 21st century: The pursuit of an alternative to Portland cement. *Cem Concr Res*. **2011**;41(7):750-763.
[6] J. L. Provis, J. S. J. van Deventer, eds., Alkali Activated Materials, *RILEM State-of-theArt Reports*, **2014**; 13, 388.
[7] Komnitsas K, Zaharaki D. Geopolymerisation: A review and prospects for the minerals industry. *Miner Eng*. **2007**;20(14):1261-1277.

Davidovits even proposes that the pyramids were not constructed from natural stone but from man-made binders. Based on chemical and mineralogical studies, suggests that the pyramid blocks were composed of a mixture of limestone sand, calcium hydroxide, sodium carbonate, and water. According to his research, the pyramid blocks were not formed from fossilized layers of calcium, as is typical in natural stones, but rather from randomly oriented materials characteristic of an artificial binder. X-ray diffraction analysis of the pyramid specimens indicates that calcium carbonate ($CaCO_3$) is the main crystalline phase. However, an amorphous material composed of aluminosilicates and a zeolitic material ($Na_2O{\cdot}Al_2O_3{\cdot}4SiO_2{\cdot}2H_2O$) was also identified [7].

Researchers define geopolymers as inorganic polymer material formed by the reaction between aluminosilicate sources and a highly alkaline silicate solution, followed by curing at room temperature or slightly higher.

For the chemical designation of silico-aluminate-based geopolymers, the term poly(sialate) has been suggested. Sialate stands for silicon-oxo-aluminate, where the network consists of SiO_4 and AlO_4 tetrahedra linked alternately by sharing all the oxygen atoms. Positive ions (such as Na^+, K^+, Li^+, Ca^{2+}, Ba^{2+}, NH_4^+, H_3O^+) must be present in the framework cavities to balance the negative charge of Al^{3+} in four-fold coordination [8].

The formula for poly(silicates) is as follows:

$$Mn\ [-(SiO_2)\ z - AlO_2 -)]n,\ wH_2O$$

Where "M" represents a cation such as potassium, sodium, or calcium, "n" is the degree of polycondensation, and "z" can be 1, 2 or 3. Poly(sialates) are chain and cycle polymers with Si^{4+} and Al^{3+} in four-fold coordination with oxygen, ranging from amorphous to semi-crystalline structures (Figure 1.1)[9].

During geopolymerization, when the aluminosilicate is mixed with the alkaline solution, it forms a paste that quickly hardens into a geopolymer. This rapid transformation leaves insufficient time and space for the gel or paste to develop into a well-crystallized structure, which is the fundamental difference between zeolites and geopolymers. Due to their shorter setting and curing times, compact polycrystalline geopolymers exhibit better mechanical properties compared to the cage-shaped, lower density, crystalline zeolites [10].

[8] Pacheco-Torgal F, Castro-Gomes J, Jalali S. Alkali-activated binders: A review. Part 1. Historical background, terminology, reaction mechanisms and hydration products. *Constr Build Mater*. **2008**;22(7):1305-1314.

[9] Davidovits J. Properties of Geopolymer Cements: First International Conference on Alkaline Cements and Concretes, **1994**; 131–149.

[10] Davidovits J. Geopolymers and geopolymeric materials. *J Therm Anal*. **1989**;35(2):429-441.

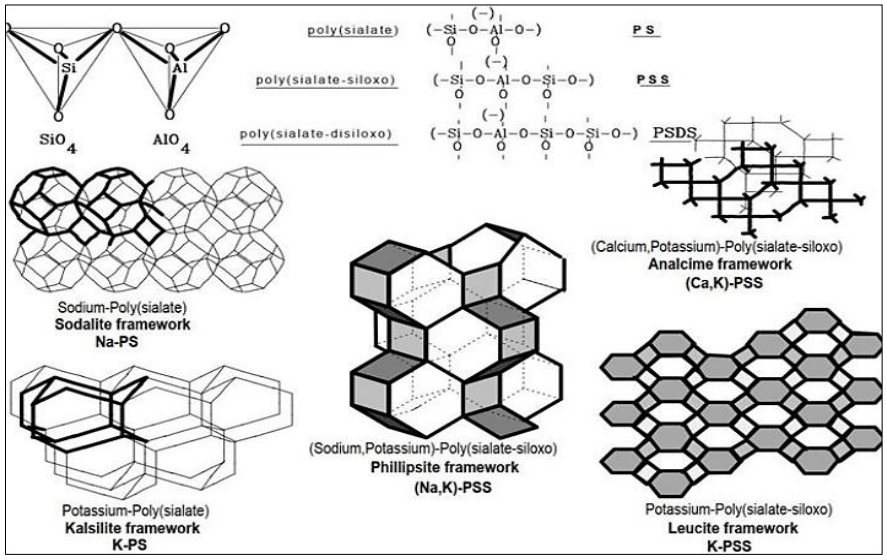

Figure 1.1. Representation of the different sialates present in the structure of a geopolymer[9].

Figure 1.2 illustrates the primary processes involved in transforming a solid aluminosilicate source into a synthetic alkaline aluminosilicate. Although depicted linearly for simplicity, these processes are largely interconnected and occur simultaneously.

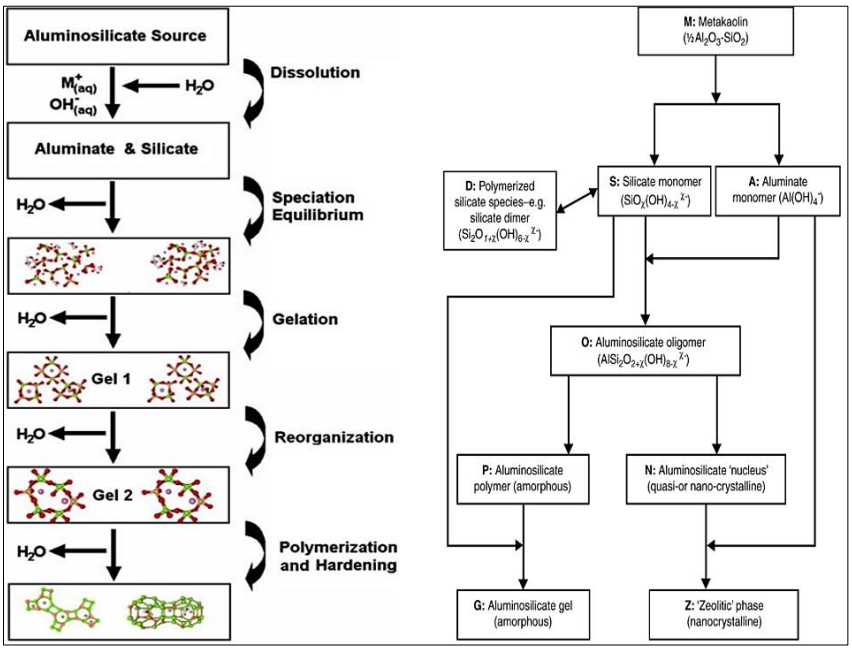

Figure 1.2. (right) Reaction mechanism of geopolymerization proposed by Duxson et *al* [11]. (left) Schematic of reaction processes involved in geopolymerization [12].

[11] Provis J, Rees C. Geopolymer synthesis kinetics. In: *Geopolymers*. **2008**. p. 118-136.
[12] Duxson P, Fernández-Jiménez A, Provis JL, Lukey GC, Palomo A, Van Deventer JSJ. Geopolymer technology: The current state of the art. *J Mater Sci*. **2007**;42(9):2917-2933.

In the 1950s, Glukhovsky proposed a general mechanism for the alkaline activation of materials primarily composed of silica and reactive alumina. The Glukhovsky model divides the process into three stages: destruction-coagulation, coagulation-condensation, and condensation-crystallization [5, 11].

- During the dissolution stage, the solid aluminosilicate source undergoes alkaline hydrolysis, consuming water and producing aluminate and silicate species, likely in monomer form. These species are then incorporated into the aqueous phase, which contains silicate from the activating solution. This leads to the formation of a complex mixture of silicate, aluminate, and aluminosilicate species. The dissolution of amorphous aluminosilicates is typically very rapid in a high pH environment, quickly creating a "supersaturated aluminosilicate solution".
- During the condensation (gelling) phase, when the system reaches an adequate concentration, a gel forms as the oligomers in the aqueous phase form large networks. The water consumed during the dissolution stage returns to the solution. The gel formed during this step has a bi-phasic structure, consisting of an aluminosilicate binder and water. The gel formation time greatly depends on the types of aluminosilicates (raw materials) and the chemical activators used [8].
- After gelling, the system continues to reorganize, increasing the connectivity of the gel network. This results in the formation of the "three-dimensional aluminosilicate network" characteristic of geopolymers.

Moreover, geopolymerization is influenced by the choice of source materials and alkaline activators:

- Source materials: Various authors have noted that all sources containing silicates or aluminates can serve as precursors for geopolymers. However, the most commonly used raw materials include kaolinite, metakaolinite, fly ash, dairy, or a combination of two or more of these materials [6, 8].
- Alkaline activators: Two models of alkaline activation can be identified based on the raw materials used [13]. The first model involves the activation of blast furnace slag (containing Si and Ca) with a slightly alkaline solution, resulting in the formation of calcium silicate hydrate (C-S-H) as the main reaction product. In the second model (involving Si and Al), a common example is the alkaline activation of metakaolin with medium to high alkaline solutions, leading to a final product characterized by a polymeric structure and high mechanical strength.

Strong alkalis are necessary to activate the silicon and aluminum components in the raw materials, enabling the partial or complete transformation of the vitreous structure into a highly compacted composite. Soluble silicate is mixed with fly ash, cement, lime, slag, or other sources containing multivalent metal ions, which promote gelation and silicate

[13] Provis JL, Duxson P, van Deventer JSJ, Lukey GC. The Role of Mathematical Modelling and Gel Chemistry in Advancing Geopolymer Technology. *Chem Eng Res Des*. **2005**;83(7):853-860.

precipitation. The more NaOH interacts with the reactive solid, the more silicate and aluminate monomers are released [14].

In his 1981 study [8], Glukhovsky categorized chemical activators into six groups, where M represents an alkaline ion:

1. Alkaline hydroxides (MOH)
2. Weak acid salts (M_2CO_3, M_2SO_3, M_3PO_4, MF)
3. Silicates ($M_2O.\ nSiO_3$)
4. Aluminates ($M_2O.\ nAl_2O_3$)
5. Aluminosilicates ($M_2O.\ Al_2O_3.\ (2–6)\ SiO_2$)
6. Strong acid salts (M_2SO_4)

Katz has investigated the activation of slags by alkalis (NaOH) and demonstrated an increase in mechanical strength with higher activator concentrations[15]. Similar behavior was observed by other researchers using alkali-activated metakaolin[8].

In the alkali activation of fly ash, Palomo et *al.,* found that a 12 M activator concentration yielded better results than a 18 M concentration[13]. They noted that the alkaline activator plays a crucial role in the polymerization reaction, which occurs more rapidly in the presence of soluble silica. Criado et *al*. suggested that sodium silicate (also named water glass) enhances the polymerization process, resulting in a reaction product with higher Si content and greater mechanical strength [16]. Fernandez-Jimenez and Palomo observed an increase in strength from 40 to 90 MPa after just one day of curing when an alkaline activator (sodium silicate or sodium carbonate) was used with NaOH, compared to NaOH alone [17, 18].

In the study by Fansuri et *al.,* a trend was observed where changes in the SiO_2/Na_2O ratio negatively impacted compressive strength when activating various types of fly ash. As the ratio increased, the compressive strength decreased [19]. Similarly, Fernandez-Jiménez and Palomo reported the same phenomenon [17, 18]. Kirschener and Harmuth examined the activation of metakaolin with NaOH and sodium silicate, nothing that mechanical strength improved as the Na_2O/SiO_2 molar ratio decreased[20].

---

[14] Palomo A, Grutzeck MW, Blanco MT. Alkali-activated fly ashes: A cement for the future. *Cem Concr Res*. **1999**;29(8):1323-1329.
[15] Katz A. Microscopic Study of Alkali-Activated Fly Ash. *Cem Concr Res*. **1998**;28(2):197-208.
[16] Li Y, Dai S, He X, Su Y. Influences of Ultrafine Slag Slurry Prepared by Wet Ball Milling on the Properties of Concrete. *Adv Mater Sci Eng*. **2018**;2018.
[17] Fernández-Jiménez A, Palomo A. Composition and microstructure of alkali activated fly ash binder: Effect of the activator. *Cem Concr Res*. **2005**;35(10):1984-1992.
[18] García-Lodeiro I, Fernández-Jiménez A, Palomo A. Alkali-activated based concrete. Eco-Efficient Concr. Published online January 1, **2013**:439-487.
[19] Fansuri H, Prasetyoko D, Zhang Z, Zhang D. The effect of sodium silicate and sodium hydroxide on the strength of aggregates made from coal fly ash using the geopolymerisation method. *Asia-Pacific J Chem Eng*. **2012**;7(1):73-79.
[20] Kirschner A V, Harmuth H. INVESTIGATION OF GEOPOLYMER BINDERS WITH RESPECT TO THEIR APPLICATION FOR BUILDING MATERIALS. *Orig Pap Ceram – Silikáty*. **2004**;48(3):117-120.

Several authors have highlighted the significance of the H_2O/SiO_2 molar ratio in the synthesis of geopolymers and other aluminosilicates like zeolites. The mineralizing and stabilizing effects of water play a crucial role in the dissolution and polycondensation processes of zeolites and geopolymeric precursors [21, 22].

Van Jaarsveld and van Deventer activated various fly ash using a combination of sodium silicate and sodium or potassium hydroxide. They observed that the K_2O/SiO_2 ratio influenced compressive strength, with the optimal resistance observed at a ratio between 0.75 and 1.5 (achieving 20 MPa at 7 days) [23].

In the study performed by Kovalchuk et *al.*, a mixture of sodium hydroxide and sodium silicate was used for fly ash activation[24]. They investigated the effect of SiO_2/Al_2O_3 and Na_2O/Al_2O_3 ratios on compressive strength. They found that the SiO_2/Al_2O_3 ratio did not vary linearly with mechanical strength, with optimal molar ratios between 3.5 and 4.0. Higher ratios resulted in a significant decrease in strength. An optimal Na_2O/Al_2O_3 ratio of 1.0 was identified, where the charges on Al^{3+} and Na^{+} ions balanced the negative net Si-Al charges from structural replacements. Any imbalance in this ratio could negatively affect the material's mechanical strength.

In a study by Kumar et al., various amounts of blast furnace slag (BFS) (ranging from 0 to 50 % by weight) were added to geopolymers prepared using Class F fly ash (FA) and a 6M sodium hydroxide solution. The samples were cured at 27 °C for different durations (as shown in Figure 1.3)[25].

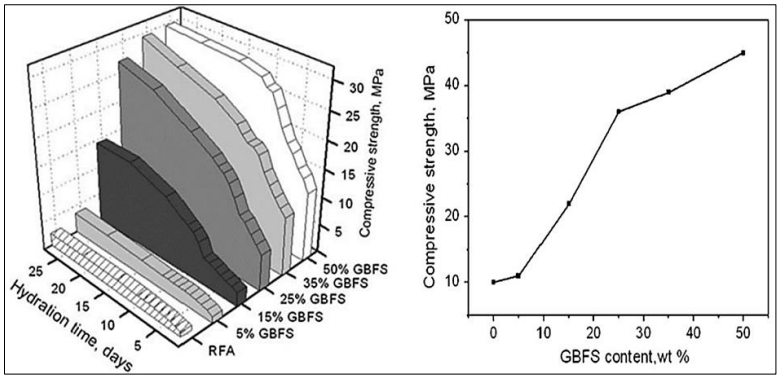

Figure 1.3. (left) Effect of GBFS addition on compressive strength versus hydration time at 27 °C, (right) for hydration of 27 °C for 48h followed by 4h to 60 °C [25].

[21] Van Jaarsveld JGS, Van Deventer JSJ, Schwartzman A. The potential use of geopolymeric materials to immobilise toxic metals: Part II. Material and leaching characteristics. *Miner Eng*. **1999**;12(1):75-91.
[22] Kamalloo A, Ganjkhanlou Y, Aboutalebi S. H, Noranian H. *Transactions A: Basics Int. J. Eng.* **2010;** (23), 145.
[23] Van Jaarsveld JGS, Van Deventer JSJ. Effect of the alkali metal activator on the properties of fly ash-based geopolymers. *Ind Eng Chem Res*. **1999**;38(10):3932-3941.
[24] Kovalchuk G, Fernández-Jiménez A, Palomo A. Alkali-activated fly ash. Relationship between mechanical strength gains and initial ash chemistry. *Mater Construcción*. **2008**;58(291):35-52.
[25] Kumar S, Kumar R, & Mehrotra S. P. Influence of granulated blast furnace slag on the reaction, structure and properties of fly ash based geopolymer. *J. Mater. Sci*. **2010**; *45*, 607-615.

The compressive strength of geopolymers was tested at different curing times and for various BFS addition rates. It was observed that increasing the amount of BFS resulted in higher compressive strength of the geopolymers, with an optimum strength of 10 MPa after 1 day and 30 MPa after 28 days for samples with 50 % BFS. Compressive strength increased most effectively with the addition of more than 15 % BFS. According to the authors, the increase in strength over time is primarily due to the formation of C-S-H. Additionally, the authors thermally treated samples at 60 °C for 48 hours after initially curing them at 27 °C for 48 hours.

The authors observed that heat treatment significantly enhanced the increase of compressive strength. For geopolymers with 100 % fly ash, the compressive strength increased to 10 MPa with heat treatment, compared to less than 5 MPa without treatment. For the geopolymer labelled "50 LHF/50 CV," the compressive strength reached 45 MPa. Calorimetric analysis of samples cured at 27 °C or heat-treated at 60 °C revealed that at 27 °C, the calorimetric response was primarily governed by the dissolution and precipitation of C-S-H gel due to the alkaline activation of slags. At 60 °C, with the addition of BFS, two reaction mechanisms occurred simultaneously: the formation of N-A-S-H and C-S-H.

In the study by Panagiotopoulou et al., geopolymers were prepared using blast furnace slag with a mixture of NaOH and sodium silicate. The compressive strength was measured after curing for 48 hours at 70 °C. The study observed that increasing the SiO_2/Al_2O_3 ratio enhanced the compressive strength, with an optimum value of 3.5, achieving a compressive strength of 112 MPa. However, when the ratio exceeded 3.5, the compressive strength decreased, dropping to 95 MPa at a ratio of 4 and to 75 MPa at a ratio of 4.5 [26].

In the study by Chang et al., slag was activated using different chemical activators (potassium hydroxide and sodium silicate). Various results were obtained, particularly for slag activated with KOH at different concentrations, which underwent a pre-treatment at 60 °C for 3 hours followed by conventional curing at room temperature. The authors found that the concentration of KOH affected the compressive strength, with the best results obtained at a concentration of 10M. For analyses conducted from 1 to 28 days, the compressive strength consistently exceeded 60 MPa. For slag activated with sodium silicate and 10M KOH, a $SiO_2/Al2O_3$ ratio of 3.36 yielded the highest compressive strength of 70 MPa, while higher ratios resulted in decreased strength. Additionally, when different levels of metakaolinite were added, the maximum compressive strength of 79 MPa was observed at a SiO_2/Al_2O_3 ratio of 3.16 [27].

[26] Panagiotopoulou C, Kakali G, Tsivilis S, Perraki T, Perraki M. Synthesis and characterisation of slag based geopolymers. *Mater Sci Forum*. **2010**;636-637:155-160.
[27] Cheng TW, Chiu JP. Fire-resistant geopolymer produced by granulated blast furnace slag. *Miner Eng*. **2003**;16(3):205-210.

In the study by Khater et al., metakaolinite (MK) based geopolymers were prepared with the addition of NaOH and sodium silicate activators[28]. The results showed an increase in compressive strength in all mixtures as hydration progressed, attributed to the pozzolanic reaction of the MK and slag samples. Compressive strength values increased with the addition of slag up to 40 %, at which point a significant improvement in strength compared to MK-based samples was observed. At 90 days, the strength of the 100 % MK sample was 105 kg/cm² for a SiO_2/Al_2O_3 ratio of 1.68, while the strength of the 40 % slag sample was 866 kg/cm² for a $SiO_2/Al2O_3$ ratio of 2. This result was attributed to the reaction of calcium produced by the slag with excess dissolved silicate, forming additional C-S-H gel that acts as a nucleative agent for geopolymer formation and accumulation. C-S-H formation during MK activation was also observed in several studies [29,30].

In the study by Rowles et al. [31], the authors used kaolinite calcined at 750 °C for 24 hours and activated it with sodium hydroxide and sodium silicate. They varied the Na_2O/Al_2O_3 ratio by adjusting the amount of activator added, and the SiO_2/Al_2O_3 ratio by incorporating silica fume[32]. In Figure 1.4, the authors illustrated the variation of compressive strength as a function of the two ratios Na_2O/Al_2O_3 and SiO_2/AlO_3. The optimal strength of 62 MPa was achieved with a SiO_2/AlO_3 ratio of 2.5 and a Na_2O/Al_2O_3 ratio of 1.29. This demonstrates that the compressive strength of the geopolymers produced in their study is highly dependent on the Na:Al and Si:Al ratios.

[28] Khater H. M, Ezzat M, and Abdeen M. El Nagar. Alkali activated eco-friendly metakaolin/slag geopolymer building bricks. *Chem. Mater. Res*. **2016**;21-32.
[29] Wang SD, Scrivener KL. Hydration products of alkali activated slag cement. *Cem Concr Res*. **1995**;25(3):561-571.
[30] Richardson IG, Brough AR, Groves GW, Dobson CM. The characterization of hardened alkali-activated blast-furnace slag pastes and the nature of the calcium silicate hydrate (C-S-H) phase. *Cem Concr Res*. **1994**;24(5):813-829.
[31] Rowles, M.R. and O'Connor, B.H. (2009), Chemical and Structural Microanalysis of Aluminosilicate Geopolymers Synthesized by Sodium Silicate Activation of Metakaolinite. Journal of the American Ceramic Society, 92: 2354-2361.
[32] Rowles M, O'Connor B. Chemical optimisation of the compressive strength of aluminosilicate geopolymers synthesised by sodium silicate activation of metakaolinite. *J Mater Chem*. **2003**;13(5):1161-1165.

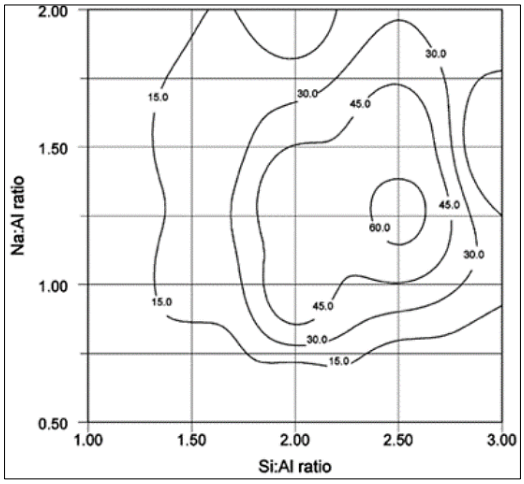

Figure 1.4. Compression strength contours for aluminosilicate polymers. The first contour is 15 MPa and the contour interval is 15 MPa [31].

To enhance the performance and rheological properties of geopolymers, researchers have focused on modifying the characteristics of raw materials prior to their combination with chemical activators.

Madai et al. utilized class F fly ash with a SiO_2/Al_2O_3 ratio of 2.26, which was dried and ball-milled for various durations (10, 20, 30, and 60 minutes). Geopolymers were prepared by adding sodium hydroxide with a liquid-to-solid ratio (L/S) of ½. Heat treatment was applied to samples aged for 20 hours at 150 °C for 4 hours, followed by compression testing after 7 days. The fly ash-based geopolymers exhibited low strength (0.4 MPa), with grinding duration significantly affecting mechanical performance. An optimum strength of 10.56 MPa was achieved with a milling duration of 30 minutes and a specific surface area (Blaine 2500 $cm^2 \cdot g$-1/BET 7.649 m^2/g)[33].

Marjanović et al. observed a similar trend in their studies, where they used four different Class F fly ashes. These fly ashes were crushed with a planetary ball mill for various durations (15, 30, 45, and 60 minutes) at a speed of 380 RPM. Geopolymer mortars were prepared by adding soda silicate and heat-treated at 95 °C for 4 hours. The effects of grinding on the fly ash particles were evident, with compressive strength values ranging from 0 to 5.24 MPa for geopolymers prepared with untreated fly ash, and significantly higher values of 51.37 to 70.32 MPa for geopolymers prepared with crushed fly ash. These studies highlight the importance of fly ash particle size in the development of compressive strength in fly ash-based geopolymers [32,34].

[33] Mádai F, Kristály F, Mucsi G. MICROSTRUCTURE, MINERALOGY AND PHYSICAL PROPERTIES OF GROUND FLY ASH BASED GEOPOLYMERS. *Ceramics-Silikáty*. **2015**;59(1):70-79.
[34] Marjanović N, Komljenović M, Baščarević Z, Nikolić V. Improving reactivity of fly ash and properties of ensuing geopolymers through mechanical activation. *Constr Build Mater*. **2014**;57:151-162.

In a study by Alex et al.[35], slag from zinc production was used to prepare geopolymers. The slag was ground using a planetary ball mill for 3 minutes, achieving a relative bond work index (RBP) of 6.2. The authors produced different types of crushed slag by using two different grinding atmospheres: one under air and the other under CO2. They observed that slag crushed under CO2 had a higher fineness compared to that crushed under air. The geopolymers were prepared with the addition of 6M NaOH, and the geopolymer pastes were stored at 20 °C. Compressive strength (RC) results showed that geopolymers prepared with CO_2-crushed slag (GP1) exhibited significantly better performance than those prepared with air-crushed slag (GP2). For instance, the 1-day RC for GP1 was 20 MPa compared to 10 MPa for GP2. This trend persisted at 180 days of curing, with GP1 showing an RC of 90 MPa and GP2 at 70 MPa. Unfortunately, the authors did not provide information on the RC of non-crushed slag-Zn-based geopolymers, which limits the assessment of the grinding efficiency on geopolymer performance. However, it is evident that the finest slags (crushed under CO_2) produced the most resistant geopolymers.

1.2. Geopolymer concrete and OPC concrete

Concrete, a mix of cement and aggregate, is the most commonly used building material globally, second only to water in terms of consumption, with an average use of 1 m^3 per person per year [36]. Big construction and infrastructure projects demand vast amounts of concrete, with Portland cement as its binder. The production of Portland cement is associated with significant carbon dioxide (CO_2) emissions. This growing global demand for concrete presents a significant opportunity for the development of geopolymer cements, which have much lower CO_2 emissions [37]. Figure 1.5 illustrates a CO_2 emissions system diagram for the production of 1 m^3 of concrete [38].

[35] Alex TC, Kalinkin AM, Nath SK, et al. Utilization of zinc slag through geopolymerization: Influence of milling atmosphere. *Int J Miner Process*. **2013**;123:102-107.
[36] Gartner E. Industrially interesting approaches to "low-CO2" cements. *Cem Concr Res*. **2004**;34(9):1489-1498.
[37] Edward G. N. Concrete Construction Engineering Handbook, 2nd edition, CRC Press, New York. **2008**.
[38] Turner LK, Collins FG. Carbon dioxide equivalent (CO2-e) emissions: A comparison between geopolymer and OPC cement concrete. *Constr Build Mater*. **2013**;43:125-130.

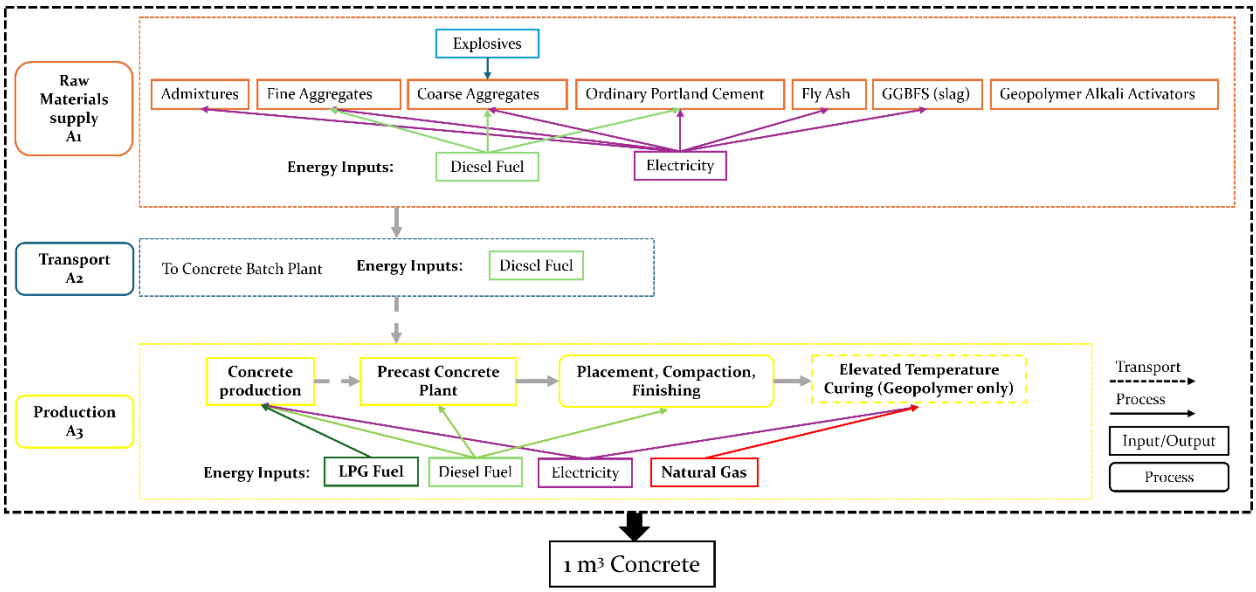

Figure 1.5. CO_2 emissions system diagram for production of 1 m³ concrete [37].

Indeed, Portland Cements (PC) are produced through the calcination of limestone, a process that can be represented by the following reaction:

$$5CaCO_3 + 2SiO_2 \rightarrow (3CaO,SiO_2)(2CaO,SiO_2) + 5CO_2$$

Furthermore, the high energy consumption involved in manufacturing, particularly in heating raw materials to temperatures exceeding 1400 °C, exacerbates this pollution [35]. Consequently, Portland cement is major contributors to high greenhouse gas emissions, and there is currently no widely recognized industrial technology that significantly reduces carbon dioxide emissions from Portland cement production.

In contrast, geopolymer cement does not rely on calcium carbonate and emit much less CO_2 during manufacturing. Several studies have reported a reduction in CO_2 emissions ranging from 26 % to 80 % compared to Portland cement production.

However, the actual reduction can vary based on factors such as local conditions of raw material sourcing, types of manufacturing facilities, climate, energy sources, and

transportation distances [39] [40] [41] [42] [43] [44] [45]. Amorphous geopolymer materials are produced at low temperatures through chemical reactions between various aluminosilicate oxides and silicates under highly alkaline conditions, forming polymeric Si-O-Al-O bonds, as described by the formula[46]:

$$Mn\,[\,-(Si-O_2)z-Al-O\,]n\cdot wH_2O$$

(where M is an alkaline element, the symbol '–' indicates the presence of a bond, z is 1, 2, or 3, and n is the degree of polymerization).

The hardening processes of the two materials differ: Portland cement (PC) hardens through the simple hydration of Calcium Silicate to form Calcium Di-Silicate hydrate (CSH) and lime Ca(OH)2, whereas Geopolymer cement (GP) sets through the polycondensation of Potassium Oligo-(sialate-siloxo) to form a cross-linked network of Potassium Poly(sialate-siloxo) (Figure 1.6)[47].

On the other hand, K. L. Turner et al. mentioned the significant environmental impact of alkali activator production, which requires a substantial amount of electrical energy (1915 kg CO_2-eq). Consequently, they estimate that geopolymer cement production is only 8 % less carbon-intensive than Portland cement production [37]. Additionally, the choice of precursors can present challenges. For example, metakaolin, commonly used in geopolymer synthesis, is produced from the dehydroxylation of kaolin, requiring considerable thermal energy for calcination and a large amount of water.

[39] Duxson P, Provis JL, Lukey GC, van Deventer JSJ. The role of inorganic polymer technology in the development of 'green concrete.' *Cem Concr Res*. **2007**;37(12):1590-1597.
[40] Stengel T, Reger J, Heinz D. Life Cycle Assessment of Geopolymer Concrete – What is the Environmental Benefit ? Concr Solut 09. **2009**;(1):1-10
[41] Witherspoon R, Wang H, Aravinthan T, Omar T. Energy and Emissions Analysis of Fly Ash Based Geopolymers. SSEE 2009 Conf Melb **2009**; 1-11. 6
[42] Van Deventer JSJ, Provis JL, Duxson P, Brice DG. Chemical research and climate change as drivers in the commercial adoption of alkali activated materials. Waste and Biomass Valorization. **2010**;1(1):145-155.
[43] Habert G, D'Espinose De Lacaillerie JB, Lanta E, Roussel N. Environmental evaluation for cement substitution with geopolymers. In: 2nd International Conference on Sustainable Construction Materials and Technologies. ; **2010**:1607-1615. 9
[44] Habert G, D'Espinose De Lacaillerie JB, Roussel N. An environmental evaluation of geopolymer based concrete production: Reviewing current research trends. J Clean Prod. **2011**;19(11):1229-1238.
[45] McLellan BC, Williams RP, Lay J, Van Riessen A, Corder GD. Costs and carbon emissions for geopolymer pastes in comparison to ordinary portland cement. J Clean Prod. **2011**;19(9-10):1080-1090.
[46] Mallicoat S, Sarin P, Kriven WM. Novel, Alkali-Bonded, Ceramic Filtration Membranes. In: John Wiley & Sons, Ltd; **2008**:37-44.
[47] Davidovits J. Geopolymer Cement a review, published in Geopolymer Science and Technics, Technical Paper #21, *Geopolymer Institute Library*, **2013**; www.geopolymer.org.

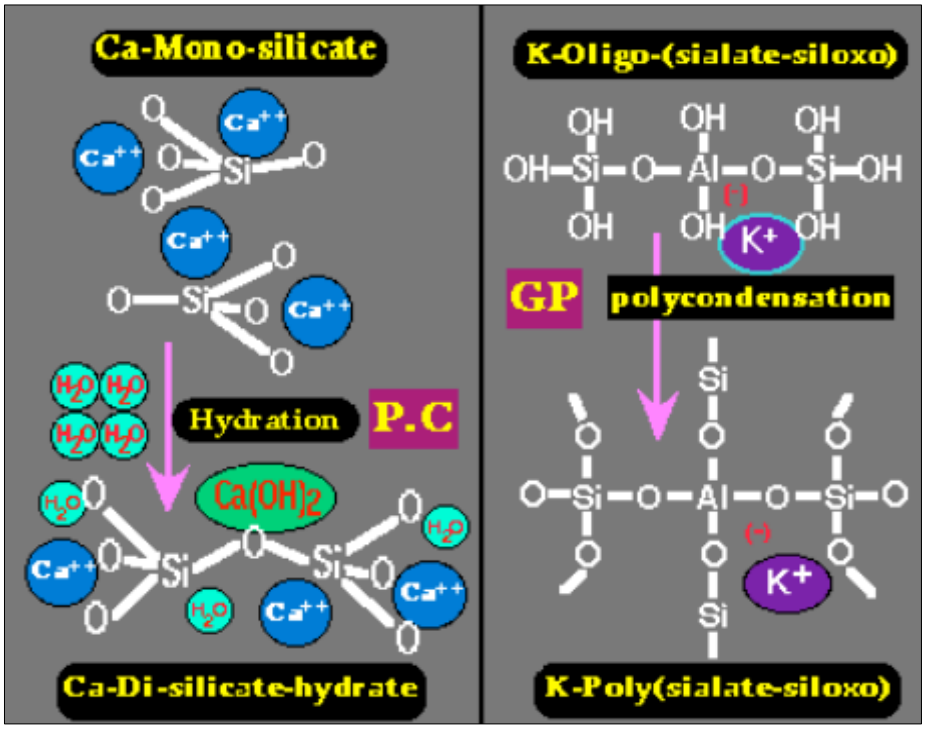

Figure 1.6. Difference between Portland Cement chemistry and geopolymer cement chemistry [47].

Recently, there has been a growing trend towards using residues and by-products (such as fly ash, granulated blast furnace slag (GBFS), steel slag, tailings, red mud, construction and demolition waste, etc.) for geopolymer synthesis. Many scientific articles are adopting this approach, as these materials offer better resistance and durability than metakaolin-based geopolymers. They also exhibit improved dimensional stability, flowability, cost-effectiveness, and easy availability, while maintaining similar molecular and nano-structural properties [48].

Significant efforts have been made to conduct comparative studies between geopolymer and Portland cements, aiming to pave the way for sustainable practices, as illustrated in Figure 1.7 [48].

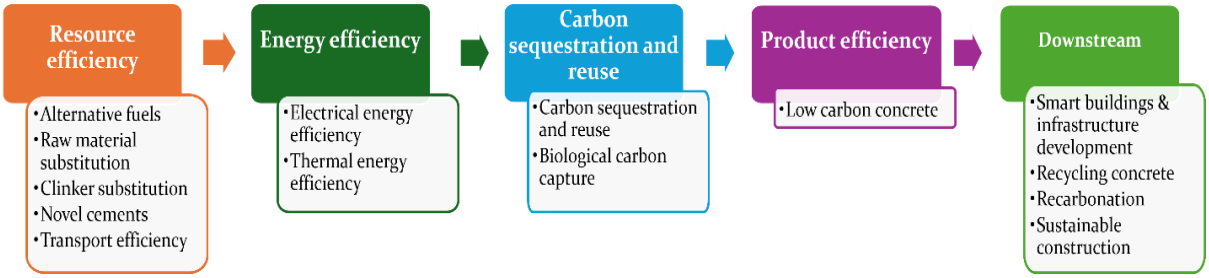

Figure 1.7. Five routes to achieve sustainability [48].

[48] Kumar S, Kumar R. Geopolymer : Cement for low carbon economy. Indian Concr J. **2014**;88(7):29-37.

As depicted in Figure 1.8, there has been a notable increase in scientific research focusing on the synthesis of geopolymers from residues and by-products. This interest has tripled over five years, from 2007 to 2012. This trend underscores the strong interest in geopolymers compared to Ordinary Portland Cements (OPCs), as geopolymers are more aligned with sustainable development criteria and offer the potential to enhance application properties while meeting environmental and economic requirements [47].

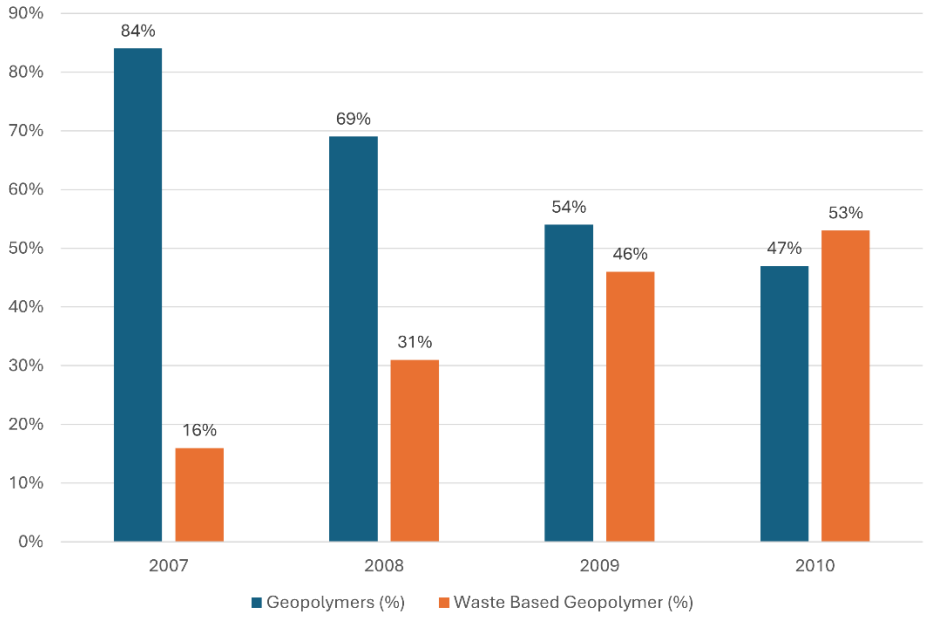

Figure 1.8. Shift in trend in geopolymer research with increasing focus on waste and by-products (2007-2012)[48].

The study also discusses various properties of the final material, as well as the economic and environmental impact of the production process. There is a growing interest in comparing geopolymer concrete with OPC, highlighting the importance of comparative studies to enhance geopolymer properties. However, geopolymer use in the construction sector is limited due to resistance issues with the reaction mixture content or to higher temperatures, unlike OPCs [47].

Conventional concretes, also known as OPC conventional concretes, are predominantly used in residential, industrial, commercial, and agricultural fields. They are considered composite materials, with sand and stone particles dispersed in a multiphase matrix of Portland cement paste (Figure 1.9) [49]. Conventional concrete differs from other composites due to its porosity and the composition of the cement, which varies with time, temperature, and humidity, there by affecting its strength and durability. This indicates that research is more focused on the paste rather than on the size and nature of sand or stone granules, which can be controlled [47].

[49] National Research Council, Nonconventional Concrete Technologies, Renewal of the Highway Infrastructure, Washington, DC: The National Academies Press, **1997**.

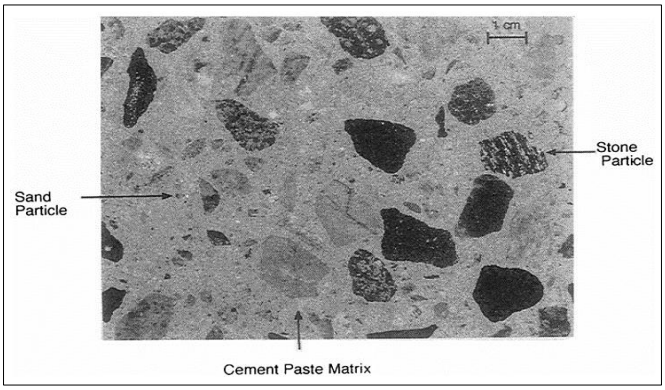

Figure 1.9. Macrophotograph of a plain polished section of concrete showing sand and stone particles in a cement paste matrix [49].

Table 1.1 reports the comparison of the properties and impact between OPCs and GPs.

Table 1.1. Comparison of physico-mechanical properties and environmental impact between OPCs and GPs [48].

Properties	OPCs	GP	Remarks
	Physico-Mechanical Properties		
Setting time	30 to 300 min	10-60 min	Usually set faster than Portland cement, but depends on raw material reactivity and alkali concentration
Compressive strength	33-53 MPa after 28 days	30-120 MPa after 7 days	Strength can be tailored by optimising raw material reactivity and alkali concentration
Durability	Moderate	More durable than Portland cement	Geopolymer systems are aluminosilicate-based system which are resistant to acid attack
	Environmental Impact		
CO_2 emission	800-900 kg/ton	150-200 kg/ton	CO_2 emission in geopolymer is during production of alkali

			hydroxide and silicate from carbon
Embodied energy	4000-4400 MJ/ton	2200-2400 MJ/ton	As it mostly uses waste and by-products with no embodied energy
Water requirement	~600 liters/ton	~450 liters/ton	Geopolymer do not need curing with water unlike Portland cement

The table below presents a performance comparison between geopolymer concrete and conventional concrete [50].

Table 1.2. Performance of geopolymer concrete compared to conventional concrete.

Property	Performance of geopolymer concrete
Compressive Strength	Similar, higher rate of early strength gain
Tensile Strength	Indirect tensile strength typically higher for similar compressive strength
Flexural Strength	Similar to higher depending on the alkali activator, higher rate of early strength gain
Modulus of Elasticity	Typically lower
Density	Similar to lower
Poison's Ratio	Typically lower or similar
Shrinkage	Lower to similar
Creep Coefficient	Lower
Bond Strength to Reinforcement	Similar for similar compressive strengths; higher for higher compressive strengths
Carbonation Coefficient	Higher
Chloride Diffusion Coefficient	Lower than conventional concrete
Rapid Chloride Permeability	Lower to similar depending on mix proportions
Sorptivity	Higher than conventional concrete
Sulfate Resistance	Higher than conventional concrete
Acid Resistance	More resistant to organic and inorganic acid attack
Alkali-Silica Reaction	Varies
Fire Resistance	High resistance

[50] Afrin, H. Life cycle assessment and sustainability aspects of using waste materials in concrete. Macquarie University. Thesis, **2022**.

Freeze-Thaw Durability	More durable
Volume of Permeable Voids	Varies depending on mix proportions
Water Absorption	Similar to conventional concrete

1.3. Common employed starting materials and activators

1.3.1. Source materials

The preceding discussion underscores the importance of selecting appropriate sources for material synthesis throughout their entire life cycle, from construction to demolition. Making a wise choice in this regard can be challenging, requiring careful consideration of cost, performance characteristics, and environmental properties [51].

- During the production phase, the selection of materials reveals their environmental qualities and the user's precautions.

- During the use phase, the choice may vary depending on the company's design and/or customer criteria. Attention is paid to maintenance and renovation until the material reaches the end of its life.

- At the end of its life, biodegradable materials should be reused or recycled to minimize waste impact.

Transportation is a key consideration throughout the entire life cycle.

As mentioned earlier, there is a growing interest in recycling or reusing waste for concrete manufacturing, which helps reduce pollution and enhances economic security by ensuring domestic sources. This includes waste from:

- Industry (Electric Arc Furnace Dust and Slag: EAF-DS).
- Household activities (plastic bags, glass containers, PET bottles).
- Construction and demolition sites, where waste such as steel, wood products, plaster, brick, and clay tile are generated.

1.3.1.1. Clay

Clay is a natural material composed of hydrated silicates or aluminosilicates with a lamellar structure, often resulting from the alteration of silicates with a three-dimensional framework. While clay offers many advantages, such as abundant availability and low cost, it also presents some challenges. These can include low strength, excessive settlement, high plasticity, swelling, dispersity, erodibility, high compressibility, and sensitivity to environmental conditions. However, these drawbacks can be mitigated through various methods. One such method involves mixing binders like cement, lime,

[51] Figiela B, Brudny K, Lin WT, Korniejenko K. Investigation of Mechanical Properties and Microstructure of Construction-and Demolition-Waste-Based Geopolymers. *J Compos Sci*. **2022**;6(7):191.

fly ash, gypsum, and other additives with the soil to form stone columns of hardened material. This enhances the soil's classification properties and strength parameters [52].

Clays have demonstrated excellent pozzolanic properties under specific calcination conditions or surface modifications. This makes them valuable alternatives to cement, helping to develop sustainable concretes with reduced costs and environmental impacts. Clays can be used in their raw, calcined, or modified forms, as shown in Figure 1.10 [53] [54] [55].

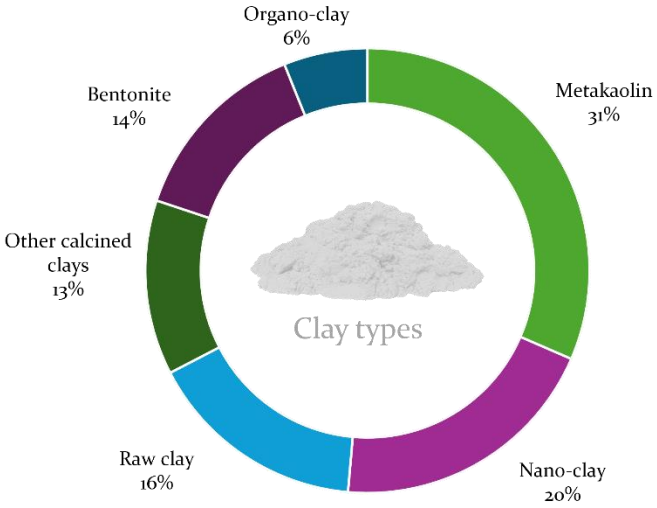

Figure 1.10. Types of clay used in literature [55].

The properties of clay-based concrete, both in its fresh and hardened states, as well as its durability, are significantly influenced by the type of clay used [54].

1.3.1.2. Metakaolin

Kaolin, a natural material, can also be obtained as a primary industrial by-product, such as from paper sludge waste and oil sands tailings. Metakaolin, also known as calcined clay, is produced by heating a source of kaolinite to between 700 °C and 850 °C. Optimal results are achieved within this temperature range, as calcination below 700 °C results in low-reactive metakaolin, while temperatures above 800 °C reduce reactivity due to the crystallization process. Metakaolin is classified as a pozzolanic material with a smaller particle size than Portland cement, which helps accelerate the reactions that harden

[52] Hamidi S, Marandi SM. Clay concrete and effect of clay minerals types on stabilized soft clay soils by epoxy resin. *Appl Clay Sci*. **2018**;151:92-101.
[53] lujas A, Fernández R, Quintana R, Scrivener KL, Martirena F. Pozzolanic reactivity of low grade kaolinitic clays: Influence of calcination temperature and impact of calcination products on OPC hydration. *Appl Clay Sci*. **2015**;108:94-101.
[54] Tironi A, Trezza MA, Scian AN, Irassar EF. Kaolinitic calcined clays: Factors affecting its performance as pozzolans. *Constr Build Mater*. 2012;28(1):276-281. doi:10.1016/J.CONBUILDMAT.2011.08.064
[55] Mousavi SS, Bhojaraju C, Ouellet-Plamondon C. Clay as a Sustainable Binder for Concrete—A Review. *Constr Mater* ***2021****, Vol 1, Pages 134-168*. 2021;1(3):134-168.

concrete. It improves the long-term strength and durability of concrete, reduces the effects of alkali-silica reactions, enhances resistance to chemical attack, and strengthens the bond between the cement paste and aggregate particles. Additionally, it increases the density of the cement paste [56] [57] [58].

Figure 1.11 summarizes the study by El-Din et al. (2017), which found that after 28 days, an optimal dosage of 15 % metakaolin resulted in a 21.96 % increase in compressive strength for specimens with 0 % steel fiber volume fraction. This increase in strength was more significant for specimens with higher steel fiber volume fractions, showing a 27.51 % increase for 0.25 % steel fiber and a 43.34 % increase for 0.50 % steel fiber.

However, the use of metakaolin can lead to an increase in water demand during concrete production, unless suitable water-reducing admixtures are used. Additionally, it can increase the risk of corrosion of carbon (black) steel reinforcement by reducing resistance to carbonation [59] [60].

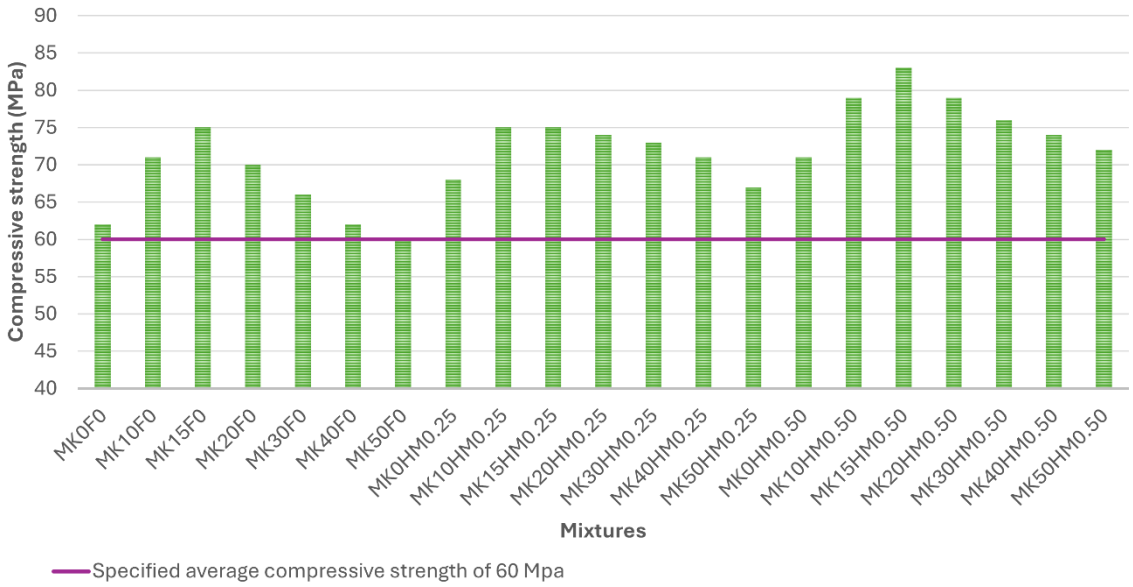

Figure 1.11. Compressive strength of metakaolin after 28 days of curing [60].

[56] Ding JT, Li Z. Effects of metakaolin and silica fume on properties of concrete. *ACI Mater J*. **2002**;99(4):393-398.
[57] Xie J, Zhang H, Duan L, et al. Effect of nano metakaolin on compressive strength of recycled concrete. *Constr Build Mater*. **2020**;256:119393.
[58] Güneyisi E, Gesoğlu M, Mermerdaş K. Improving strength, drying shrinkage, and pore structure of concrete using metakaolin. *Mater Struct*. **2008**;41(5):937-949
[59] Li Z, Ding Z. Property improvement of Portland cement by incorporating with metakaolin and slag. *Cem Concr Res*. **2003**;33(4):579-584.
[60] Shehab El-Din HK, Eisa AS, Abdel Aziz BH, Ibrahim A. Mechanical performance of high strength concrete made from high volume of Metakaolin and hybrid fibers. Constr Build Mater. **2017**;140:203-209.

1.3.2. Alkaline activators

Alkaline activation is a process that involves the chemical reaction, at room temperature, between a solid aluminosilicate precursor and an alkaline activator, resulting in a cured solid product [61]. The activators can be alkali hydroxides, silicates, carbonates, sulfates, aluminates, or oxides-essentially any soluble substance capable of providing alkali metal cations, increasing the pH of the reaction mixture, and accelerating the dissolution of the solid precursor [62].

Many studies have investigated the effects of the type and concentration of alkaline activator on the geopolymerization process and the mechanical properties of the final products [63] [64] [65]. Alkaline activator solutions contribute to SiO_2 and alkalinity, which help initiate the reactions and enhance the mechanical strength during geopolymerization. The cost and properties of these compounds are crucial factors in their selection [66].

1.3.2.1. Sodium hydroxide

Also known as sodium hydrate or caustic soda (NaOH), this white solid has been produced since ancient times, with records of its manufacture in ancient Egypt by mixing sodium carbonate with lime. NaOH finds application in numerous industries, including agronomy, petrochemistry, and cosmetics. However, it is considered a hazardous product for concentrations exceeding 2 %. NaOH is recognized for several chemical properties, such as non-flammability, instability at high temperatures or pressures, and its strong affinity for water molecules [67].

1.3.2.2. Sodium silicate

Also known as sodium silicate or water glass ($Na_2O(SiO_2)x.(H_2O)x$), this clear to cloudy, viscous liquid is known for its stability under ordinary conditions of use and storage. Prolonged contact with metals can result in the production of hydrogen gas. When mixed with acids, it forms gels. The solution is a strong base, reacting with acids,

---

[61] Bernal S. A, Mejía de Gutierrez R, & Rodríguez E. D. Alkali-activated materials: cementing a sustainable future. *Ingeniería y competitividad*, **2013**; *15*(2), 211-223.

[62] Torres-Carrasco M, Puertas F. La activación alcalina de diferentes aluminosilicatos como una alternativa al Cemento Portland: cementos activados alcalinamente o geopolímeros. Revista ingeniería de construcción. **2017** Aug;32(2):05-12.

[63] Álvarez-Ayuso E, Querol X, Plana F, et al. Environmental, physical and structural characterisation of geopolymer matrixes synthesised from coal (co-)combustion fly ashes. *J Hazard Mater*. **2008**;154(1-3):175-183.

[64] Rattanasak U, Chindaprasirt P. Influence of NaOH solution on the synthesis of fly ash geopolymer. *Miner Eng*. **2009**;22(12):1073-1078.

[65] Zhang Z, Wang H, Provis JL, Bullen F, Reid A, Zhu Y. Quantitative kinetic and structural analysis of geopolymers. Part 1. The activation of metakaolin with sodium hydroxide. *Thermochim Acta*. **2012**;539:23-33.

[66] Oshani F, Allahverdi A, Kargari A, Mahmoodi NM. Effect of preparation parameters on properties of metakaolin-based geopolymer activated by silica fume- sodium hydroxide alkaline blend. *J Build Eng*. **2022**;60:104984.

[67] Sodium Hydroxide: Management of Ocular and Cutaneous Chemical Splashes

organic anhydrides, alkylene oxides, epichlorohydrin, aldehydes, alcohols, glycols, phenols, cresols, and caprolactam solution. Sodium silicate is not considered a fire hazard or an explosion hazard [68].

1.4. Hybrid and sustainable functional geopolymeric materials

Hybrid geopolymer is considered nowadays as the new trend for the development of geopolymer. The objective of this research is to develop products with good compressive strength as well as good flexural strength. Inorganic-organic hybrid geopolymer that has been developed are lightweight and less brittle than conventional geopolymer with 3D framework structure [46].

Indeed, any material interacts with its environment via its surface and all interactions with this environment depend on the material's surface properties. Indeed, the objective of functionalization consists of a controlled modification of the surface physico-chemical properties, by obtaining a hybrid organo-mineral material to associate the properties of the porous inorganic framework with the chemical reactivity of the organic group[69]. This functionalization can be done during the synthesis, or in post-synthesis.

The table 1.3 shows the most recent studies on functionalized geopolymers.

Table 1.3. Organic–inorganic hybrid geopolymers present in literature.

Inorganic substrate	Organic agent	References
Metakaolin-based geopolymer	(3-Aminopropyl)triethoxysilane (APTES)	[70]
Geopolymer concrete waste	Vinyl trimethoxy silane (VTP) + recycled polypropylene (rPP)	[71]
Metakaolin-based geopolymer	Polypropylene fiber (PP), polyvinyl alcohol fiber (PVA)	[72]

[68] Description P, Identification H, Measures FA, Procedures F. Safety Data Sheet Sodium Silicate Solution Hazard Identification Composition / Information on Ingredients First Aid Measures. :1-4.

[69] Livre blanc : Matériaux Fonctionnels et Fonctionnalisation de Surfaces, Techniques de l'Ingénieur, (2015).

[70] Zhang, C.; Hu, Z.; Zhu, H.; Wang, X.; Gao, J. Effects of silane on reaction process and microstructure of metakaolin-based geopolymer composites. *J. Build. Eng.* **2020**, *32*, 101695.

[71] Ramos FJHTV, da Silva MHP, Monteiro SN, Grafov A, Grafova I. Recycled polypropylene matrix nanocomposites reinforced with silane functionalized geopolymer concrete waste. *J Mater Res Technol*. **2020**;9(4):7540-7550.

[72] Guo L, Wu Y, Xu F, et al. Sulfate resistance of hybrid fiber reinforced metakaolin geopolymer composites. *Compos Part B Eng*. **2020**;183:107689.

Metakaolin-based geopolymer	Unsaturated orthophtalic polyester resin	[73]
Metakaolin-based geopolymer	polyacrylate	[74]
Fly ash- based geopolymer	Oligomeric dimethylsiloxane	[75]
Kaolin-based geopolymer	Methyl-polysiloxane (MK), methyl-phenyl-polysiloxane (H44), tetraethyl-ortho-silicate (TEOS) and 3-amino-propyl-triethoxysilane (APTES)	[76]
Metakaolin-based geopolymer	Polyurethane powders wastes (polyurethane foam and polyisocyanurate foam)	[77]
Metakaolin-based geopolymer	Commercial oligomeric dimethylsiloxane mixture and epoxy resin	[78]
Fly ash-based geopolymer	Organic molecules deriving from the decomposition of rice husk: D-glucose, native cellulose, phenolic compounds and sucrose	[79]

[73] Fiset, J.; Cellier, M.; Vuillaume, P.Y. Macroporous geopolymers designed for facile polymers post-infusion. Cem. Concr. Compos. **2020**, 110, 103591

[74] Chen, X.; Zhou, M.; Ge, X.; Niu, Z.; Guo, Y. Study on the microstructure of metakaolin-based geopolymer enhanced by polyacrylate. *J. Ceram. Soc. Jpn.* **2019**, *127*, 165–172

[75] Roviello, G.; Ricciotti, L.; Molino, A.J.; Menna, C.; Ferone, C.; Cioffi, R.; Tarallo, O. Hybrid Geopolymers from Fly Ash and Polysiloxanes. *Molecules* **2019**, *24*, 3510.

[76] Dos Reis, G.S.; Lima, E.C.; Sampaio, C.H.; Rodembusch, F.S.; Petter, C.O.; Cazacliu, B.G.; Dotto, G.L.; Hidalgo, G.E.N. Novel kaolin/polysiloxane based organic-inorganic hybrid materials: Sol-gel synthesis, characterization and photocatalytic properties. *J. Solid State Chem.* **2018**, *260*, 106–116.

[77] Bergamonti, L.; Taurino, R.; Cattani, L.; Ferretti, D.; Bondioli, F. Lightweight hybrid organic-inorganic geopolymers obtained using polyurethane waste. *Constr. Build. Mater.* **2018**, *185*, 285–292.

[78] Roviello, G.; Menna, C.; Tarallo, O.; Ricciotti, L.; Messina, F.; Ferone, C.; Asprone, D.; Cioffi, R. Lightweight geopolymer-based hybrid materials. *Compos. Part B Eng.* **2017**, *128*, 225–237

[79] Amritphale, S.S.; Mishra, D.; Mudgal, M.; Chouhan, R.K.; Chandra, N. A novel green approach for making hybrid inorganicorganic geopolymeric cementitious material utilizing fly ash and rice husk. *J. Environ. Chem. Eng.* **2016**, *4*, 3856–3865

Metakaolin-based geopolymer	Polyethylene glycol (PEG)	[80]
Metakaolin-based geopolymer + sepiolite	Methylene blue (MB) and methyl red (MR)	[81]
Metakaolin-based geopolymer	Polyethylene (PE)	[82]
Metakaolin-based geopolymer	Commercial epoxy resin	[83]
Metakaolin-based geopolymer	Epoxy resins formed by N,N-diglycidyl-4-glycidyl-oxyaniline with bis-(2-aminoethyl)amine and N,N-diglycidyl-4-glycidyl-oxyaniline with bis-(2-aminoethyl)amine and 2,4-diaminotoluene)	[84]
Metakaolin-based geopolymer	Polyethylene glycol (PEG)	[85]
Kaolin-based geopolymer	Epoxide matrix constituted by bisphenol a diglycidyl ether	[86]

[80] Catauro, M.; Papale, F.; Lamanna, G.; Bollino, F. Geopolymer/PEG Hybrid Materials Synthesis and Investigation of the Polymer Influence on Microstructure and Mechanical Behavior. *Mater. Res.* **2015**, *18*, 698–705.
[81] Ouellet-Plamondon, C.; Aranda, P.; Favier, A.; Habert, G.; van Damme, H.; Ruiz-Hitzky, E. The Maya blue nanostructured material concept applied to colouring geopolymers. *RSC Adv.* **2015**, 5, 98834–98841.
[82] Yuan, X.W.; Easteal, A.J.; Bhattacharyya, D. Geopolymer Reinforced Polyethylene Nanocomposites. *Compos. Technol. For. 2020* **2004**, 796–802
[83] Colangelo, F.; Roviello, G.; Ricciotti, L.; Ferone, C.; Cioffi, R. Preparation and Characterization of New Geopolymer-Epoxy Resin Hybrid Mortars. *Materials* **2013**, *6*, 2989–3006.
[84] Ferone, C.; Roviello, G.; Colangelo, F.; Cioffi, R.; Tarallo, O. Novel hybrid organic-geopolymer materials. *Appl. Clay Sci.* **2013**, *73*, 42–50
[85] Lamanna, G.; Soprano, A.; Bollino, F.; Catauro, M. Mechanical Characterization of Hybrid (Organic-Inorganic) Geopolymers. *Key Eng. Mater.* **2013**, *569–570*, 119–125.
[86] Hussain, M.; Varely, R.; Cheng, Y.B.; Mathys, Z.; Simon, G.P. Synthesis and thermal behavior of inorganic–organic hybrid geopolymer composites. *J. Appl. Polym. Sci.* **2005**, *96*, 112–121.

1.4.1. Starting secondary raw materials

The incorporation of secondary raw materials, such as industrial wastes and by-products, in geopolymer production can yield notable environmental and economic advantages. Environmentally, this practice helps in waste reduction and promotes the conservation of natural resources, resulting in lower carbon emissions and decreased ecological impact. In addition, economically, it can lead to cost savings, create new revenue streams, and contribute to more sustainable resource management practices.

1.4.1.1. Electric Arc Furnace Slag

Electric Arc Furnace slag (DS), also known as black slag or oxidizing slag, is a dark-grey stony by-product of the steelmaking industry that holds significant potential for use in structural concrete (Figure 1.12). EAF slag can be effectively utilized as a coarse aggregate in concrete production due to its favorable physical, chemical, and mineralogical properties. It is obtained after cooling from temperatures of up to 1300 °C to ambient conditions and can be classified as an industrial aggregate suitable for use in structural concrete. EAF slag contains a small proportion of amorphous silicon and a high proportion of iron oxide [87].

Research has shown that concrete made with EAF slag exhibits higher compressive strength and improved mechanical properties compared to concrete made with natural aggregates [88] [89]. Additionally, concrete containing EAF slag exhibits satisfactory durability in aggressive environments, maintaining its mechanical properties over time (Manso et al., 2004). This makes it suitable for high-performance concrete applications, enhancing both its mechanical properties and durability [90] [91].

[87] Mombelli D, Mapelli C, Barella S, Cecca C, Saoût G, Garcia-Diaz E. The effect of microstructure on the leaching behaviour of electric arc furnace (EAF) carbon steel slag. Process Safety and Environmental Protection. **2016**;102:810-821.
[88] Faleschini F, Brunelli K, Zanini M, Dabalà M, Pellegrino C. Electric Arc Furnace Slag as Coarse Recycled Aggregate for Concrete Production. Journal of Sustainable Metallurgy. **2016**;2:44-50.
[89] Faleschini F, Fernández-Ruiz M, Zanini M, Brunelli K, Pellegrino C, Hernández-Montes E. High performance concrete with electric arc furnace slag as aggregate: Mechanical and durability properties. Construction and Building Materials. **2015**;101:113-121.
[90] Abu-eishah SI, El-Dieb A, Bedir MS. Performance of concrete mixtures made with electric arc furnace (EAF) steel slag aggregate produced in the Arabian Gulf region. Construction and Building Materials. **2012**;34:249-256
[91] Kim SW, Lee YJ, Kim KH. Flexural Behavior of Reinforced Concrete Beams with Electric Arc Furnace Slag Aggregates. Journal of Asian Architecture and Building Engineering. **2012**;11:133-138.

Figure 1.12. Electric arc furnace slag as aggregate for concrete production [93].

Its properties generally depend on factors such as the type of steel produced in the furnace, the composition of the scrap used, the method and rate of slag cooling, and weathering processes. There are two main types of EAF slag, depending on the production process mentioned above [92]:

- EAF slag formed with a major content of iron oxides, characterized by low porosity and high density.
- EAF slag formed with lower iron oxide content, resulting in lower density.

According to Euroslag, an international organization focusing on iron and steel slag matters, approximately 25.9 % of steel slags produced in Europe are EAF slags from carbon steel production, while 5.9 % are EAF slags from stainless or high alloy steel production [93].

1.4.1.2. Brick waste

Brick waste is a significant by-product of the construction and demolition industry, comprising largely of leftover bricks from the building process or broken bricks from demolition sites. The accumulation of brick waste poses both economic and environmental challenges, including air and water contamination from dust emissions, alterations in vegetation cover, and a reduction in the economic value of affected sites. Effective management and recycling of brick waste can mitigate these impacts and contribute to sustainable construction practices[94].

Many reports highlight the inadequate management of construction and demolition waste (CDW) in the infrastructure sector, given its substantial contribution to global solid

[92] Euro*slag.Pdf*. https://www.euroslag.com/products/eaf/.
[93] Pellegrino C, Faleschini F, Meyer C. *Recycled Materials in Concrete*. Elsevier LTD; **2019**.

[94] Dubale, M.; Vasić, M. V.; Pathade, G. R.; Kalamdhad, A. S.; Singh, L. B. Utilization of Construction and Demolition Mix Waste in the Fired Brick Production: The Impact on Mechanical Properties. *Materials*. **2022**, *16*, 262

waste (30-40 %) [95]. CDW often consists of up to 80 % brick, mortar, concrete, and ceramic waste [96]. For example, large quantities of clay bricks are produced and accumulate annually during the demolition of old buildings. This situation has economic and environmental consequences, including air and water contamination from dust emissions, alteration of vegetation cover, and a decrease in the economic value of the site [97].

To address this issue, utilizing waste clay bricks in the production of construction materials, such as geopolymer concrete, emerges as an interesting and promising solution. This approach can help mitigate both the environmental problems associated with cement production and the accumulation of waste bricks [98].

The carbonation of certain construction and demolition waste components can facilitate the transformation of hydrated calcium silicates and aluminates into calcium carbonate, as well as amorphous silica/alumina. This conversion process makes these wastes suitable for geopolymer synthesis. Red bricks contain a significant amount of SiO_2 (49.9 %) and Al_2O_3 (16.6 %) [99] [100].

1.4.1.3. Volcanic rock

Scoria is a highly vesicular, dark-colored volcanic rock formed from basaltic or andesitic magma during explosive volcanic eruptions [101] [102]. It is characterized by numerous bubble-like cavities, known as vesicles, which are created by trapped gas bubbles as the lava cools and solidifies quickly in the air. This gives scoria a lightweight and porous texture, making it useful in various applications such as construction, horticulture, and environmental purification. Studies have shown that scoria can

[95] López Ruiz LA, Roca Ramón X, Gassó Domingo S. The circular economy in the construction and demolition waste sector – A review and an integrative model approach. *J Clean Prod*. **2020**;248:119238.
[96] Özalp F, Yilmaz HD, Kara M, Kaya Ö, Şahin A. Effects of recycled aggregates from construction and demolition wastes on mechanical and permeability properties of paving stone, kerb and concrete pipes. *Constr Build Mater*. **2016**;110:17-23.
[97] Atta, I. A.; Bakhoum, E. S. Environmental Feasibility of Recycling Construction and Demolition Waste. *Int. J. Environ. Sci. Technol.* **2023**, *20*, 2553-2564.
[98] Pericot NG, Solar P Del. Optimizing the recycling rate on construction waste: the approach of sustainability tools SEE PROFILE. Published online **2013**.
[99] Dadsetan, S.; Siad, H.; Lachemi, M.; Şahmaran, M. Construction and Demolition Waste in Geopolymer Concrete Technology: A Review. *Magazine of Concrete Research*. **2019**, *71*(22), 1147-1160.
[100] Sikander, B.; Salminen, T. Efflorescence Mitigation in Construction and Demolition Waste (CDW) Based Geopolymer. *Journal of Building Engineering*. **2022**, *48*, 105001.
[101] Best, M.G. (2003). Igneous and Metamorphic Petrology. Wiley-Blackwell.
[102] Scoria." (2018). In *Encyclopaedia Britannica*. Retrieved from britannica.com

effectively replace traditional aggregates in concrete, improving its strength and durability, and can also be used as a cement additive and water purifier [103] [104] .

1.4.2. Functional additives

Functional additives in geopolymer materials play a crucial role in improving their mechanical, chemical, and thermal properties. In the realm of functional additives for geopolymers, three significant categories include sol-gel-based, polymers, and nanofillers additives.

Researchers have explored different types of additives, including silane coupling agents, which reduce mesoporosity and improve mechanical properties and drying resistance [105]. Chemical admixtures like sulfates, selenates, and hydroxycarboxylic acid salts have been shown to improve rheological properties, facilitating uniform mixing and enhancing the transport and finishing capabilities of geopolymer cements[106]. Organic acids and sugars can increase the strength and usability of geopolymers for construction purposes [107] [108]. Additionally, foaming agents have been developed to control and delay foam generation, simplifying the production process[109]. Each of these additives contributes uniquely to the overall functionality and application of geopolymer materials.

1.4.2.1. Sol-gel based

Involve a process where a colloidal solution (sol) transforms into an integrated network (gel). These additives can enhance the homogeneity, mechanical properties and surface properties of geopolymers by providing a more uniform distribution of reactive species, leading to improved bonding and reduced porosity. For example, sol-gel processing can be used to incorporate silicon or aluminum oxides, which improve the thermal stability and mechanical strength of geopolymers[110].

---

[103] Galal, Fares., Abdulrahman, M., Alhozaimy. Assessment of Pozzolanic Activity of Ground Scoria Rocks under Low- and High-Pressure (Autoclave) Steam Curing. Materials, **2022**;15(13):4666-4666

[104] Yin L, Huang Y, Dang Y, Wang Q. Bond of Seawater Scoria Aggregate Concrete to Stainless Reinforcement. *J Renew Mater*. **2023**;11(1):209-231.

[105] Glad BE, Kriven WM. Geopolymer with Hydrogel Characteristics via Silane Coupling Agent Additives. *J Am Ceram Soc*. **2014**;97(1):295-302.

[106] Kinney, Frederick., Patel, Rajeshkumar. Additives for geopolymer cements. (**2020**).

[107] Karthik A, Sudalaimani K, Vijaya Kumar CT. Investigation on mechanical properties of fly ash-ground granulated blast furnace slag based self curing bio-geopolymer concrete. *Constr Build Mater*. **2017**;149:338-349.

[108] Karthik A, Sudalaimani K, Vijayakumar CT, Saravanakumar SS. Effect of bio-additives on physico-chemical properties of fly ash-ground granulated blast furnace slag based self cured geopolymer mortars. *J Hazard Mater*. **2019**;361:56-63.

[109] Glad BE, Kriven WM. Geopolymer with Hydrogel Characteristics via Silane Coupling Agent Additives. Colombo P, ed. *J Am Ceram Soc*. **2014**;97(1):295-302.

[110] Glad BE, Kriven WM. Geopolymer with Hydrogel Characteristics via Silane Coupling Agent Additives. Colombo P, ed. *J Am Ceram Soc*. **2014**;97(1):295-302.

1.4.2.2. Polymeric based

They can be incorporated into the geopolymer matrix to enhance its performance such as flexibility, durability, toughness, and water resistance. For example, polyvinyl alcohol (PVA) or acrylate-functional silane coupling agents work by creating polymer networks within the geopolymer matrix, which can absorb stress and prevent crack propagation. For instance, the addition of silane coupling agents has been shown to reduce mesoporosity and enhance drying resistance, thereby improving the overall durability of the geopolymer[111] [112].

1.4.2.3. Nanofiller

Nanofillers are used to improve the microstructural properties of geopolymers, providing benefits such as increased strength, durability, and reduced environmental impact[113]. Nano-silica, nano-titania, or carbon nanotubes are used to improve the mechanical properties and durability of geopolymers at a microstructural level. These nanomaterials can fill the microvoids within the geopolymer matrix, leading to increased density and strength. Additionally, nanofillers can enhance the thermal and electrical properties of geopolymers, making them suitable for advanced engineering applications. For example, nano-silica has been found to significantly increase the compressive strength and reduce the permeability of geopolymer composites[114] [115].

1.5. Advantages and disadvantages of geopolymer materials

Geopolymer materials are an emerging material in the construction industry, known for their environmental benefits and superior mechanical properties. However, they also have several disadvantages:

Benefits:

- Low Carbon Footprint: Geopolymers can significantly reduce CO_2 emissions compared to traditional Portland cement, contributing to sustainability [116].

---

[111] Chang L, Wang H, Xie Y, et al. Enhancement of mechanical properties and microstructure of geopolymers using polyvinyl alcohol (PVA) fibers. Constr Build Mater. **2018**;163:395-405.
[112] Glad BE, Kriven WM. Geopolymer with hydrogel characteristics via silane coupling agent additives. J Am Ceram Soc. **2014**;97(1):1-9.
[113] Valente M, Sambucci M, Sibai A. Geopolymers vs. Cement Matrix Materials: How Nanofiller Can Help a Sustainability Approach for Smart Construction Applications—A Review. Nanomaterials. **2021**;11(8):2007.
[114] Provis JL, Lukey GC, Van Deventer JS. Do geopolymers actually contain nanocrystalline zeolites? A reexamination of existing results. Chem Mater. **2005**;17(12):3075-3085
[115] Fernández-Jiménez A, Palomo A. Nanostructure/microstructure of fly ash geopolymers. In: Provis JL, Van Deventer JSJ, eds. Geopolymers: Structures, Processing, Properties and Industrial Applications. Woodhead Publishing; **2009**:185-207.
[116] Duxson P, Provis JL, Lukey GC, Van Deventer JS. The role of inorganic polymer technology in the development of 'green concrete'. Cem Concr Res. **2007**;37(12):1590-1597.

- High Thermal Stability: They exhibit excellent thermal resistance, making them suitable for high-temperature applications [117].
- Excellent Mechanical Properties: Geopolymers often display high compressive and tensile strength, enhancing their durability and structural integrity [118].
- Chemical Resistance: They are highly resistant to chemical attacks, including acids and sulfates, which extends their lifespan in harsh environments [119].
- Utilization of Industrial Waste: Geopolymers can incorporate industrial by-products like fly ash and blast furnace slag, promoting waste recycling and reducing landfill usage [120].
- Fire Resistance: Due to their inorganic nature, geopolymers have superior fire resistance compared to conventional concrete [121].

Disadvantages:

- High Costs of Starting Materials: The raw materials and alkali activators used in geopolymer production can be more expensive than those for traditional cement[122].
- Limited Long-Term Durability Data: There is a lack of comprehensive long-term durability studies, which creates uncertainty about their performance over time[123].
- Low Workability: Geopolymer mixtures often have lower workability, requiring the use of plasticizers and other admixtures to improve handling and placement [116].
- Heat Treatment Requirements: Many geopolymer formulations require heat curing to achieve optimal mechanical properties, complicating on-site applications [118].
- Specialized Knowledge and Handling: The production and application of geopolymers require specialized knowledge and handling techniques, which can limit widespread adoption [124].

[117] Provis JL, Bernal SA. Geopolymers and Related Alkali-Activated Materials. Annu Rev Mater Res. **2014**;44:299-327.
[118] Zhang Z, Provis JL, Reid A, Wang H. Geopolymer foam concrete: An emerging material for sustainable construction. Constr Build Mater. **2014**;56:113-127.
[119] Davidovits J. Geopolymer Chemistry and Applications. 4th ed. Geopolymer Institute; **2008**.
[120] Mehta A, Siddique R. An overview of geopolymers derived from industrial by-products. Constr Build Mater. **2016**;127:183-198.
[121] Arioz O, Kilinc K, Arioz E, Tuncan A, Tuncan M. Elevated temperature effects on properties of fly ash based geopolymer. Procedia Eng. **2012**;42:646-655.
[122] Singh B, Ishwarya G, Gupta M, Bhattacharyya SK. Geopolymer concrete: A review of some recent developments. Constr Build Mater. **2015**;85:78-90.
[123] Komnitsas K, Zaharaki D. Geopolymerisation: A review and prospects for the minerals industry. Miner Eng. **2007**;20(14):1261-1277.
[124] Xu H, Van Deventer JS. The geopolymerisation of alumino-silicate minerals. Int J Miner Process. **2000**;59(3):247-266.

- Variability in Raw Materials: The properties of geopolymers can vary significantly depending on the source and composition of the raw materials used, leading to inconsistencies [125].

1.6. Applications of geopolymer concrete

Geopolymers are finding increasing applications, including in archaeology and the removal of certain toxic chemicals. However, they are rarely used by civil engineers globally due to limited information about their durability, low workability, the need for large quantities of admixtures to slow their setting, and the challenges related to on-site manufacturing, which requires heat treatment for acceptable mechanical performance.

The table 1.4 below summarizes the applications of geopolymer materials.

Table 1.4. Applications of geopolymers.

Area	Applications	Ref.
Repair Materials	Concrete patching materials; waterproof, hydrophobic, fast-curing, high-strength geopolymer repair material	[126]
Marine Constructions	Chemical resistance for marine environments; anti-corrosive coatings	[127]
Pavement Base Materials	Sustainable pavement materials; reduced CO_2 emissions; improved durability	[128]
3D Printing Materials	Geopolymer formulations for 3D printing; improved mechanical properties and stability	[129]
Functional Applications	Fire-resistant materials; high-temperature materials	[130]

[125] Rangan BV. Fly ash-based geopolymer concrete. In: Concrete Construction Engineering Handbook. 2nd ed. CRC Press; **2008**:1-23.
[126] Yodsudjai W, Phoo-ngernkham T, Wazien A, Duan P, Robayo-Salazar RA, Kuo W, Zailani WN. Geopolymer mortars as a substitute for concrete repair engineering. Constr Build Mater. **2010.**
[127] Bondar D, Hassan A, Reddy BJ, Zhang Y, Chindaprasirt P, Chalee W, Pasupathy K, Alzeebaree R, Nuaklong P. Geopolymer concrete for marine constructions. Constr Build Mater. **2012**.
[128] rovis JL, Deventer JS, Shi C, Roy DM, Hoy M, Phummiphan I, Sun W, Rosyidi SA. Geopolymers for pavement base materials. Constr Build Mater. **2014**.
[129] Panda B, Xia M, Nematollahi B, Bong S, Ma GW, Thang N. Geopolymer materials for 3D printing. Constr Build Mater. **2017**.
[130] Cheng TW, Chiu JP, Shuai S, Tchakoute HK, Thang N, Nuaklong P, Masi A, Wang Y, Zhao H, Rickard WDA, Lahoti M. Functional applications of geopolymer materials. Constr Build Mater. **2003**.

Wastewater Treatment	Adsorption, degradation, filtration, and solidification/stabilization of pollutants from water	[131]
Others	Paints, Coatings, Adhesive	[132]

Based on the previous studies, the development of geopolymers focuses on four main areas as detailed in Figure 1.13:

- Developing processes and products using high-temperature processing.
- Geopolymerization at ambient temperatures.
- Preprocessing raw materials.
- Hybrid geopolymer materials.

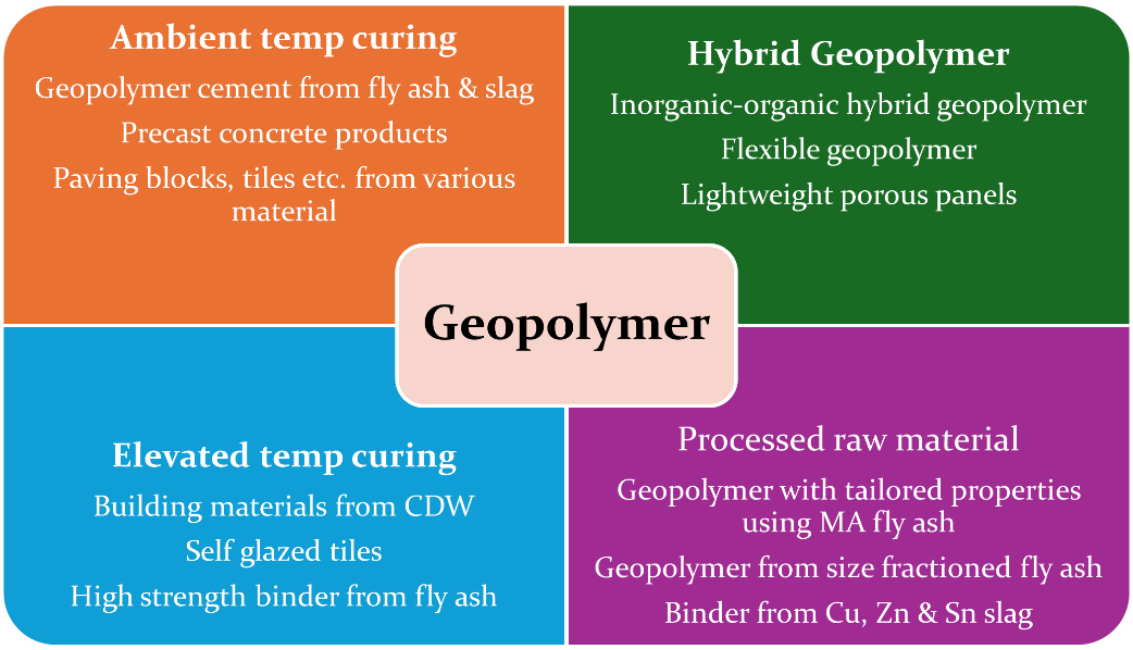

Figure 1.13. Geopolymer research activities [48].

[131] Al-Zubaid ZY, Mosa J, Kareem M, Dulaimi A. Geopolymers as sustainable eco-friendly materials: Classification, synthesis routes, and applications in wastewater treatment. Environ Technol Innov. **2021**;24:102267.
[132] Łach M, Róg G, Ochman K, Pławecka K, Bąk A, Korniejenko K. Assessment of Adhesion of Geopolymer and Varnished Coatings by the Pull-Off Method. *Eng*. **2022**;3(1):42-59.

1.7. Aim of the PhD thesis

This PhD thesis aims to explore the socio-economic implications of utilizing new building materials called "geopolymers," which are synthesized from local industrial by-products and natural raw materials. The focus of this research is on Electric Arc Furnace Slag and Brick Waste as industrial by-products, while also incorporating other materials such as clay, metakaolin, and volcanic rock. These materials are investigated for their potential to reduce production costs, air pollution, and the carbon footprint associated with traditional building materials. The overarching goal is to propose ecologically sound and sustainable building materials suitable for human habitation.

The primary objective of this PhD thesis is to synthesize and evaluate geopolymers made from a combination of industrial by-products (Electric Arc Furnace Slag and Brick Waste) and naturally materials (clay, metakaolin, and volcanic rock). The research focuses on assessing the physicochemical, mechanical, and environmental properties of the resulting geopolymers, with the goal of developing low-carbon binders for sustainable construction.

The specific objectives of this research are to: 1) conduct a detailed characterization of raw materials, including their chemical composition, physical properties, and mineralogy, to assess their suitability for geopolymer synthesis; (2) develop experimental protocols for synthesizing geopolymers using both treated and untreated precursors, while analyzing the influence of activation solutions and organic modifiers on the final material properties; (3) evaluate the compressive strength and water absorption of the synthesized geopolymers over different curing periods; (4) optimize the geopolymer formulation by exploring the effects of combining different raw materials, activation solutions, and curing conditions to enhance both mechanical performance and environmental sustainability; and (5) finally, perform a life cycle assessment (LCA) after the experimental phase to compare the environmental and economic benefits of geopolymers relative to traditional cementitious materials, with a focus on reducing the carbon footprint in construction.

By focusing on these materials, the research aims to shift civil engineering practices towards developing low-carbon binders. While previous studies have focused on using metakaolin or fly ash in geopolymer production, this research explores the potential of other industrial by-products, such as Electric Arc Furnace Slag and Brick Waste, which are currently underutilized.

1.8. Thesis overview

This thesis is structured into six chapters, each addressing a different aspect of geopolymeric materials, hybrid geopolymers, and their applications. The following provides an overview based on the detailed table of contents.

Introduction: This chapter provides a comprehensive introduction to geopolymeric materials, comparing them with Ordinary Portland Cement (OPC) concrete. It covers the composition, properties, sources, activating solutions, applications, and benefits of geopolymers. The chapter also discusses hybrid and sustainable functional geopolymeric materials, detailing the use of secondary raw materials like Electric Arc Furnace Slag, brick waste, and slag. It further explores functional additives, including sol-gel-based, polymeric-based, and nanofillers, and their roles in enhancing the properties of geopolymers. Additionally, the chapter covers the advantages, disadvantages and applications of geopolymer concrete and introduces the concept of Life Cycle Assessment (LCA) in the context of this study.

Geopolymeric Materials: This chapter discusses the choice of best-performing raw materials and their characterization before and after treatment. It includes physicochemical, mineralogical, geotechnical, physical, and mechanical properties, as well as synthetic procedures and conditions for geopolymer materials. It also covers the development of geopolymeric blended materials.

Functional Hybrid Geopolymer Materials: This chapter focuses on the development and testing of functional hybrid geopolymer materials. It details the integration of functional additives and their impact on the properties of geopolymers.

Life Cycle Assessment: This chapter explores the Life Cycle Assessment (LCA) of building materials, emphasizing sustainable development and eco-construction. It details the methodology of LCA, including goal and scope, inventory analysis, impact assessment, and interpretation. The chapter also will examine the LCA of geopolymers, covering raw materials, energy, transport, manufacturing, usage, and end-of-life stages.

Conclusions and Final Remarks: This chapter summarizes the key findings of the thesis, highlighting the overall contributions to the field of geopolymeric materials and sustainable construction. It also outlines potential future research directions.

Materials and Methods: This chapter will present the materials, methods, and the various characterization techniques employed in this thesis. It will describe the principles of operation, manipulation, and preparation of the samples.

CHAPTER 2

GEOPOLYMERIC MATERIALS

This chapter explores the synthesis, characterization, and performance evaluation of various geopolymeric materials derived from different local Sicilian raw materials: Electric Arc Furnace Slag (DS), clay, brick waste (BW), kaolin (K), and volcanic rock (slag). The chapter begins with the selection and detailed characterization of these raw materials that are evaluated for their chemical composition, physical properties, and suitability for geopolymer synthesis. The primary focus is on identifying the optimal raw material that enhances the final properties of geopolymers. Mechanical test, X-Ray Diffraction (XRD), Fourier-Transform Infrared Spectroscopy (FTIR) and Scanning Electron Microscopy (SEM) are employed to investigate the structural and compositional attributes of the selected geopolymers.

2.1. Abstract

This study investigates the suitability of five Sicilian raw materials including electric arc furnace slag (DS), clay, brick waste (BW), kaolin (K), and volcanic rock (slag) for geopolymer synthesis. These industrial and by-products raw materials were utilized to prepare various geopolymer pastes, with the aim of evaluating their suitability for sustainable construction applications. To achieve this, a series of experiments were performed to analyze both the starting materials and the prepared geopolymer samples. The general experimental process, including the preparation and analysis of geopolymer samples, followed these steps:

1. Selecting the starting materials;
2. Specimen preparation;
3. Analyzing and determining the optimal conditions;
4. Preparation of geopolymer paste under the optimized conditions.

Therefore, the raw materials were analyzed using various techniques to characterize their chemical and physical properties. Clay and kaolin (K) were thermally treated to enhance their reactivity, resulting in calcined clay (C-Clay) and metakaolin (MK_T), respectively. Additionally, these materials (C-Clay, MK_T and DS) were ground, and the ground electric arc furnace slag referred to as DS_g. Geopolymer pastes were then prepared by activating these materials with sodium hydroxide solutions at different concentrations (6 M and 8 M) and curing them at different temperatures (25 °C and 85 °C). The study also explored the development of a geopolymeric mixture by combining different precursors in equal proportions. Based on our research findings, we selected C-Clay and DS_g mixture for further investigation. This mixture was activated using both an "alkaline activator liquid" (A.A.L) and an "alkaline activator powder" (A.A.P) to characterize the produced geopolymer (Figure 2.1). Hence, the results indicate that C-Clay and DS_g mixtures activated with A.A.L show strong potential for producing high-performance geopolymers.

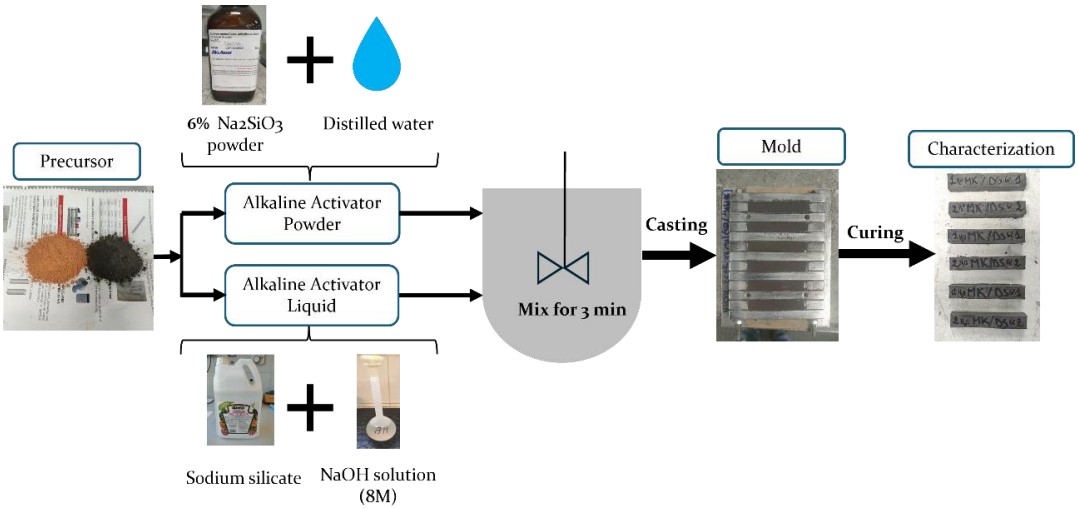

Figure 2.1. Graphical representation of C-Clay and DS_g geopolymer preparation.

2.2. Results and discussion

2.2.1. Choosing the best performing raw materials and characterization

The selection of raw materials for geopolymer synthesis is critical in determining the final properties of the resulting geopolymer material. The present study evaluated five Sicilian raw materials (figure 2.2), including electric arc furnace slag (DS), clay, brick waste (BW), kaolin (K), and volcanic rock (slag).

Figure 2.2. Starting materials: (a) DS, (b) clay, (c) BW, (d) K and (e) Slag.

2.2.1.1. Chemical, physical and grain size analysis

The chemical and physical properties of the raw materials (DS, clay, BW, K, and slag) were analyzed to assess their suitability for geopolymer synthesis. X-ray fluorescence (XRF) results presented in Table 2.1 revealed that DS is rich in CaO (35.28 %) and Fe_2O_3 (29.32 %), while clay contains high amounts of SiO_2 (40.07 %) and CaO (16.62 %), and BW predominantly consists of SiO_2 (61.83 %) and Al_2O_3 (17.39 %). K is mainly composed of SiO_2 (51.97 %) and Al_2O_3 (40.70 %), with minimal impurities, and volcanic rock has significant levels of CaO (45.08 %) and Fe_2O_3 (11.93 %). The data of particle size under 63 µm and 45 µm are presented in Table 2.1., moisture content and loss on ignition of all raw materials were provided in Chapter 6 (Table 6.4 and Table 6.5). DS, with its coarse granulated structure, had 31.4 % and 26.4 % of particles passing through 63 µm and 45 µm mesh sizes, respectively, with a moisture content of 0.1263 % and a loss on ignition (LOI) of 0.31 %. Clay had a finer particle, 80 % and 77.3 % of particles passing through 63 µm and 45 µm sieves, and a moisture content of 1.0790 % with an LOI of 16.74 %. BW, also fine-grained, had 95.8 % and 89 % of particles passing through 63 µm and 45 µm, with a moisture content of 0.0636 % and an LOI of 1.26 %. K displayed ultra-fine particles, with 98 % and 91 % passing through 63 µm and 45 µm mesh sizes, a moisture content of 0.1482 %, and an LOI of 3.29 %. Volcanic rock had also fine particles, with 80.9 % and 70.3 % passing through 63 µm and 45 µm, with a moisture content of 0.2654 % and an LOI of 4.33 %. The finer particle size of clay, BW, K, and volcanic rock suggests a higher reactivity due to their larger surface areas, potentially enhancing the geopolymerization process and improving the final properties of the geopolymer materials.

Table 2.1. Chemical composition (% by mass) and particle size under 63 μm and 45μm of all of raw materials.

	DS	Clay	BW	K	volcanic rock (slag)
SiO_2	13.18	40.07	61.83	51.97	18.48
Al_2O_3	10.35	12.36	17.39	40.70	4.83
Fe_2O_3	29.32	7.45	5.78	1.40	11.93
CaO	35.28	16.62	5.41	0.16	45.08
MgO	3.21	1.91	1.46	0.27	7.98
Cr_2O_3	1.51	0.02	0.02	/	0.28
Na_2O	0.35	0.62	2	/	0.28
K_2O	0.07	2.56	3.3	1.46	0.09
TiO_2	0.68	0.88	0.67	0.52	0.38
MnO	4.34	0.15	0.09	/	4.87
Other	1.4	0.62	0.79	0.29	1.47
LOI	0.31	16.74	1.26	3.23	4.33

Mesh size		
	< 63 μm (%)	< 45 μm (%)
DS	31.4	26.4
Clay	80	77.3
BW	95.8	89
K	98	91
volcanic rock (slag)	80.9	70.3

The ternary diagram in Figure 2.3 shows the major elemental compositions of the raw materials. It represents how these materials are distributed based on their silicon dioxide (SiO_2), alumina (Al_2O_3), and calcium oxide (CaO) contents. DS is positioned near the CaO corner, indicating its high calcium content. Clay is situated between the Al_2O_3 and CaO axes, reflecting its balanced composition of alumina and calcium. BW has very high silica content, being closest to the SiO_2 corner. K has high alumina content, located near the Al_2O_3 corner. The slag has the highest calcium oxide content.

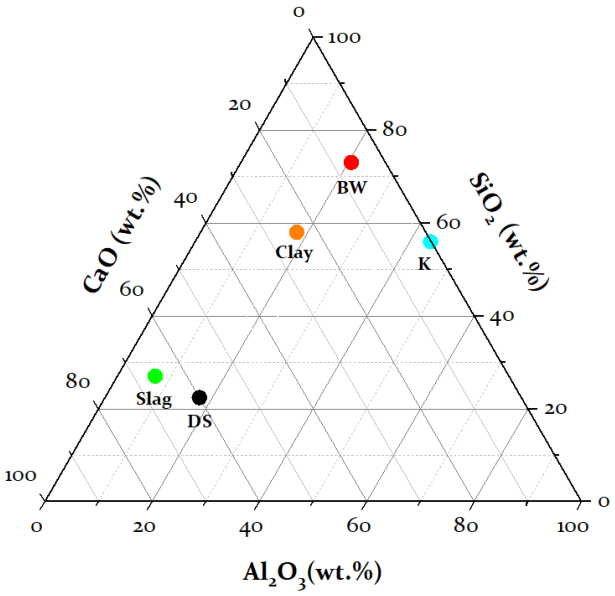

Figure 2.3. The SiO_2-Al_2O_3-CaO ternary diagram of raw materials.

2.2.1.2. X-ray diffraction (XRD)

X-ray diffraction (XRD) diffractograms were recorded for the raw materials to analyze their crystalline structure (Figure 2.4). The chemical composition of the DS is approximately 78 % iron, calcium, and silicon oxides. The XRD patterns of the DS (Figure 2.4 a) indicates the presence of multiple crystalline phases. The primary crystalline phases identified include wüstite (FeO), larnite (Ca_2SiO_4), magnetite (Fe_3O_4), and gehlenite. Additionally, the presence of calcite ($CaCO_3$), quartz (SiO_2), and magnesite ($MgCO_3$) was detected in the sample. These mineral components align with the typical composition of Electric Arc Furnace slag (EAF), corroborating findings reported in several research studies [1, 2, 3]. The presence of these phases indicates the potential for diverse applications of EAF slag in construction materials, particularly in the formulation of geopolymers and other cementitious products. The clay (Figure 2.4 b) indicates that the main crystalline phases contained are Quartz (SiO_2), Calcite ($CaCO_3$), and Muscovite. Other phases present include Cristobalite, Lawsonite, and Garronite. Quartz is a common mineral in clay, contributing to its mechanical strength and thermal stability [4]. The X-ray diffraction (XRD) analysis of kaolin (K) powder (Figure 2.4 c) reveals the presence of both crystalline and amorphous phases. The major crystalline phases identified are quartz (SiO_2), mullite

[1] Rashad AM, Khafaga SA, Gharieb M. Valorization of fly ash as an additive for electric arc furnace slag geopolymer cement. *Constr Build Mater*. **2021**;294:123570.

[2] Menad N, Kana N, Kanari N, Pereira F, Seron A. Process for Enhancing the Valuable Metal Recovery from "Electric Arc Furnace" (EAF) Slags. *Waste and Biomass Valorization*. **2021**;12(9):5187-5200.

[3] Teo P Ter, Zakaria SK, Salleh SZ, et al. Assessment of Electric Arc Furnace (EAF) Steel Slag Waste's Recycling Options into Value Added Green Products: A Review. Met **2020**, Vol 10, Page 1347. **2020**;10(10):1347.

[4] Pan X, Li S, Li Y, Guo P, Zhao X, Cai Y. Resource, characteristic, purification and application of quartz: a review. *Miner Eng*. **2022**;183:107600.

($Al_4Si_2O_{10}$), and kaolinite ($Al_2Si_2O_5(OH)_4$). Mullite enhances its thermal stability and refractory properties [5]. Although kaolinite retains its crystalline structure, its inherent properties, such as reactivity and pozzolanic potential [6]. Additionally, the diffraction peaks around 2θ = 8.87, 17.75° and 27° 2θ are assigned to illite based on the chemical composition of the samples.

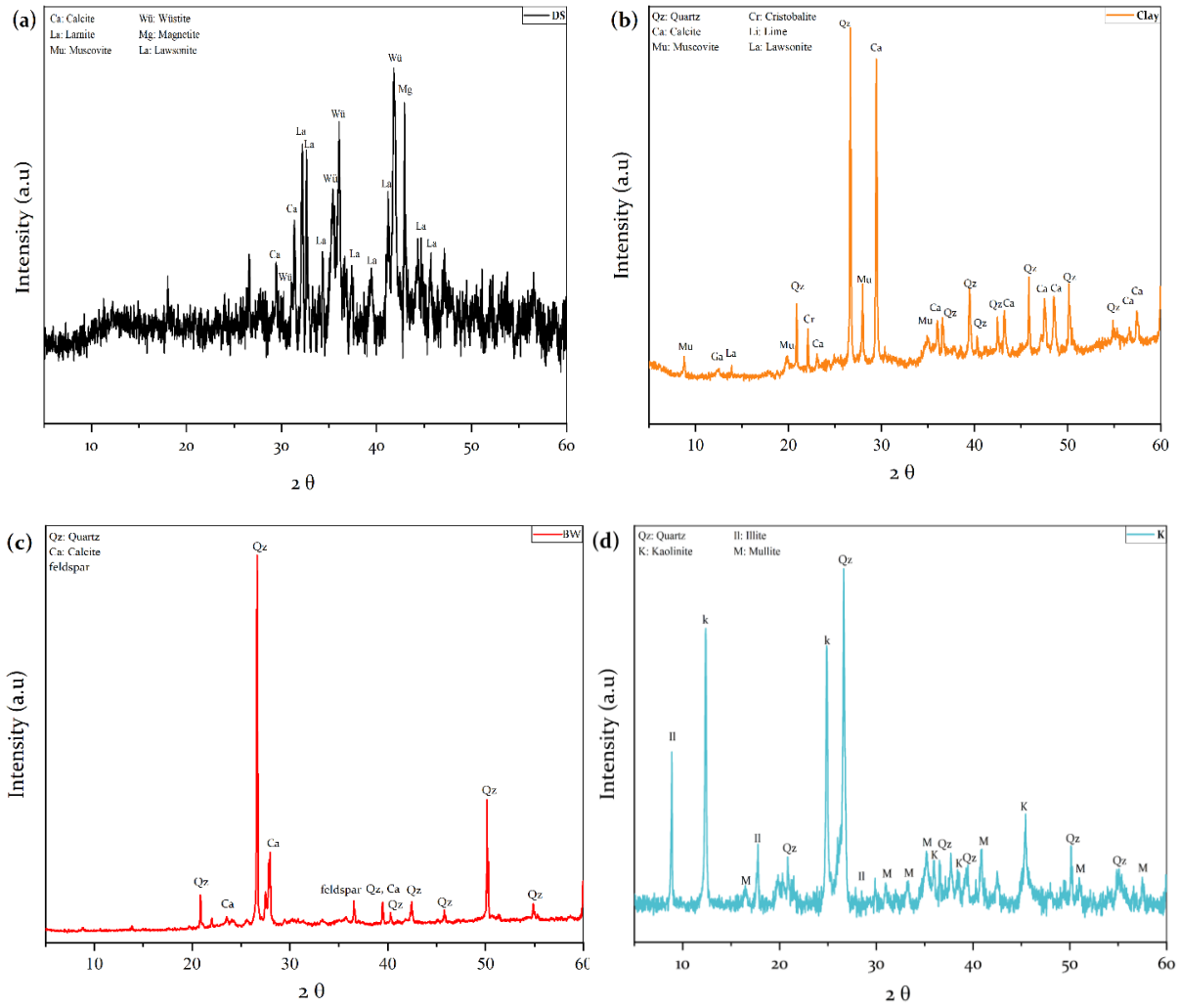

[5] Lima LKS, Silva KR, Menezes RR, Santana LNL, Lira HL. Mullite: a review microstructural characteristics, properties, synthesis and applications of m. *Cerâmica*. **2022**;68(385):126-142.

[6] Moya JS, Cabal B, Lopez-Esteban S, Bartolomé JF, Sanz J. Significance of the formation of pentahedral aluminum in the reactivity of calcined kaolin/metakaolin and its applications. *Ceram Int*. **2024**;50(1):1329-1340.

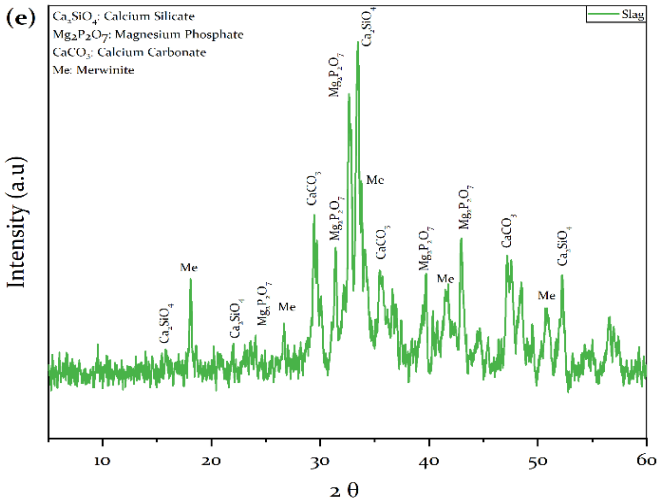

Figure 2.4. XRD patterns of raw materials (a) DS; (b) clay; (c) BW; (d) K and (e) volcanic rock (slag).

The XRD diffractogram patterns of the brick waste (BW) powder (Figure 2.4 d) show that quartz (SiO_2) is the major phase, with well-defined peaks observed at 26.7° and 50.2°. Additionally, the presence of feldspar minerals is identified in the BW sample. Variations in peak intensity reflect changes in the degree of crystallinity, where higher intensity indicates greater crystallinity of the compound [7].

The XRD pattern of the volcanic rock (slag) (Figure 2.4 e) displays broad halos, indicating an amorphous structure with poor to moderate crystal formation. The analysis confirms that the slag sample contains a high content of calcite ($CaCO_3$), merwinite ($Ca_{12}Mg_4Si_8O_{32}$), and magnesium phosphate ($Mg_2O_7P_2$).

2.2.1.3. Enhancing the reactivity of the raw materials: thermal and grinding treatments

Based on the characterization results of the raw materials, DS, Kaolin, and clay were selected for further treatment to enhance their reactivity and improve their performance in geopolymer synthesis. In general, thermal and mechanical treatments are commonly used techniques to enhance the reactivity of precursors. The calcination process is intended to transform crystalline phases into more reactive amorphous phases, which enhances the material's pozzolanic properties. The calcination conditions (temperature and duration) are crucial, as excessive calcination can lead to the formation of non-reactive crystalline phases. During this process, chemically bound water is removed, and the structure of the material undergoes significant changes. When optimized, calcination increases the amount of amorphous content, thereby enhancing the reactivity, which resulting in stronger geopolymer bonds[8].

[7] Taweetamnusin D, Narasingha M, Panasupamassadu K, et al. Analysis of chemical-mineralogical content of brick waste as a pozzolan substitute material in blended cement. *IOP Conf Ser Earth Environ Sci*. **2024**;1312(1):012047.

[8] Shinkafi AB. Mechanical Properties and Internal Mechanisms Characterization of Calcined Clay Geopolymer Concrete.; 2020. https://pure.coventry.ac.uk/ws/portalfiles/portal/43077553/Shinkafi2020.pdf

2.2.1.3.1. Thermal treatments

For both Clay and Kaolin, thermal treatment was employed to enhance their reactivity. This process, typically performed at temperatures between 600-800 °C, dehydrates the kaolinite and disrupts its crystalline structure, converting it into a highly reactive amorphous aluminosilicate [9]. Clay and Kaolin were calcined at 750 °C for 3 hours using a laboratory muffle furnace (SATER). The temperature was chosen based on TGA results and literature [10].

The thermal analysis of the untreated clay and kaolin samples is shown in Figure 2.5. In the DTG curves of the clay sample (Figure 2.5 a), three major peaks are observed. The first peak around 47°C is attributed to the dehydration of adsorbed water and the water molecules contained in the clay[11]. The second peak at a temperature of ≈ 486°C, is due to the dehydroxylation reactions of kaolinite and illite/muscovite[12]. The third peak observed at 710 °C is related to decarbonization, which corresponds to releasing CO_2 upon the decomposition of calcite[13]. From the DTG curves shown in Figure 2.5 (b), the exothermic peak at 512.61°C is due to dehydroxylation of the kaolinite present in the kaolin[8]. K shows more thermal stability compared to clay (weight loss of K around 3.57 % while clay 16.96 %).

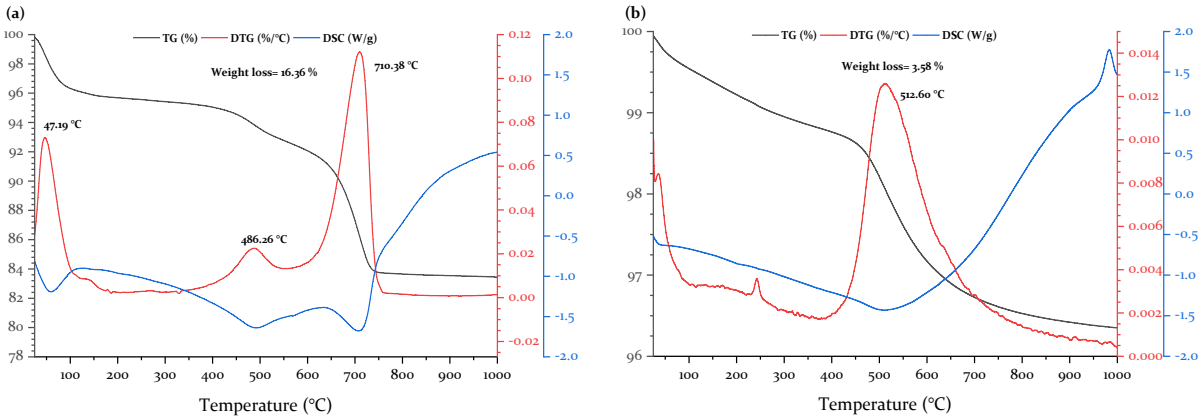

Figure 2.5. TG/DTG/DSC curves of (a) clay and (b) K before thermal treatment.

The thermally treated clay will be referred to as calcined clay (C-Clay), while the thermally treated kaolin will be indicated hereafter as metakaolin (MK_T).

[9] Balczár I, Korim T, Kovács A, Makó E. Mechanochemical and thermal activation of kaolin for manufacturing geopolymer mortars – Comparative study. *Ceram Int*. 2016;42(14):15367-15375.
[10] Uchima JS, Restrepo OJ, Tobón JI. Pozzolanicity of the material obtained in the simultaneous calcination of biomass and kaolinitic clay. *Constr Build Mater*. **2015**;95:414-420.
[11] Heller-Kallai L. Chapter 7.2 Thermally Modified Clay Minerals. *Dev Clay Sci*. **2006**;1(C):289-308.
[12] Gualtieri A, Bellotto M. Modelling the structure of the metastable phases in the reaction sequence kaolinite-mullite by X-ray scattering experiments. *Phys Chem Miner*. **1998**;25(6):442-452.
[13] Mohammed S, Elhem G, Mekki B. Valorization of pozzolanicity of Algerian clay: Optimization of the heat treatment and mechanical characteristics of the involved cement mortars. *Appl Clay Sci*. **2016**;132-133:711-721.

2.2.1.3.2. Mechanical treatments

Mechanical treatment, such as grinding, was employed to reduce the particle size and increase the surface area of DS. After the thermal treatment, MK_T and C-Clay were also ground into a fine powder using a laboratory ball mill under ambient conditions to ensure the destruction of any small aggregates that may have formed during calcination. As shown in Figure 2.6, more than 80 % of the treated sample particles (DS and C-Clay) are smaller than 30 µm while MK_T particles are less than 40 µm. Additionally, the $D_v(50)$ values for C-Clay, MK_T and DS are 5.65 µm, 15.2 µm and 5.63 µm, respectively. For brick waste (BW), no mechanical treatment was performed, and the $D_v(50)$ value was found to be 6.41 µm. These results demonstrate the effectiveness of the treatment in reducing the particle size of C-Clay, MK_T and DS powders.

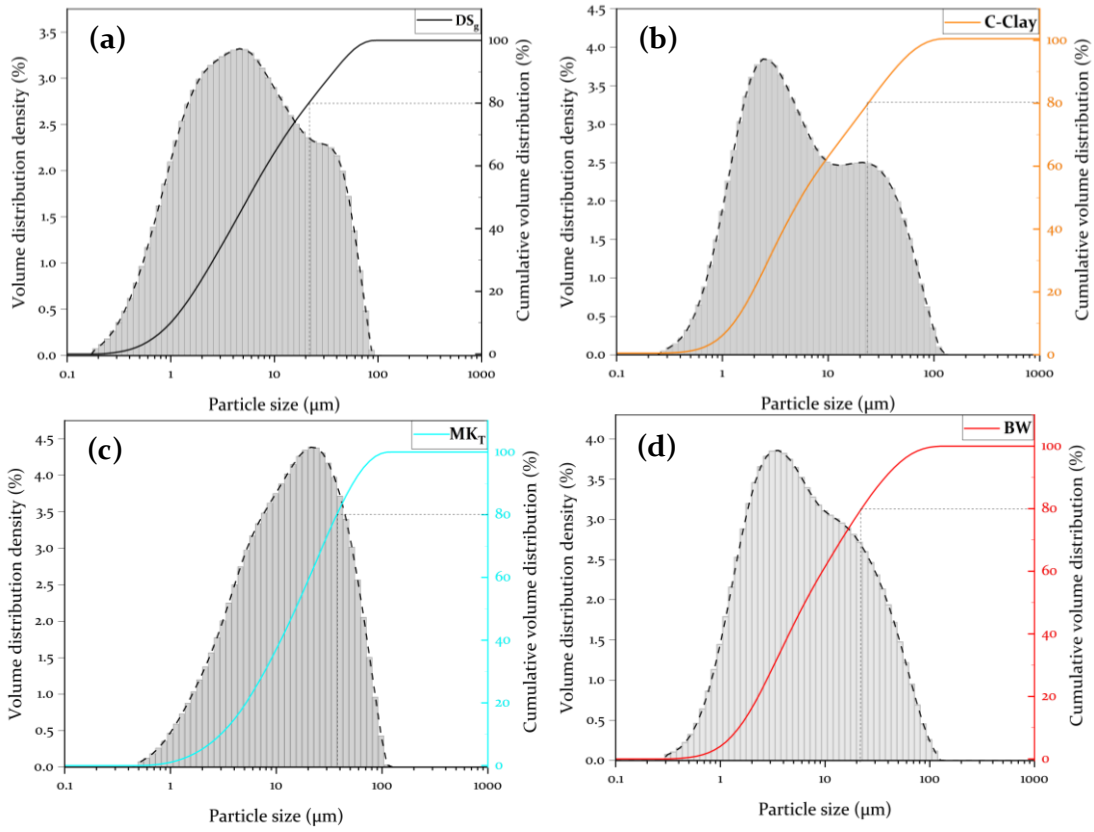

Figure 2.6. Particle size distribution of the (a) DS_g, (b) C-Clay, (c) MK_T, and (d) BW samples.

After the mechanical treatment, the Electric Arc Furnace Slag will be referred to as DS_g.

2.2.2. Synthetic procedures for best-performing geopolymers

Large quantities of geopolymer pastes were prepared in the laboratory using different NaOH solution concentration (4 M, 6 M, and 8 M) and cured at various temperatures (room temperature, 65 °C, and 85 °C). Based on the compressive strength results of the final geopolymers, the following synthetic procedures were selected for the preparation of best-performing geopolymers.

2.2.2.1. Compressive strength of raw material-based geopolymers

Table 2.2 present the compressive strength data of geopolymer paste made from volcanic rock, DS, DS_g, K, MK_T, Clay, C-Clay, and BW under different conditions (23 °C, 6 M NaOH; 85 °C, 8 M NaOH) over different curing periods (2 days, 7 days, and 28 days). The results show that the compressive strength improves with longer curing time. At 28 days, DS_g and C-Clay have the highest compressive strengths.

Table 2.2. Compressive strength results of geopolymer pastes (MPa) at 2, 7, and 28 days.

Geopolymers	Curing		
	2 days	7 days	28 days
Volcanic rock	1.3 ± 0.18	2.56 ± 0.41	8.73 ± 0.91
DS	3.46 ± 0.42	11.78 ± 1.68	17.75 ± 1.59
DS_g	7.74 ± 0.43	16.35 ± 0.80	27.33 ± 0.47
K	14.91 ± 1.03	14.97 ± 1.34	14.96 ± 0.86
MK_T	18.97 ± 0.88	22.46 ± 0.11	26.29 ± 1.22
Clay	2.33 ± 0.28	2.95 ± 0.12	3.16 ± 0.53
C-Clay	28.97 ± 1.43	34.67 ± 1.34	41 ± 0.85
BW	14.13 ± 1.18	15.12 ± 1.62	17.92 ± 0.62

The compressive strength of volcanic rock-based geopolymers cured at room temperature with 6 M NaOH shows a slight improvement over 28 days. The strength increases from 1.3 MPa after 2 days to 8.73 MPa at 28 days. However, further thermal and/or mechanical treatments of slag can enhance its reactivity, leading to better mechanical properties in slag-based geopolymers.

The compressive strength of DS significantly improved after the mechanical treatment (grinding). The compressive strength of DS_g increased from approximately 8 MPa at 2 days to around 28 MPa at 28 days. This represents a significant improvement compared to the untreated DS, which showed an increase from about 3.5 MPa at 2 days to 18 MPa at 28 days. The improvement in strength is due to the grinding process which increases the surface area and reactivity of the material, which promotes better geopolymerization.

Kaolin (K) exhibited lower compressive strength values, starting at approximately 14.91 MPa at 2 days and remaining relatively stable, reaching around 14.96 MPa at 28 days. In contrast, MK_T demonstrated a consistent development in compressive strength, starting with a higher initial strength of around 19 MPa at 2 days and increasing to 26 MPa at 28 days. The thermal treatment enhances the reactivity of K by promoting further dehydroxylation and structural changes, leading to improved geopolymerization and higher strength development.

Untreated clay shows low initial compressive strength, starting at 2.33 MPa at 2 days, with minimal improvement over time, reaching only 3.15 MPa at 28 days. This indicates

that untreated clay has limited reactivity and poor geopolymerization potential. In contrast, calcined clay (C-Clay) exhibits a remarkable increase in compressive strength. C-Clay starts at approximately 29 MPa at 2 days and reaches over 41 MPa at 28 days, showcasing its enhanced reactivity and significantly improved strength.

BW exhibited substantial early strength, achieving around 14 MPa in 2 days, which increased to 15.12 MPa by 7 days. Over 28 days, the compressive strength reached 17.92 MPa, representing a 26.81 % increase from 2 days and an 18.47 % increase from 7 days. This indicates significant progress in the geopolymerization process over time.

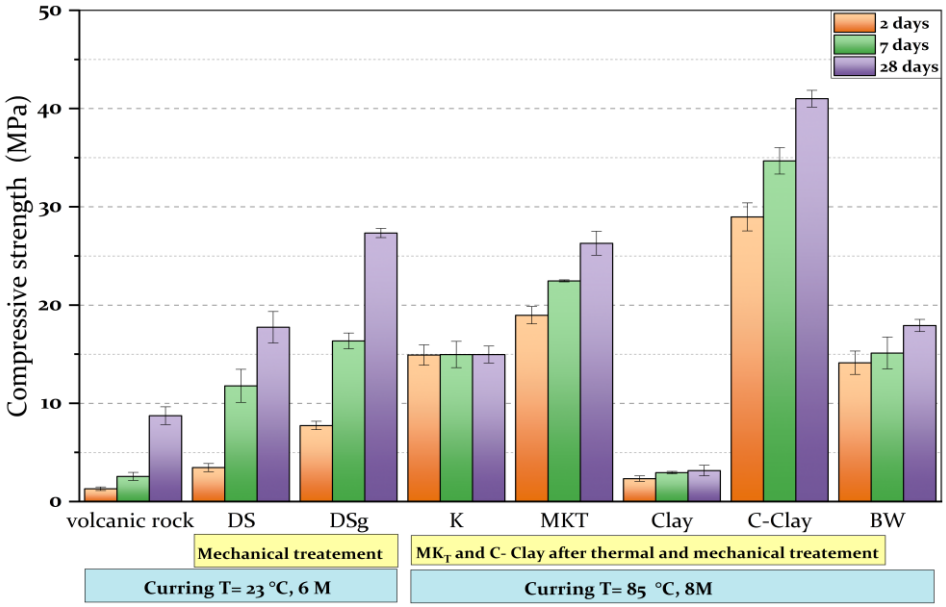

Figure 2.7. Compressive strength of geopolymers prepared using 6 M and 8 M NaOH solutions with untreated and treated precursors cured at room temperature and 85 °C.

2.2.3. Development of geopolymeric mixture

The performance of geopolymers depends significantly on the type and combination of precursors used[14]. Some studies have demonstrated that mixing two or more precursors can improve the performance of geopolymers[15, 16]. In this regard, we investigated the effects of the combinations of raw materials activated with NaOH alkali activator and cured at different temperatures on the mechanical properties of the produced geopolymer materials.

[14] Xie J, Wang J, Rao R, Wang C, Fang C. Effects of combined usage of GGBS and fly ash on workability and mechanical properties of alkali activated geopolymer concrete with recycled aggregate. *Compos Part B Eng*. **2019**;164:179-190.

[15] Zawrah MF, Gado RA, Khattab RM. Optimization of slag content and properties improvement of metakaolin-slag geopolymer mixes. *Open Mater Sci J*. **2018**;12:40-57.

[16] Driouich A, El Hassani SA, Hamah Sor N, et al. Mix design optimization of metakaolin-slag-based geopolymer concrete synthesis using RSM. *Results Eng*. **2023**;20:101573.

Based on the previous analysis results, the following mixtures have been proposed for further study to enhance the properties of geopolymer pastes:

- (a) MK_T + DS_g (Thermally treated kaolin + Electric Arc Furnace Slag after ground);
- (b) MK_T + BW (Thermally treated kaolin + Brick Waste);
- (c) C-Clay + DS_g (Calcined Clay + Electric Arc Furnace Salg after ground);
- (d) C-Clay + BW (Calcined Clay + Brick Waste);
- (e) BW + DS_g (Brick Waste + Electric Arc Furnace Salg after ground).

2.2.3.1. Effect of curing temperature on the compressive strength

The mixture (50 % MK_T @ 50 % DS_g) of 50 % thermally treated Kaolin (MK_T) and 50 % ground electric arc furnace slag (DS_g) activated with 6 M of NaOH solution and cured at different temperatures (25 °C, 65 °C, and 85 °C) demonstrates that higher curing temperatures significantly improve the compressive strength (Figure 2.8).

Table 2.3. Compressive strength results for 50 % MK_T and 50 % DS_g mixture at different temperatures (25°c, 65°c, 85°c) over 2, 7, and 28 days.

Curing temperatures	**50 % MK_T @ 50 % DS_g**		
	2 days	7 days	28 days
25 °C	2.10 ± 0.03	13.02 ± 0.52	15.23 ± 1.45
65 °C	14.51 ± 1.48	19.99 ± 1.97	20.65 ± 1.49
85 °C	8.60 ± 0.81	15.62 ± 1.34	21.40 ± 1.73

The compressive strengths after 28 days at 25 °C, 65 °C, and 85 °C, indicating that there is a significant improvement from 25 °C to 65 °C of curing temperature. The increase from 65 °C to 85 °C is negligible (less than 4 %). These findings highlight the importance of curing conditions to enhance the mechanical properties of geopolymer materials.

As a result, 65 °C was chosen as the optimal curing temperature for the synthesis of all geopolymer mixtures due to its significant impact on strength without the need for higher energy input associated with curing at 85 °C, thus supporting the goal of producing cost- effective and environmentally sustainable geopolymer materials.

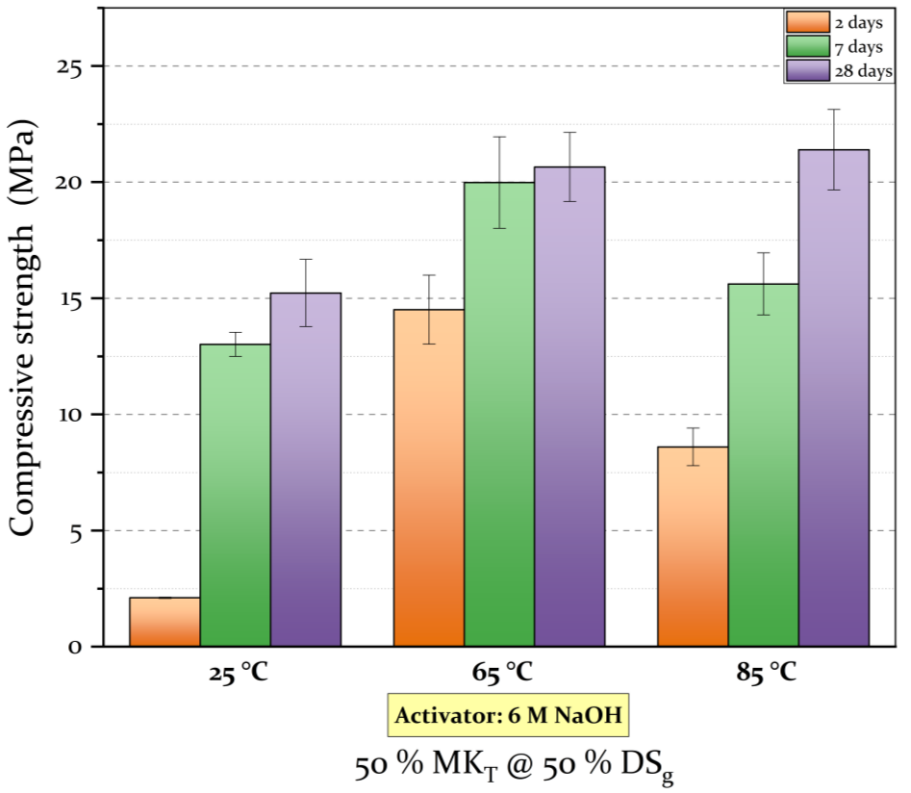

Figure 2.8. The effect of curing temperature on the compressive strength mixture of 50 % MK_T and 50 % DS_g geopolymer mixture activated with 6 M NaOH solution.

2.2.3.2. Compressive strength for the mixture of (MK_T @ BW) and (C-Clay @ DS_g and C-Clay @ BW)

The compressive strength results for the mixture of MK_T with BW and C-Clay with both DS_g and BW are shown in Figure 2.9. Detailed results for these mixtures are provided in Table 2.4.

Table.2.4. Compressive strength results for geopolymers mixture at 65 °C with 6 M Solution over 2, 7, and 28 days.

Geopolymers	**Curing**		
	2 days	7 days	28 days
MK_T @ BW	8.62 ± 0.48	10.06 ± 1.03	13.60 ± 0.28
C-Clay @ DS_g	24.07 ± 1.95	27.64 ± 5.87	41.66 ± 2.72
C-Clay @ BW	43.45 ± 1.62	44.36 ± 2.45	47.90 ± 1.77

The compressive strength of the 50 % MK_T @ 50 % BW geopolymer mixture shows a steady and significant increase over the 28-day curing period (Figure 2.9 a). Initially, at 2 days, the compressive strength is 8.62 MPa, indicating the early formation of the geopolymer matrix. By 7 days, the strength increased to 10.06 MPa, reflecting a 16.73 % improvement, which suggests ongoing geopolymerization. At 28 days, the compressive strength reached 13.60 MPa, representing a substantial 57.76 % increase from the 2-day

strength. This progression highlights the effectiveness of the MK_T and BW combination in producing a geopolymer material with enhanced compressive strength over time.

Both mixtures of (50 % C-Clay @ 50 % DS_g and 50 % C-Clay @ 50 % BW) show the highest compressive strengths after 28 days, with values reaching up to about 42 MPa and 48 MPa, respectively (Figure 2.9b and 2.9c). The C-Clay @ BW mixture achieves a slightly higher compressive strength compared to the C-Clay @ DS_g mixture at 28 days. These results demonstrate the effectiveness of the mechanical and thermal treatments applied to DS and clay in enhancing the reactivity and compressive strength of the resulting geopolymer matrices.

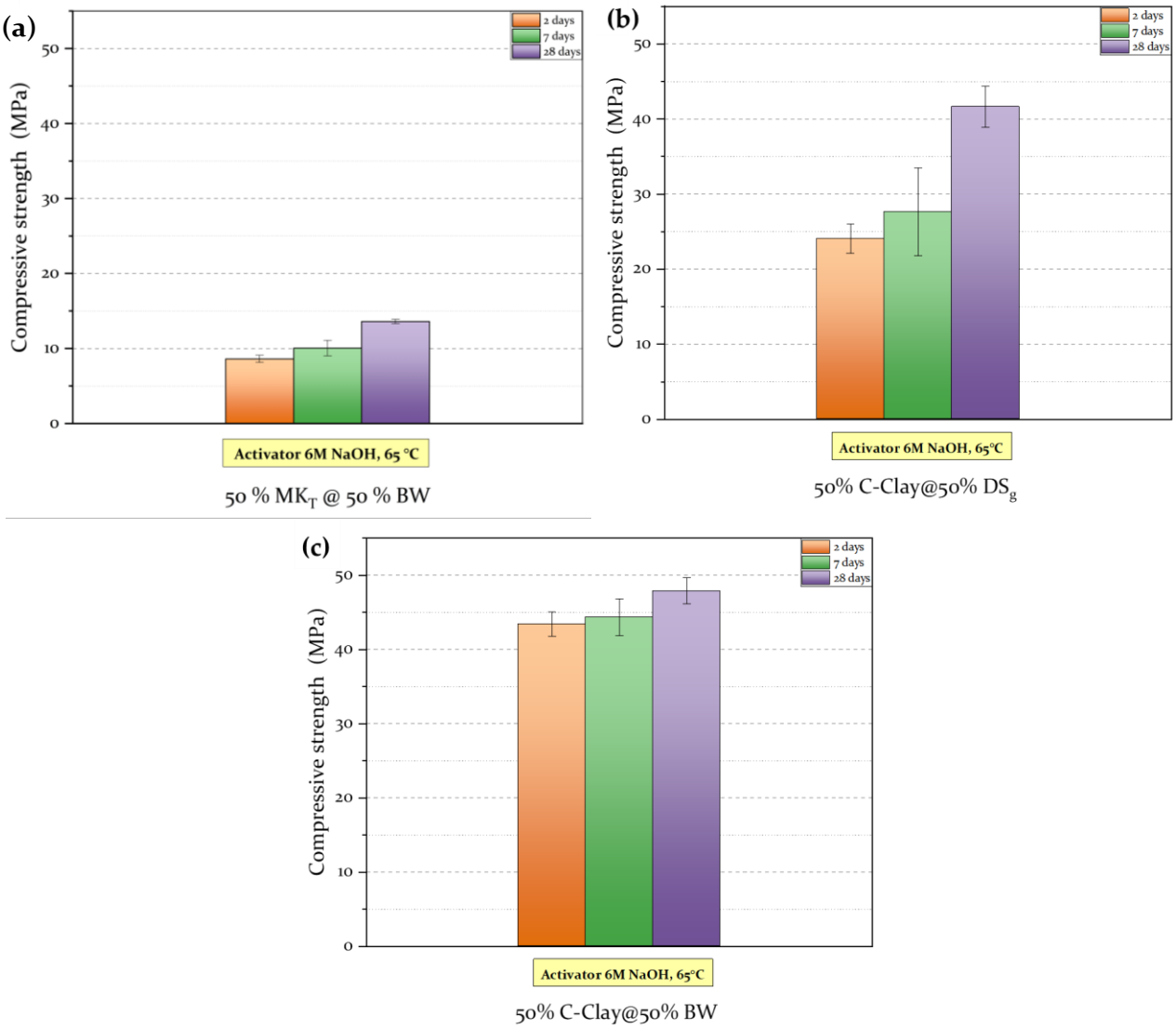

Figure 2.9. Compressive strength of the mixtures (a) MK_T @ BW, (b) C-Clay @ DS_g, and (c) C-Clay @ BW activated with 6 M NaOH and cured at 65 °C.

2.2.3.3. Effect of NaOH concentration on compressive strength

Figure 2.10 shows the compressive strength of the (50 % MK_T @ 50 % DS_g) and (50 % BW @ 50 % DS_g) mixtures cured at 65 °C. The compressive strength data, measured at 2, 7, and 28 days, are summarized in Table 2.5 for geopolymers prepared with 6 M and 8 M NaOH solutions.

The increase in NaOH concentration from 6 M to 8 M resulted in notable improvements in compressive strength at 28 days. for the 50 % MK_T @ 50 % DS_g mixture, strength increased from 20.65 MPa to 24.24 MPa, while for the BW mixture, it rose from 20.53 MPa to 25.66 MPa. This indicated that a higher NaOH concentration enhanced geopolymerization, promoting better dissolution of the aluminosilicate materials and creating stronger, denser structures. Although the impact was less significant at 2 and 7 days, the results confirmed that higher NaOH concentrations positively influenced both early and long-term compressive strength, emphasizing its importance in optimizing geopolymer properties.

Table 2.5. Compressive strength results of geopolymer mixtures cured at 65 °C with 6 M and 8 M NaOH solutions over different curing periods.

Geopolymers	**Curing**		
	2 days	7 days	28 days
MK_T @ DS_g (6 M)	14.51 ± 1.48	19.99 ± 1.97	20.65 ± 1.49
MK_T @ DS_g (8 M)	19.42 ± 1.04	20.23 ± 1.35	24.24 ± 1.41
BW @ DS_g (6 M)	12.91 ± 0.57	14.99 ± 1.00	20.53 ± 0.48
BW @ DS_g (8 M)	16.41 ± 0.80	17.58 ± 0.51	25.66 ± 1.18

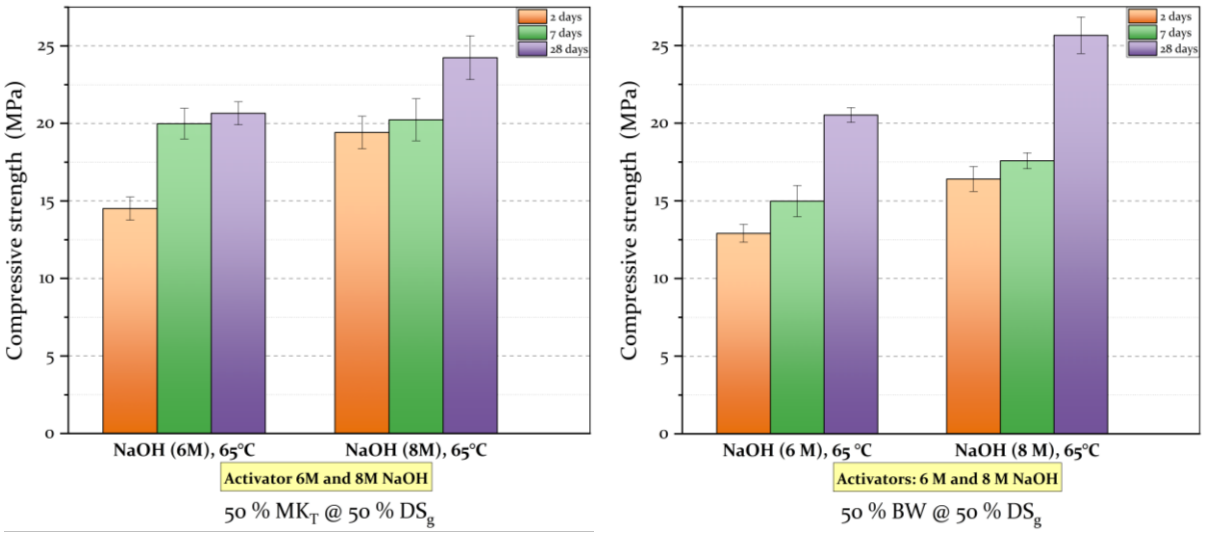

Figure 2.10. Compressive strength of the mixtures: (left) 50 % MK_T @ 50 % DS_g and (right)50 % BW@50 % DS_g, activated with 6M and 8M NaOH solutions and cured at 65 °C.

Finally, the findings from the previous results, along with observations from the water droplet test, were used to guide the selection of these mixtures for further study:

a) 50 % C-Clay + 50 % DS_g (65 °C, 6 M NaOH);
b) 50 % C-Clay + 50 % BW (65 °C, 6 M NaOH);
c) 50 % MK_T + 50 % DS_g (65 °C, 8 M NaOH).

In the light of these results, the 8 M NaOH solution is selected as the optimal alkaline condition for all the next geopolymer syntheses.

2.2.4. Development of geopolymeric mixtures using various alkaline activators

Further experiments focused on the investigation of the mechanical properties of various geopolymer mixtures. The mixtures examined include C-Clay @ DS_g, C-Clay @ BW, and MK_T @ DS_g, and activated with two different types of alkaline activators: Alkaline Activator Liquid (A.A.L), and Alkaline Activator Powder (A.A.P). More details on the experimental procedures can be found in Chapter 6, Table 6.3.

The compressive strengths of geopolymer specimens synthesized with different alkali activators are shown in Figure 2.11. The study results demonstrate that the choice of alkaline activator significantly impacts the compressive strength of geopolymer mixtures. It can be observed that the compressive strength of the specimens manufactured by A.A.L is higher than those prepared by A.A.P at all testing ages. Additionally, the compressive strength results for A.A.P samples indicate that the age of the samples has no significant impact on the final compressive strength, suggesting that A.A.P does not facilitate ongoing strength development over time. These findings align with previous studies, confirming that a part of the water remained free and unbound during the mixing stage, increasing the water-to-binder ratio and thus reducing the compressive strengths [17].

The compressive strength data for the different geopolymer mixtures and alkaline activators over 2, 7, and 28 days is presented in **Table 2.6** below.

Table 2.6. Compressive strength of geopolymer samples activated with A.A.L. and A.A.P. over 2, 7, and 28 days of curing.

Geopolymers		**Curing**		
		2 days	7 days	28 days
A.A.L.	C-Clay @ DS_g	40.17 ± 2.11	41.37 ± 2.36	45.20 ± 2.12
	C-Clay @ BW	40.32 ± 2.35	49.20 ± 1.44	54.38 ± 1.43
	MK_T @ DS_g	29.82 ± 0.13	37.71 ± 0.75	43.40 ± 1.49
A.A.P.	C-Clay @ DS_g	32.43 ± 1.65	34.93 ± 2.19	37.32 ± 0.52
	C-Clay @ BW	10.50 ± 0.53	13.18 ± 0.55	14.60 ± 0.30
	MK_T @ DS_g	1.60 ± 0.17	1.41 ± 0.07	1.59 ± 0.16

[17] Dong M, Elchalakani M, Karrech A. Development of high strength one-part geopolymer mortar using sodium metasilicate. *Constr Build Mater*. **2020**;236:117611.

The mixture of 50 % C-Clay and 50 % DS_g shows high compressive strengths with both activators, reaching around 45 MPa with A.A.L and 37 MPa with A.A.P. (Figure 2.11 a). The average compressive strengths for MK_T @ DS_g geopolymer made with A.A.L at 2, 7, and 28 days were 29.82 ± 0.13 MPa, 37.71 ± 0.75 MPa, and 43.40 ± 1.49 MPa, respectively. In contrast, the corresponding compressive strengths for samples made with A.A.P were 1.60 ± 0.17 MPa, 1.41 ± 0.07 MPa, and 1.59 ± 0.16 MPa. Thus, can be attributed to several factors such as: A.A.P could lead to a higher water-to-binder ratio, producing a weaker matrix; the distribution of A.A.L is more uniform promoting a consistent and effective geopolymerization process, whereas A.A.P may not distribute as evenly.

When comparing the mixture of C-Clay @ BW prepared with A.A.P and A.A.L shows a remarkable difference in strength, with an increase approximately of 284 % at 2 days and 272 % at 28 days, respectively (Figure 2.11 b).

The compressive strength of mixture MK_T @ DS_g activated with A.A.L starts at 29.82 MPa after 2 days and increases to 37.71 MPa at 7 days reaching a peak of 43.4 MPa at 28 days (Figure 2.11 c). This demonstrates the effective geopolymerization facilitated by the sodium hydroxide and sodium silicate, which show better dissolution and distribution into the matrix leading to a high compressive strength. In contrast, the samples activated with A.A.P show very low compressive strengths. The strength after 2 days of curing is only 1.6 MPa, which slightly decreases to 1.59 MPa after 28 days. This negligible improvement indicates that the A.A.P is not as effective as the A.A.L.

Based on the research findings, the chemical-physical, structural and morphological properties of the C-Clay and DS_g combination will be explored in the next sections. This decision is based on the outstanding compressive strength performance of this combination when activated with both Alkaline Activator Liquid (A.A.L) and Alkaline Activator Powder (A.A.P).

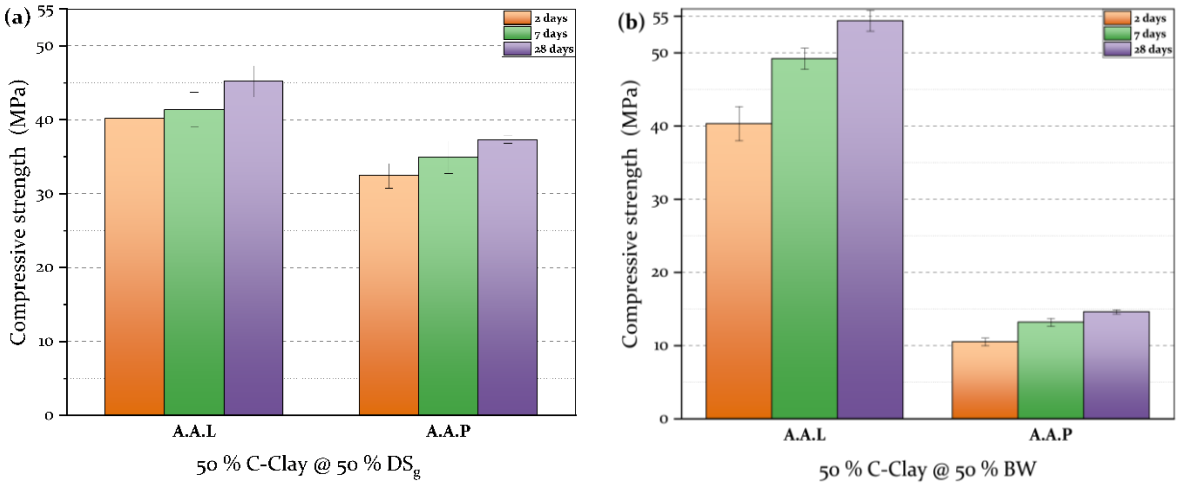

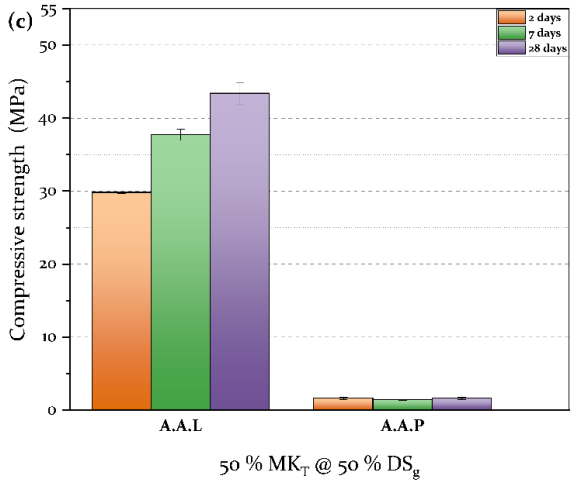

Figure 2.11. Compressive strength of the (a) C-Clay @ DS_g, (b) C-Clay @ BW, and (c) MK_T @ DS_g geopolymers activated with A.A.L and A.A.P solutions.

2.2.4.1. FTIR of 50 % C-Clay @ 50 % DS_g (A.A.L and A.A.P)

The FTIR spectra for the 50 % C-Clay @ 50 % DS_g geopolymer samples after 2 and 28 days of curing with different activators (A.A.L and A.A.P) are shown in Figure 2.12. In all spectra, the characteristic bands for stretching and bending vibrations of H–O–H bonds of water molecules appear around 3435 cm^{-1} and 1640 cm^{-1} [18]. Both bands, along with the one associated with O–H stretching, are broad, indicating a significant disorder of hydroxyl groups and water molecules. A significant peak at approximately 1000 cm^{-1} is observed, which is associated with Si–O–Si asymmetric stretching vibrations and 560 cm^{-1} (Si–O bending and Al–O vibrations), which indicates of starting the geopolymerization process [19]. The band at 695 cm^{-1} 798 cm^{-1} and 778 cm^{-1} are associated with Si–O–Si symmetrical stretching vibration in quartz in all geopolymer samples [20]. Calcite is identified by absorption bands at about 1796 cm^{-1}, 1428 cm^{-1}, 873 cm^{-1}, and 712 cm^{-1} (CO_3 deformation). Furthermore, bands in the range of 400-550 cm^{-1} can be assigned to kaolinite at 471 cm^{-1} and muscovite at 430 cm^{-1} and 531 cm^{-1}. Those results given by FTIR confirm the presence of all crystalline minerals found by X-ray diffraction in Clay and C-clay.

[18] Clausi M, Tarantino SC, Magnani LL, Riccardi MP, Tedeschi C, Zema M. Metakaolin as a precursor of materials for applications in Cultural Heritage: Geopolymer-based mortars with ornamental stone aggregates. *Appl Clay Sci*. **2016**;132-133:589-599.
[19] Phair JW, Van Deventer JSJ. Effect of the silicate activator pH on the microstructural characteristics of waste-based geopolymers. Int J Miner Process. **2002**;66(1-4):121-143.
[20] Kaufhold S, Hein M, Dohrmann R, Ufer K. Quantification of the mineralogical composition of clays using FTIR spectroscopy. *Vib Spectrosc*. **2012**;59:29-39.

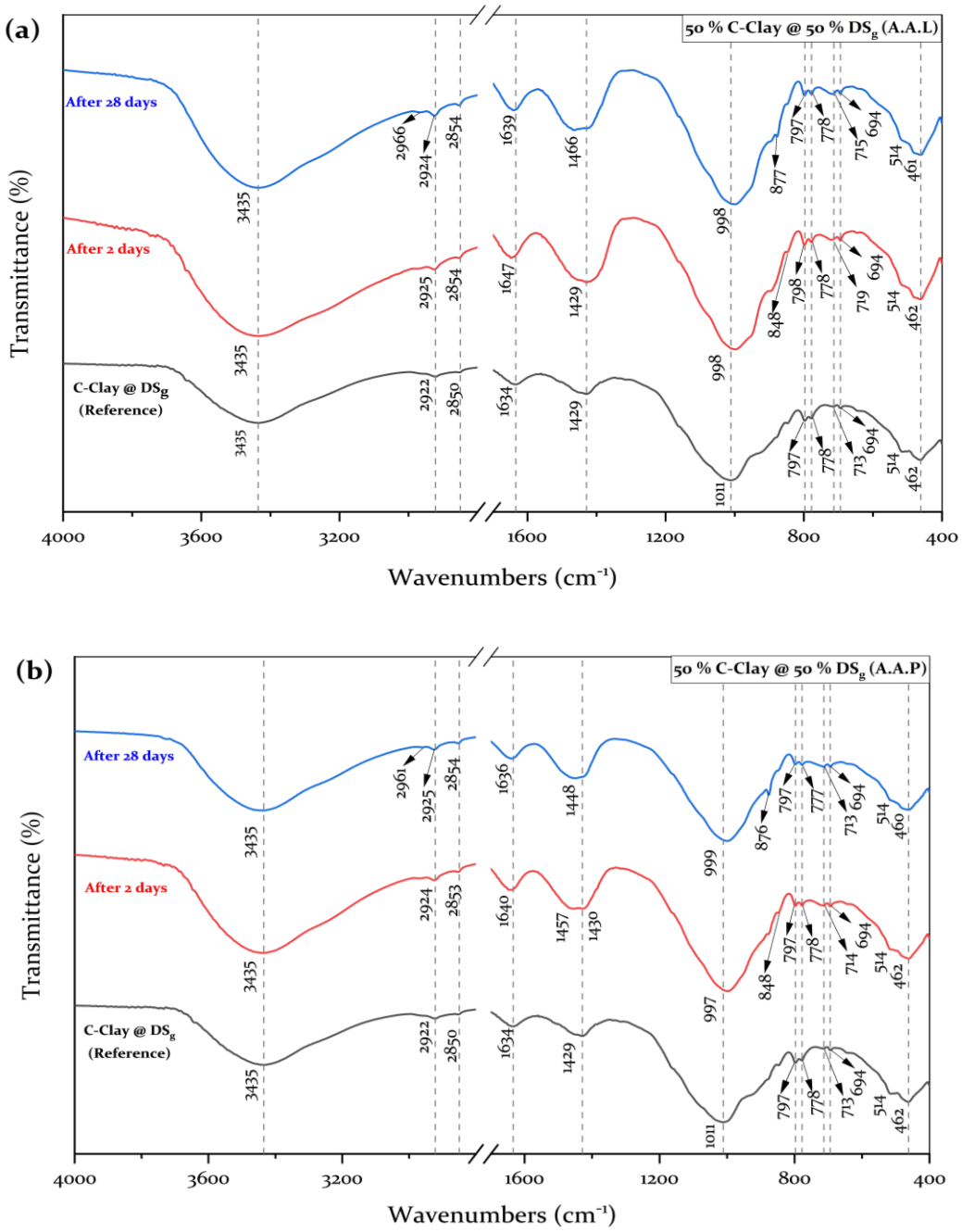

Figure 2.12. FTIR spectra of C-Clay @ DS_g geopolymers prepared with (a) A.A.L and (b) A.A.P after 2 and 28 days of curing.

2.2.4.2. Mineralogical characterization for 50 % C-Clay @ 50 % DS_g (A.A.L and A.A.P)

The X-ray diffraction (XRD) patterns for the 50 % C-Clay @ 50 % DS_g geopolymer after 2 and 28 days are shown in Figure 2.13. It can be observed that all the geopolymer samples show the same crystalline phases present in the precursors, indicating the presence of unreacted raw materials.

The XRD patterns of the C-Clay @ DS_g geopolymer, prepared using an alkaline activator liquid, along with the raw materials (C-Clay and DS_g), are shown in Figure

2.12(a). The mineralogical phases such as calcite, quartz, muscovite, calcite, wüstite, and magnetite, which were detected in the raw materials (C-Clay and electric arc furnace slag) are still present in the geopolymeric binders activated with sodium hydroxide (8 M) and sodium silicate after 2 and 28 days of curing. This observation suggests that these crystalline phases are inert to alkaline activation, remaining unchanged throughout the geopolymerization process [21].

Additionally, Figure 2.12 (b) shows the XRD pattern of the C-Clay @ DS_g geopolymer prepared using an alkaline activator powder. The same mineralogical phases from the raw materials C-Clay and DS, including quartz (Qz), muscovite (Mu), wüstite (Wü), and larnite (La) are detected. After 28 days, it is evident that some crystalline phases remain unchanged after alkali activation, confirming that these phases are inert to alkaline activation in both liquid and powder forms.

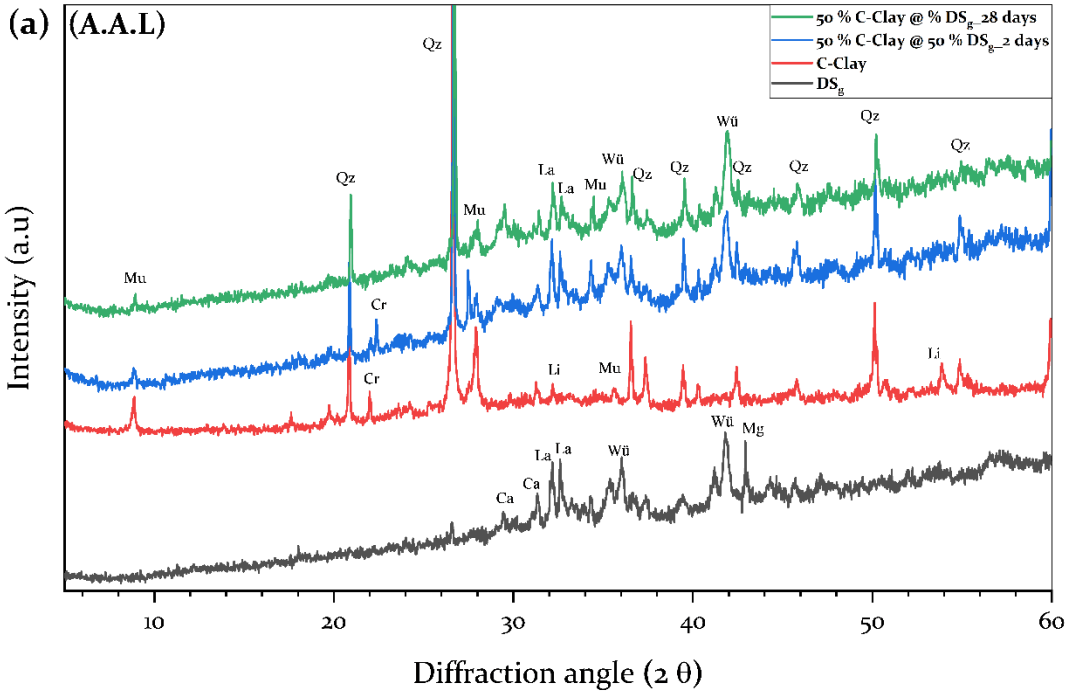

[21] Stroscio A, Barone G, Fernàndez-Jimenez A, Lancellotti I, Leonelli C, Mazzoleni P. Sicilian clay sediments as precursor for alkali activated materials. *Appl Clay Sci*. **2024**;253:107350.

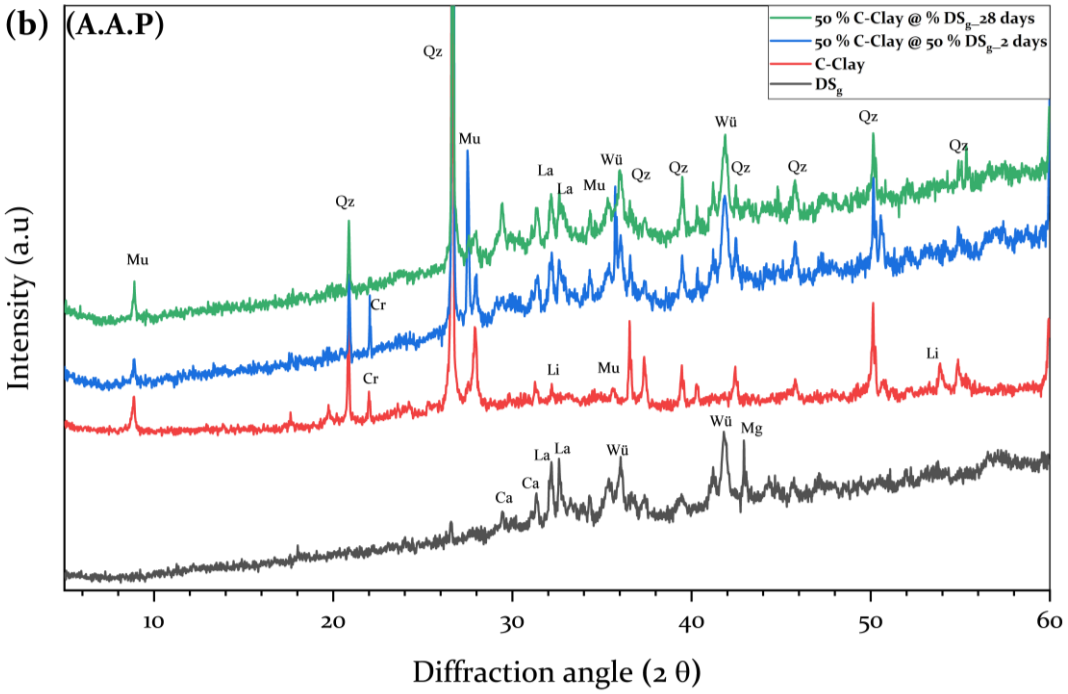

Figure 2.13. XRD patterns of the C-Clay, DS_g raw materials, and geopolymer samples made with (a) A.A.L and (b) A.A.P after 2 and 28 days.

2.2.4.3. Thermal analysis of 50 % C-Clay @ 50 % DS_g (A.A.L and A.A.P) after 28 days

TG/DTG/DSC analyses were performed on the 50 % C-Clay @ 50 % DS_g geopolymer mixture, activated with A.A.L and A.A.P in order to evaluate the thermal behavior after 28 days of curing. Figure 2.14 (a) and (b) illustrate the main thermal changes happening in the geopolymer pastes activated with A.A.L and A.A.P, respectively.

In Figure 2.14 (a), the first exothermic peak of geopolymer was observed at 50 - 200 °C. In this first stage at a low temperature of 78.42 °C, thermal dehydration is associated with the evaporation of free and physically bound water (H_2O) within the geopolymer gel phase [22]. The second exothermic peak was observed at 450 - 650 °C. In this stage at 511.78 °C, the geopolymer samples show another weight change noted due to the decomposition of carbonates of kaolinite, illite and muscovite [23], indicated by an exothermic peak in the DTG curve.

Figure 2.14 (b) shows the thermal analysis of the geopolymer sample prepared with an alkaline activator powder. A notable weight loss occurs around 43.32°C, which is due to the evaporation of water (H_2O), corresponding to a small exothermic peak in the DTG curve. Another weight loss occurs around 346°C, indicating additional dehydroxylation

[22] Yang T, Wu Q, Zhu H, Zhang Z. Geopolymer with improved thermal stability by incorporating high-magnesium nickel slag. *Constr Build Mater*. **2017**;155:475-484.
[23] Petlitckaia S, Gharzouni A, Hyvernaud E, Texier-Mandoki N, Bourbon X, Rossignol S. Influence of the nature and amount of carbonate additions on the thermal behaviour of geopolymers: A model for prediction of shrinkage. *Constr Build Mater*. **2021**;296:123752

or decomposition of remaining hydroxyl groups and organic impurities [24]. At 615.98 °C, the sample shows another weight change, likely associated with the decomposition of carbonates.

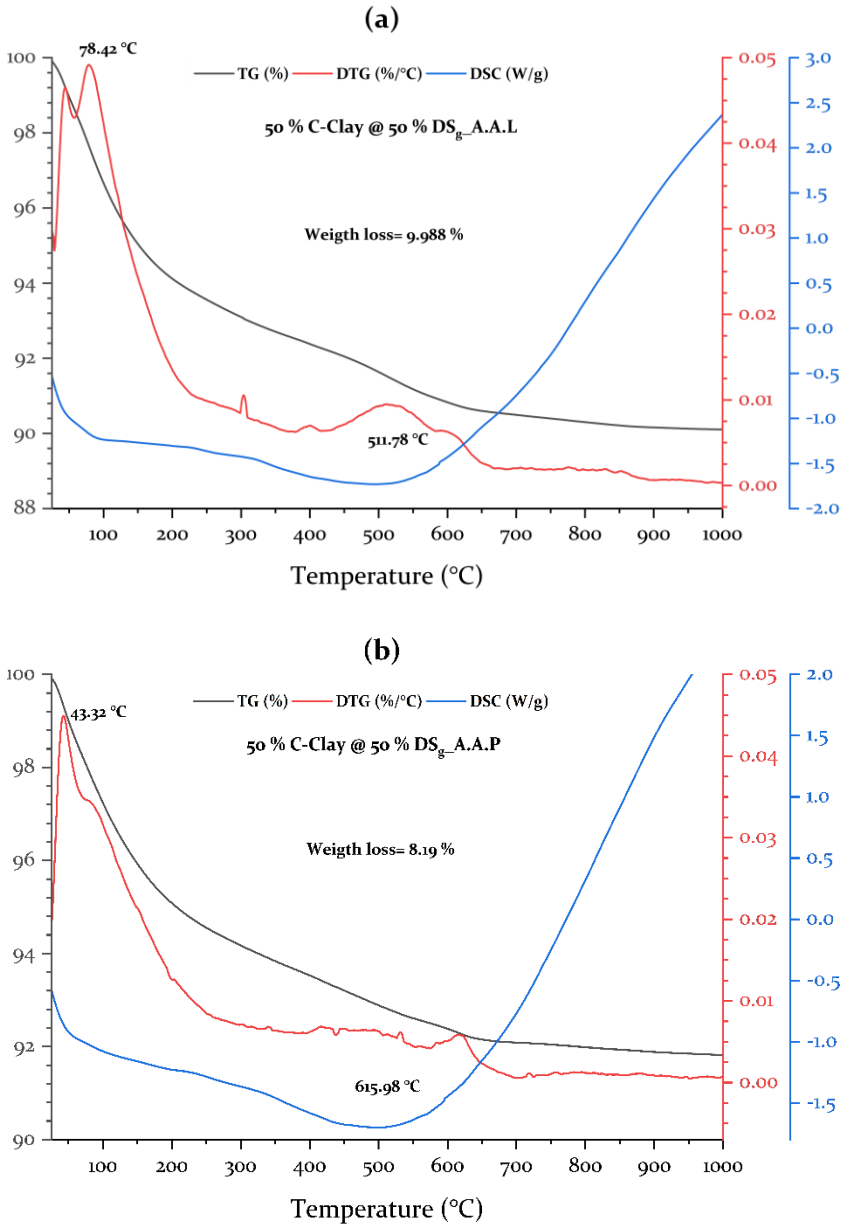

Figure 2.14. TG/DTG/DSC curves of (a) geopolymer activated by A.A.L and (b) geopolymer activated by A.A.P after 28 days of curing.

The total weight loss up to around 1000°C is approximately 9.90 % for geopolymers made with A.A.L. In contrast, the thermal analysis of the geopolymer sample activated with A.A.P shows a slightly lower total weight loss, around 8.19 %. These results indicate good thermal stability for both samples and the presence of residual components that remain stable at high temperatures.

[24] Pavese A, Artioli G, Hull S. In situ powder neutron diffraction of cation partitioning vs. pressure in Mgo.94Al2.02O4 synthetic spinel. *Am Mineral*. **1999**;84(5-6):905-912.

2.2.4.4. Morphological study of 50 % C-Clay @ 50 % DS_g geopolymers (A.A.L and A.A.P)

Scanning electron microscopy (SEM) analyses were performed on all (50 % C-Clay @ 50 % DS_g) geopolymer samples at different magnifications. The analysis of the structures was aimed to highlight the details about the microstructure and the differences between A.A.L (Figure 2.15) and A.A.P (Figure 2.16), both cured at 65 °C after 28 days.

Figure 2.15 depicts SEM images of the geopolymer made with A.A.L at different magnifications.

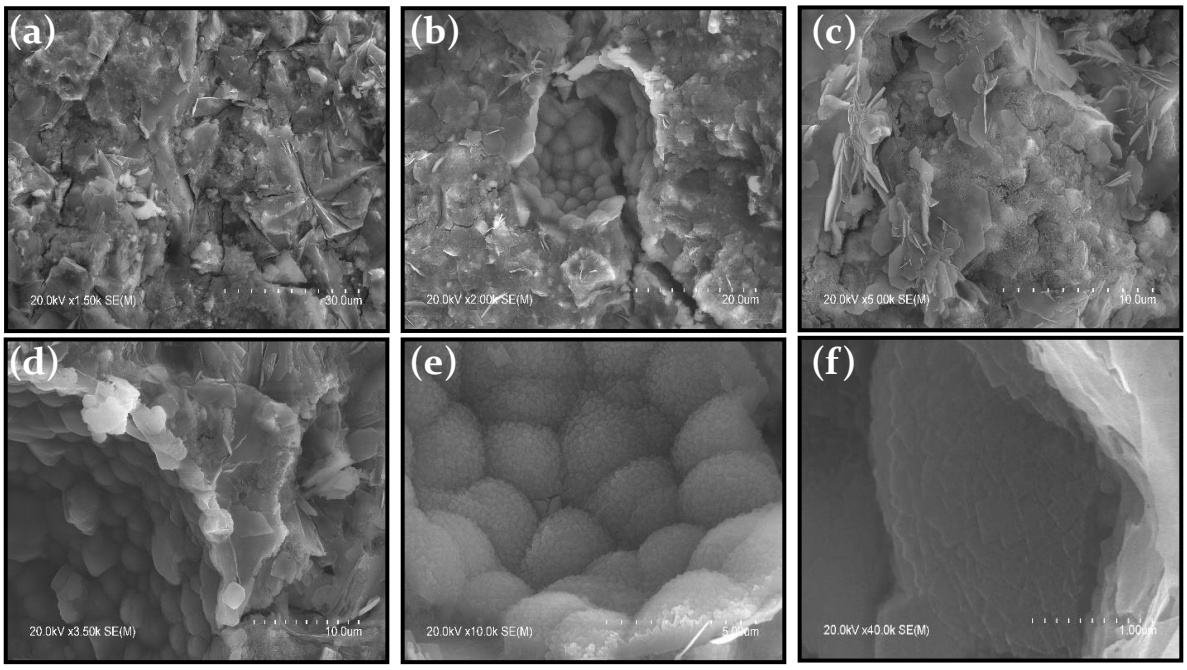

Figure 2.15. SEM micrographs of 50 % C-Clay @ 50 % DS_g geopolymer samples activated with alkaline activator liquid (28 days; 65 °C for 20 h).

At low magnification (Figure 2.15 a), a heterogeneous and compact matrix with visible solid particles is revealed. A porous structure with large voids and interconnected pores is highlighted in Figure 2.15 (b), suggesting incomplete matrix filling and the presence of unreacted precursors. Additionally, Figure 2.15 (c) displays a rough texture with flaky structures, likely remnants of raw materials such as muscovite and quartz, indicating areas where geopolymerization has not fully progressed. Furthermore, at medium magnification (Figure 2.15 d) a closer view of the matrix shows the layered and flaky nature of the sample, suggesting the formation of an aluminosilicate network. Figure 2.15 (e) reveals spherical particles in the porous regions, indicating ongoing reactions within the matrix and the presence of gel phases. Finally, at higher magnification (Figure 2.15 f) a highly magnified section of the geopolymer matrix displays fine details of the microstructure. This image highlights the dense and compact nature of the geopolymer, with very fine particles and a smooth surface texture, suggesting a well-formed and stable geopolymer network.

Figure 2.16 shows the SEM images of the geopolymer activated with A.A.P (6 % Na_2SiO_3 + water).

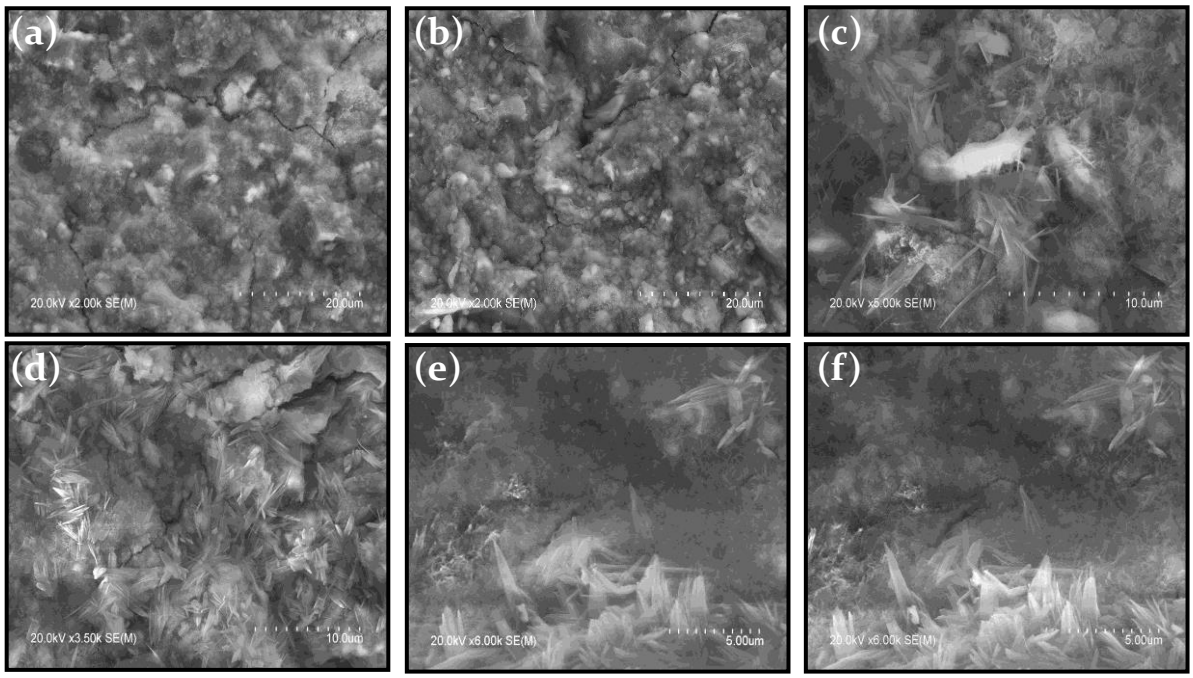

Figure 2.16. SEM micrographs of 50 % C-Clay @ 50 % DS_g geopolymer samples activated with alkaline activator powder (6 % Na_2SiO_3 and water; 28 days; 65 °C for 20 h).

The SEM figures (Figure 2.16 a, b, and d) show micro-fractures which was evidenced by the weakness in the compressive strength. Additionally, the microstructural figures show a granular geopolymeric gel that is not well compacted, surrounding raw materials particles with irregular morphologies. A less compact matrix with visible micro-fractures is shown in Figure 2.16 (a, b) with a highly porous structure with large voids, suggesting significant unreacted materials and poor matrix consolidation. Figure 2.16 (c) depicts a rough texture with flaky structures, indicating limited progress in geopolymerization. Detailed matrix layers are observed at medium magnification (Figure 2.16 d) indicating incomplete formation of the geopolymer network, while Figure 2.16 (e, f) reveals poorly reactions between raw materials within the matrix characterized by a less dense and less compact structure with a smooth surface texture, suggesting a poorly formed and unstable geopolymer network. To further understand the composition and stability of the geopolymer gels, a microanalysis such as energy-dispersive X-ray spectroscopy (EDS) would have been beneficial.

2.2.4.5. Porosity and pore size distribution

The porosity data for the 50 % C-Clay and 50 % DS_g geopolymers are summarized in Table 2.7, while the pore size distribution is illustrated in Figure 2.17. The results highlight significant differences in porosity and bulk density between the samples activated with

Alkaline Activator Liquid (A.A.L) and Alkaline Activator Powder (A.A.P) over curing periods of 2 and 28 days.

Table 2.7. Total porosity and bulk density for 50 % C-Clay @ 50 % DS_g geopolymers.

Alkaline activators	Total porosity (%)		Bulk Density (g/cm³)	
	2 days	28 days	2 days	28 days
(A.A.L) NaOH (8 M) + S.S	24.41	22.72	2.54	2.34
(A.A.P) 6 % Na.S + water	30.12	29.13	1.78	1.78

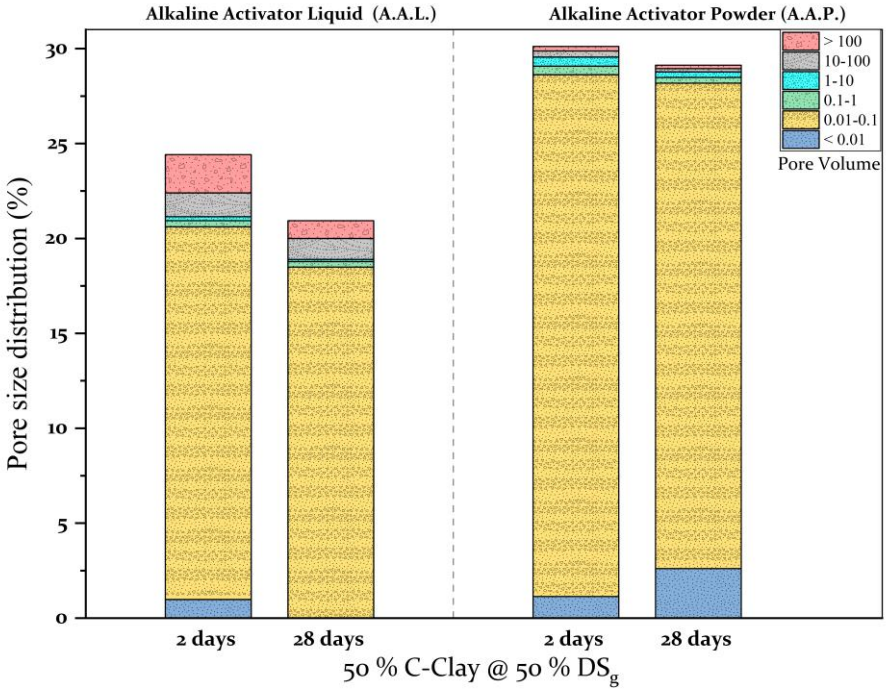

Figure 2.17. Porosity and pore size distribution of 50 % C-Clay @ 50 % DS_g geopolymers samples activated with A.A.L and A.A.P after 2 and 28 days of curing.

The total porosity of samples activated with A.A.L decreases from 24.41 % at 2 days to 22.72 % at 28 days. This reduction indicates the ongoing densification and pore refinement within the geopolymer matrix, leading to enhanced mechanical properties (see Figure 2.10 a). The bulk density remains relatively high and stable, suggesting a denser and more compact geopolymer material structure due to effective geopolymerization. It decreases from 2.54 g/cm³ at 2 days to 2.34 g/cm³ at 28 days, reflecting the reduction in porosity and increased compaction within the geopolymer structure. The total porosity of samples activated with A.A.P also slightly decreases from 30.12 % at 2 days to 29.13 % at 28 days. However, the higher overall porosity compared to A.A.L samples suggests less efficient geopolymerization and pore filling which is confirmed by the lower mechanical properties (see Figure 2.10 a). The bulk density for A.A.P- activated samples remains nearly constant at approximately 1.78 g/cm³ over the 28-day curing. This indicates a minimal change in the material's structure and density.

2.3. Conclusions

This work describes the successful design and development of geopolymeric materials using locally sourced precursors such as Electric Arc Furnace Slag (DS), clay, brick waste (BW), kaolin (K), and volcanic rock (slag), to synthesize eco-friendly and high-performance geopolymers. The experiments were conducted on various geopolymers activated with NaOH solution, as well as alkaline activators in both liquid and powder forms under different conditions. In particular, these experiments highlighted the importance of sodium hydroxide concentration, curing temperature and precursor treatment in enhancing the properties and performance of the resulting geopolymeric materials.

Further efforts were focused on the improvement of the raw material reactivity. Specifically, thermal treatment was applied to kaolin (K) and clay to convert them into more reactive materials (named MK_T and C-Clay), while mechanical treatment (grinding) was used on both electric arc furnace slag (DS) and the thermally treated samples (MK_T and C-Clay) to reduce the particle size. The results indicated that geopolymers based on thermally treated clay (C-Clay) and ground electric arc furnace slag (DS_g) demonstrated superior compressive strengths, with significant improvements observed over various curing periods due to these treatments.

Moreover, we investigated the effects of the combination of different raw materials (MK_T + DS_g, MK_T + BW, C-Clay + DS_g, and C-Clay + BW) activated with NaOH alkali activator and cured at different temperatures on the mechanical properties of the resulting geopolymer materials. The study further investigated the influence of two types of alkaline activators, Alkaline Activator Liquid (A.A.L) and Alkaline Activator Powder (A.A.P), on the compressive strength of these mixtures.

Outstanding compressive strength performances were observed in the geopolymers based on the 50 % C-Clay @ 50 % DS_g combination. Further experiments were performed to evaluate the chemical-physical, structural, morphological and mechanical properties of (50 % C-Clay @ 50 % DS_g) samples activated with A.A.P compared to those activated with A.A.L. The results showed that the geopolymeric samples activated with A.A.L are denser and stronger than activated with A.A.P.

These findings highlight the potential of utilizing industrial and construction waste materials in the development of sustainable, high-performance building materials, aligning with the goals of environmental conservation and waste management.

Furthermore, the incorporation of functional sol-gel into these mixtures could further enhance the properties of the produced geopolymers, employing eco-friendly and green practices. This approach offers a pathway to more efficient and advanced building materials, which will be discussed in the next Chapter.

CHAPTER 3

FUNCTIONAL HYBRID GEOPOLYMER MATERIALS

This chapter describes the development of hybrid organic-inorganic geopolymers which represent a novel class of composite materials formed by incorporating organic-inorganic precursors/additives into a geopolymer matrix. These additives can be in various forms, including organic polymers (plastic waste, polymer pellets), natural fibers (wood pulp, agricultural waste), nanomaterials (metal or metal-oxide nanoparticles, carbon-based or silica-based nanoparticles) and organic-inorganic precursors (superplasticizers and water-repellent agents). This combination of organic and inorganic components opens up a wide range of applications, including construction materials, coatings, composites, and even 3D printing. The great attention to these hybrid materials is associated with their unique chemical and physical properties, which result from the synergistic interaction between the two matrices. In this research work, we focused on the use of proper silane precursors, polysiloxane oligomers or acrylic polymers for the obtaining of hybrid organic-inorganic geopolymers through also the sol-gel process. The objective of this study is to investigate the effect of incorporating four different functional agents into a mixture of two precursors (i.e., calcined clay blended with electric arc furnace slag ground, and calcined clay blended with brick waste) on the processing performance and the waterproof properties, as well as the mechanical strength.

3.1. Abstract

Geopolymer materials can be functionalized to obtain organic-inorganic composite materials by incorporating an organic/inorganic component such as polysiloxane oligomers, alkoxysilane agents or epoxy/acrylic resin precursors into the alkali-activated matrix producing then a hybrid material with improved chemical, physical and viscosity of the mixture[1,2,3]. These hybrid organic-inorganic geopolymers have recently received considerable attention due to their unique properties resulting from the synergistic interaction between the organic and inorganic components. To develop these hybrid geopolymers, the sol-gel synthesis approach was used. For these purposes, four functional agents were employed as polydimethylsiloxane (PDMS), tetraethyl orthosilicate (TEOS), acrylic resin, and TP56 mixture (56 wt.% of PDMS combined with ethoxysilane and 0.05 % n-octylamine).

Therefore, this work aims to develop hybrid geopolymers and then investigate thier surface wettability, water absorption, compressive strength, SEM analysis, and porosity characteristics, with a focus on the best-performing materials. Thus, eight hybrid geopolymers (named hereafter as H-GP) based on calcined clay blended with electric arc furnace slag (50 % C-Clay @ 50 % DS_g), were prepared with two different alkaline activators (A.A.L and A.A.P) and incorporating 3 wt.% of PDMS, TEOS, resin acrylic and TP56 separately (Figure 3.1). Additionally, another four samples (C-Clay @ BW) based on calcined clay blended with brick waste (50 % C-Clay @ 50 % BW), were prepared using the same two alkaline activators (A.A.L and A.A.P), and then incorporating only PDMS and TP56 separately (Figure 3.2).

The results showed a consistent increase in compressive strength over 28 days for all samples. The addition of PDMS exhibited better mechanical properties compared to other functional agents (TEOS, Resin and TP56), though PDMS reduced slightly the thermal stability. SEM analysis revealed microcracks in C-Clay @ DS_g samples activated with both A.A.L and A.A.P The porosity and water absorption tests demonstrated that samples activated with A.A.P show improved water absorption resistance and lower porosity. Contact angle measurements confirmed that the hybrid geopolymer prepared with A.A.P. alkaline activator and functionalized with PDMS (H-GP-P@PDMS) was the most hydrophobic.

[1] Roviello G, Menna C, Tarallo O, et al. Lightweight geopolymer-based hybrid materials. *Compos Part B Eng*. **2017**;128:225-237.

[2] Colangelo F, Roviello G, Ricciotti L, Ferone C, Cioffi R. Preparation and Characterization of New Geopolymer-Epoxy Resin Hybrid Mortars. *Mater 2013, Vol 6, Pages 2989-3006*. **2013**;6(7):2989-3006.

[3] Ielo I, Galletta M, Rando G, et al. Design, synthesis and characterization of hybrid coatings suitable for geopolymeric-based supports for the restoration of cultural heritage. *IOP Conf Ser Mater Sci Eng*. **2020**;777(1):012003.

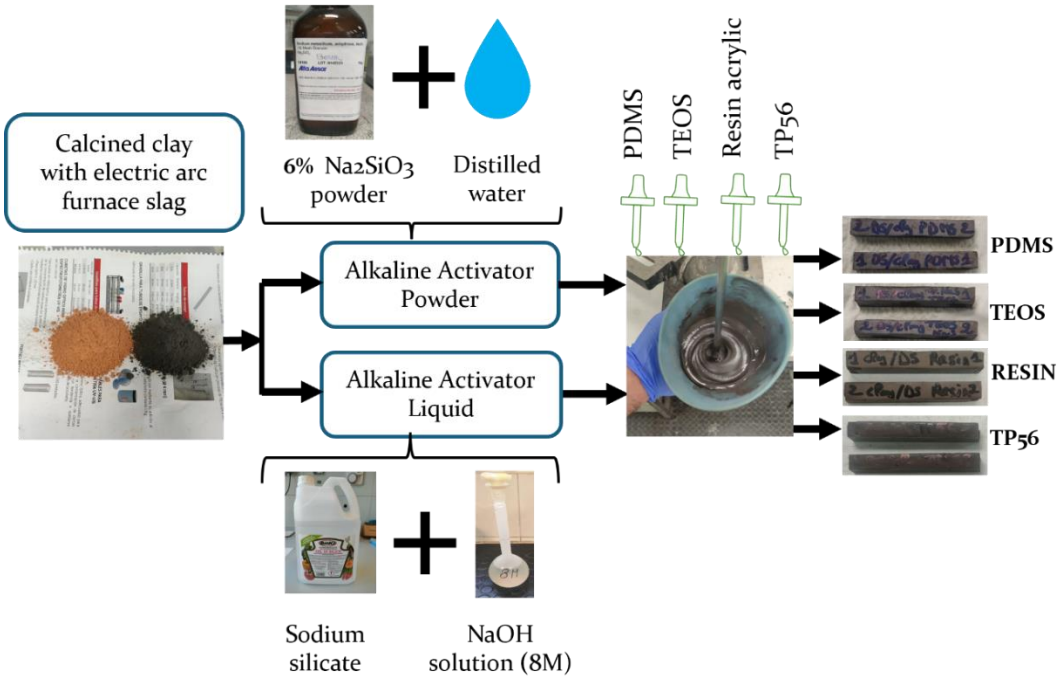

Figure 3.1. Synthesis of hybrid geopolymers (C-Clay @ DS_g) incorporating functional agents (PDMS, TEOS, resin, and TP56) with A.A.P. and A.A.L.

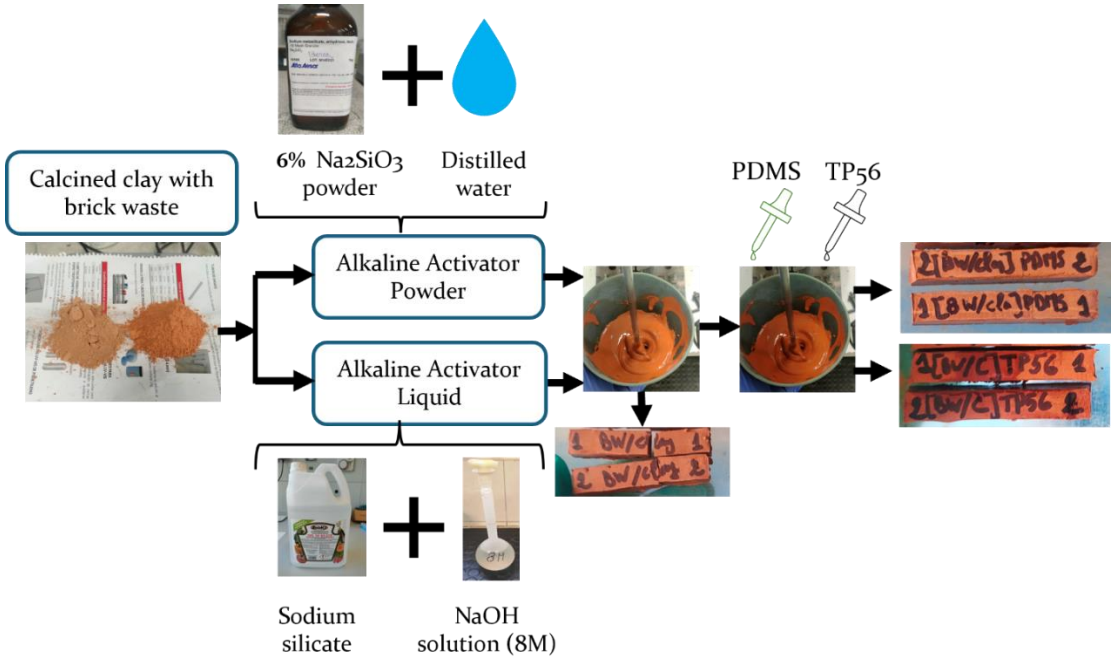

Figure 3.2. Preparation process of hybrid geopolymers (C-Clay @ BW) incorporating PDMS and TP56, using A.A.P. and A.A.L.

3.2. Results and discussion

3.2.1. Development of functional hybrid geopolymer materials

The rational design and development of functional organic-inorganic geopolymer materials aim to synthesize and optimize the formulations in order to obtain a synergy of beneficial properties between both the geopolymer matrix and the added components. In fact, it is important that these hybrid geopolymer materials are able to exhibit not only typical properties intrinsic of a geopolymer formulation but also the functional properties introduced by the combination of components and additives.

This paragraph discusses how the synthesis is performed, how to characterize the resulting material and the properties that can be achieved from the developed hybrid geopolymers. On this regard, sol-gel technology, an approach known to creating highly homogeneous formulations with enhanced properties, which was utilized to develop functional hybrid geopolymer materials (H-GP). To achieve this goal, functional agents (Figure 3.3) include polydimethylsiloxane (PDMS), tetramethyl orthosilicate (TEOS), acrylic resin and TP56 (56 wt.% of PDMS combined with ethoxysilane and 0.05 % of n-octylamine) were used. PDMS acts as a silicone-based organic polymer to enhance durability and chemical resistance of the hybrid geopolymer. TEOS plays a role as an organosilicon compound, contributes to the formation of a strong silica network for stabilization within a geopolymer matrix. Meanwhile, acrylic resin is employed to improve mechanical strength and durability.

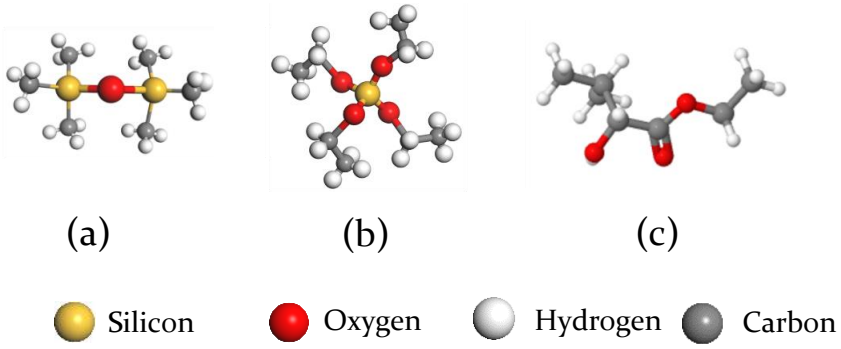

Figure 3.3. Functional agents/monomers: (a) PDMS, (b) TEOS, (c) acrylic resin used for the preparation of hybrid geopolymer materials.

3.2.2. Synthesis Process

The hybrid geopolymers were synthesized by incorporating organic components, including polydimethylsiloxane (PDMS), tetraethyl orthosilicate (TEOS), acrylic resin and TP56, into the geopolymer matrix. The geopolymer paste was prepared using calcined clay blended with electric arc furnace slag grounded (50 % C-Clay @ 50 % DS_g) and calcined clay blended with brick waste (50 % C-Clay @ 50 % BW) in equal proportion and activated with an alkaline activator liquid composed of sodium hydroxide (NaOH) and sodium silicate (Na_2SiO_3) and/or alkaline activator powder (6 % Na_2SiO_3 + water) (as

described in Chapter 6). After that, the organic components were added to the base mixture during the initial blending stage to develop the functional hybrid geopolymer materials. The synthesis approach used in the present study was designed to be ecologically friendly and sustainable by utilizing locally sourced industrial by-products and waste materials, reducing reliance on non-renewable resources, and minimizing energy consumption during the production process.

3.2.3. Characterization and performance of functional hybrid geopolymer materials

3.2.3.1. Compressive strength for 50 % C-Clay @ 50 % DS_g geopolymers

In this work, the compressive strength results of the base geopolymer (GP) and hybrid geopolymers (H-GP) incorporating PDMS, TEOS, acrylic resin and TP56 into the geopolymer matrix activated by (a) A.A.L. and (b) A.A.P. is presented in Table 3.1. Compressive strength tests were performed at 2, 7 and 28 days of curing and the results are illustrated in Figure 3.4.

Table 3.1. Compressive strength results of C-Clay @ DS_g base and hybrid geopolymer (MPa) at 2, 7, and 28 days.

C-Clay @ DS_g geopolymers		**Curing**		
		2 days	7 days	28 days
A.A.L.	GP-L	40.17 ± 2.15	41.37 ± 2.36	45.2 ± 2.12
	H-GP-L @ PDMS	27.92 ± 1.52	29.46 ± 0.46	47.39 ± 3.46
	H-GP-L @ TEOS	28.77 ± 1.84	35.75 ± 1.82	40.32 ± 2.705
	H-GP-L @ Resin	25.59 ± 1.70	32.90 ± 3.26	50.38 ± 2.87
	H-GP-L @ TP56	29.08± 2.66	32.25± 2.71	35.67± 2.42
A.A.P.	GP-P	32.43 ± 1.65	34.93 ± 2.19	37.32 ± 0.52
	H-GP-P @ PDMS	35.87 ± 3.34	36.96 ± 0.92	37.39 ± 0.62
	H-GP-P @ TEOS	26.73 ± 1.37	28.17 ± 1.76	29.30 ± 1.45
	H-GP-P @ Resin	34.81 ± 2.95	36.21 ± 2.47	36.22 ± 1.90
	H-GP-P @ TP56	25.63 ± 3.97	30.22 ± 3.98	35.60 ± 2.32

At the different stages of testing all the samples showed an increase in compressive strengths from 2 days to 28 days of curing at 65 °C, in agreement with the observations of Wang. Q et al., and Suwan. T. et al,[4,5]. This enhancement is due to the progress of the geopolymerization process. The use of A.A.L. was observed to give higher strength compared to A.A.P. for all samples as in the study of Mustafa Al Bakria AM et al [6]. After 28 days of curing, the samples activated with A.A.L: GP-L, H-GP-L @ PDMS, H-GP-L @ TEOS, H-GP-L @ Resin, and H-GP-L @ TP56, achieved compressive strengths of 45.2, 47.39, 40.32, 50.38 and 35.67 MPa, respectively (Figure 3.4 a). H-GP-L @ Resin had the

[4] Wang Q, Ran K, Ding Z, Qiu L. Research on Mechanical Properties of Geopolymer Concrete under early Stage Curing System. *Appl Mech Mater*. **2012**;164:492-496.

[5] Suwan T, Fan M, Braimah N. Micro-mechanisms and compressive strength of Geopolymer-Portland cementitious system under various curing temperatures. *Mater Chem Phys*. **2016**;180:219-225.

[6] Mustafa Al Bakria AM, Kamarudin H, Bin Hussain M, Khairul Nizar I, Zarina Y, Rafiza AR. The Effect of Curing Temperature on Physical and Chemical Properties of Geopolymers. *Phys Procedia*. **2011**;22:286-291.

highest compressive strength compared to the other samples at 28 days (50.38 MPa), followed closely by H-GP-L @ PDMS (47.39 MPa) both exceeding GP-L strength (45.20 MPa). On the other hand, the H-GP-L @ TP56 hybrid geopolymer showed a low strength value over time reaching 35.67 MPa at 28 days. The compressive strength of H-GP-L @ PDMS after 2 and 7 days was lower compared to GP-L (Figure 3.4 a). Those findings are consistent with results reported by Garcia-Lodeiro et al., who observed a reduction in strength with the addition of PDMS into the materials[7].

Meanwhile, the samples activated with A.A.P, achieved lower compressive strengths of 37.32, 37.39, 29.30, 36.22, and 35.60 MPa, respectively (Figure 3.4 b). H-GP-P @ PDMS show a better compressive strength compared to H-GP-P @ TEOS, H-GP-P @ Resin, and H-GP-P @ TP56, with a slight increase in strength from 2 days to 28 days. In contrast, H-GP-P @ TEOS had the lowest strength values reaching a maximum of 29.30 MPa at 28 days.

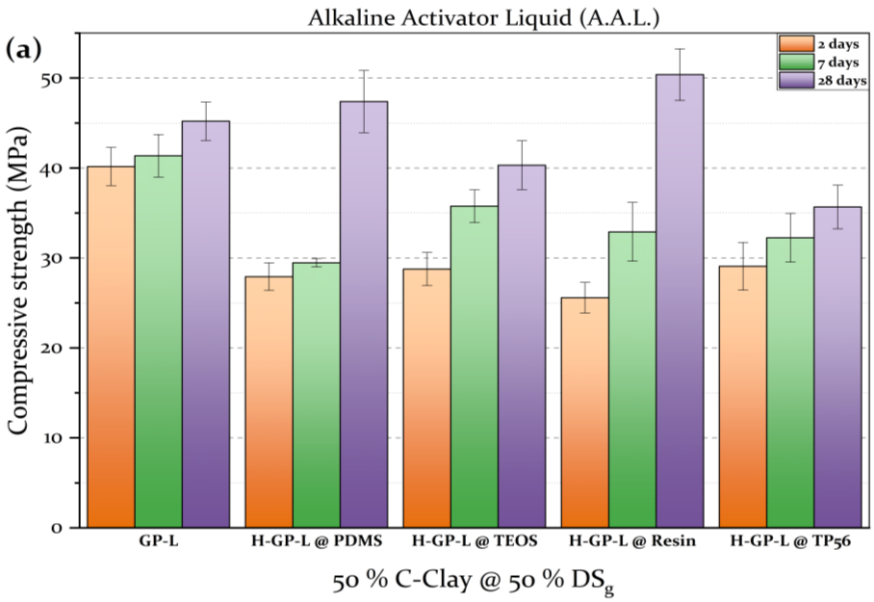

[7] Garcia-Lodeiro I, Gonzalez-Aguza S, Zarzuela R, et al. Studying the dosage-dependent influence of hydrophobic alkoxysilane/siloxane admixtures on the performance of repair micromortars. *J Build Eng*. **2022**;48:103905.

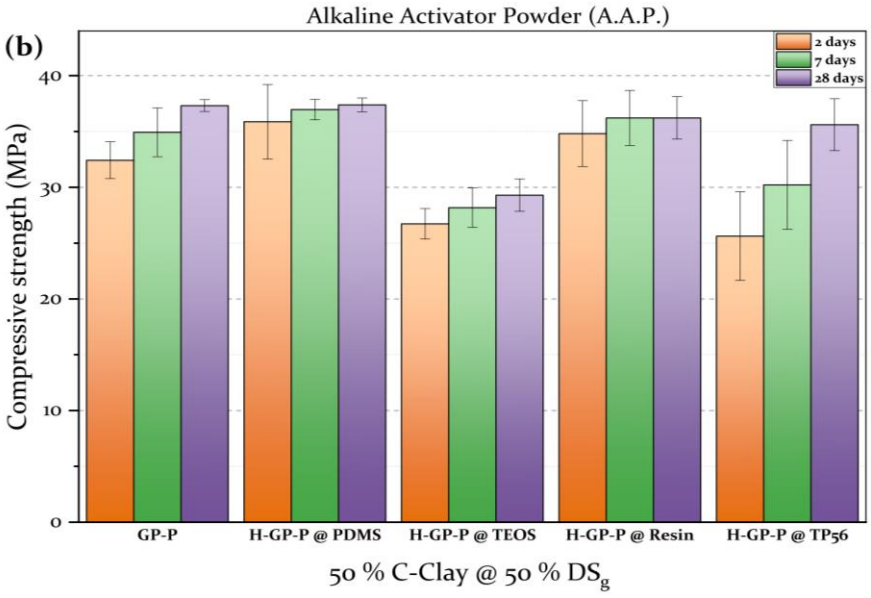

Figure 3.4. Compressive strength of the base and hybrid geopolymers C-Clay @ DS_g activated with (a) A.A.L. and (b) A.A.P.

3.2.3.2. Compressive strength for the hybrid 50 % C-Clay @ 50 % BW with PDMS and TP56

Following the previous results, the two hybrid components PDMS and TP56, were added to calcined clay and brick waste geopolymer mixture in equal proportions (50:50). These components were incorporated at 3 wt.% to form a hybrid geopolymer activated with A.A.L. and A.A.P. The selection of the mixture of calcined clay and brick waste as precursors was motivated by their abundance, low cost for BW, and water resistant. This water resistance was confirmed through a water droplet test, which showed promising results for the hydrophobic properties of the mixture. The compressive strength results for the C-Clay @ BW geopolymer and the hybrid geopolymers after 2, 7 and 28 days of curing are presented in Table 3.2.

Table 3.2. Compressive strength results of C-Clay @ BW base and hybrid geopolymer (MPa) at 2, 7, and 28 days.

	C-Clay @ BW geopolymers	**Curing**		
		2 days	7 days	28 days
A.A.L.	C-Clay @ BW-L	40.32 ± 2.35	49.2 ± 1.44	54.38 ± 1.43
	C-Clay @ BW-L_PDMS	39.31 ± 1.86	45.37 ± 3.26	48.16 ± 4.35
	C-Clay @ BW-L_TP56	36.49 ± 0.60	36.9 ± 0.76	43.15 ± 3.26
A.A.P.	C-Clay @ BW-P	10.50 ± 0.53	13.18 ± 0.55	14.6 ± 0.30
	C-Clay @ BW-P_PDMS	8.03 ± 0.52	11.49 ± 0.24	14.80 ± 1.13
	C-Clay @ BW-P_TP56	2.07 ± 0.17	3.03 ± 0.05	1.93 ± 0.28

Figure 3.5 shows the compressive strength results of hybrid geopolymers activated with A.A.L. (C-Clay @ BW-L) and A.A.P. (C-Clay @ BW-P) with the addition of PDMS and

TP56 separately. The results indicates that the compressive strength increased over time for all samples. Also, for this formulation, samples activated with A.A.L. showed significantly higher compressive strength compared to those activated with A.A.P. Specifically, the base geopolymer C-Clay @ BW-L reached 54.38 ± 1.43 MPa, while C-Clay @ BW-P achieved only 14.6 ± 0.30 MPa at 28 days of curing. However, the addition of the hybrid components PDMS and TP56 to the C-Clay @ BW-L geopolymer (obtaining C-Clay @ BW-L_PDMS and C-Clay @ BW-L_PDMS_TP56, samples respectively) resulted in a compressive strength of 48.16 ± 4.35 MPa and 43.15 ± 3.26 MPa at 28 days, respectively, which were lower than the base C-Clay @ BW-L. In contrast, the hybrid geopolymer activated with A.A.P. (C-Clay @ BW-P_PDMS and C-Clay @ BW-P_TP56) showed compressive strengths of 14.80 ± 1.13 MPa and 1.93 ± 0.28 MPa at 28 days, respectively. These results highlight that the addition of TP56 is not effective in improving the compressive strength of geopolymers.

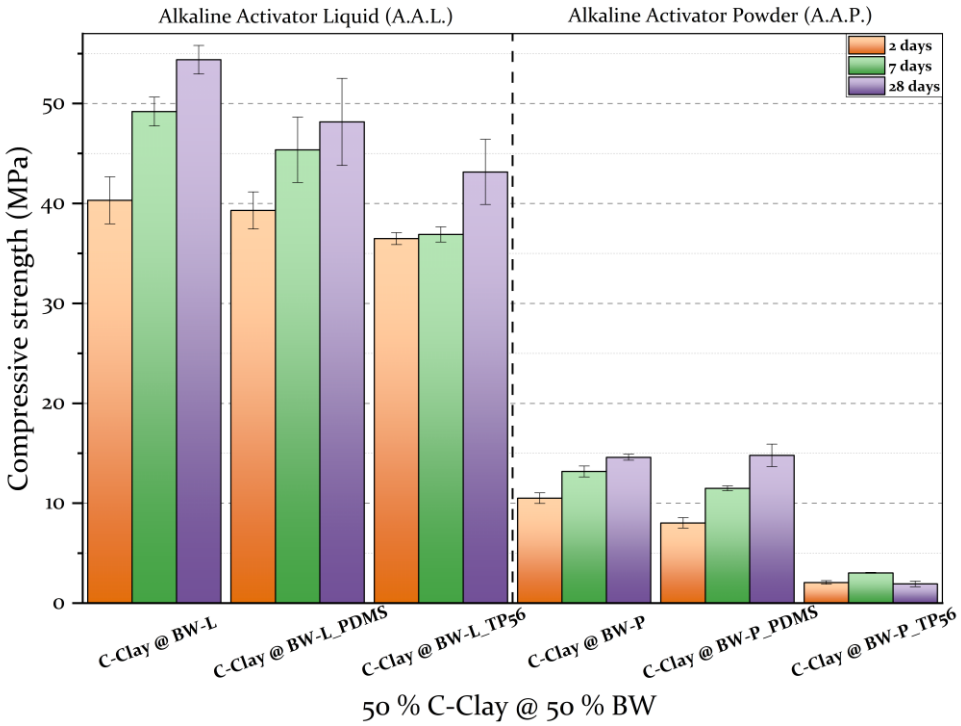

Figure 3.5. Compressive strength of the base geopolymer C-Clay @ BW with hybrid geopolymers incorporating PDMS and TP56 activated with (left) A.A.L. and (right) A.A.P.

Based on the mechanical properties, water droplet results on the surface (Figure 3.6) as well as its advantages such as low cost, non-toxicity, and low volatility, PDMS was selected as best best-performing functional agent in combination with C-Clay @ DS_g mixture. This system was studied in depth, and the results regarding its chemical-physical characterization are reported in the next paragraphs.

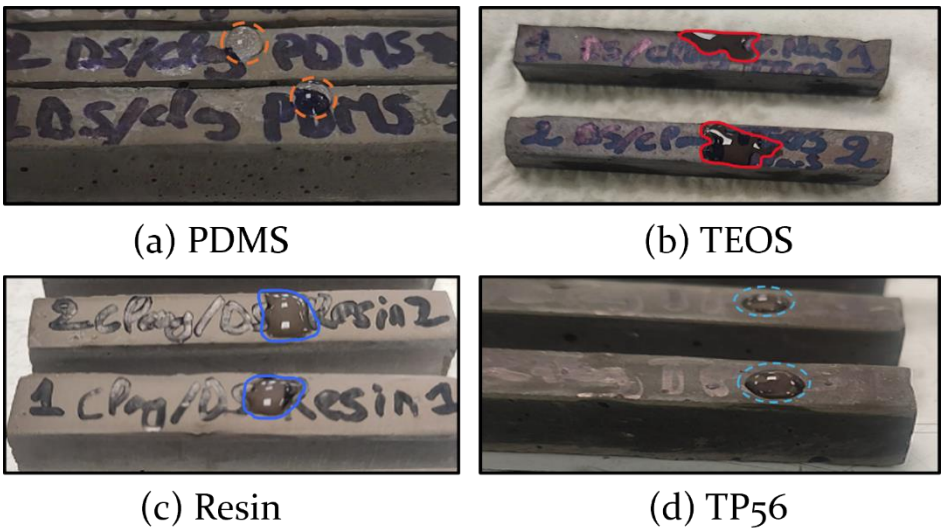

Figure 3.6. Water droplets on various C-Clay @ DS_g hybrid geopolymers.

3.2.3.3. FTIR analysis of 50 % C-Clay @ 50 % DS_g with PDMS activated by (A.A.L and A.A.P)

The FTIR spectra of the 50 % calcined clay and 50 % DS_g with 3 wt. % PDMS activated by A.A.L. and A.A.P. over 2 days and 28 days of curing age are shown in Figure 3.7. The FT-IR spectra of the base geopolymer and hybrid geopolymers were found to be quite similar. The broad peak at around 3445 cm^{-1} and 1639 cm^{-1} correspond to the O-H stretching and bending vibrations, respectively, from hydroxyl groups due to adsorbed water [8,9]. These peaks are present in all samples prepared with both A.A.L. and A.A.P. Figure 3.7 (a) shows some minor changes that occurred after 28 days of curing, with a slight increase in peak intensity. This can be attributed to the dissolution and reaction of the precursors in the alkaline activation solution through hydrolysis and condensation processes [10]. The bands between 950 and 1250 cm^{-1} have been assigned to internal asymmetric vibrations of Si–O–T (T = Al/Si) that reflect the formation of an aluminosilicate network[11]. The peaks at 1260 cm^{-1} in both H-GP-L @ PDMS and H-GP-P @ PDMS samples, after 2 and 28 days of curing, are characteristic of Si-CH_3 groups from PDMS, indicating its successful integration into the geopolymer matrix. In figure 3.7 (a), GP-L and GP-P samples display slightly reduced peak intensity compared to H-GP-L @ PDMS and H-GP-P @ PDMS after 2 and 28 days. This reduction may indicate that the incorporation of PDMS reduces the free hydroxyl groups of water content within the geopolymer matrix.

[8] Zhang Z, Wang H, Provis JL. Quantitative study of the reactivity of fly ash in geopolymerization by ftir. *J Sustain Cem Mater*. **2012**;1(4):154-166.
[9] Panias D, Giannopoulou IP, Perraki T. Effect of synthesis parameters on the mechanical properties of fly ash-based geopolymers. *Colloids Surfaces A Physicochem Eng Asp*. **2007**;301(1-3):246-254.
[10] Rees CA, Provis JL, Lukey GC, Van Deventer JSJ. In situ ATR-FTIR study of the early stages of fly ash geopolymer gel formation. *Langmuir*. **2007**;23(17):9076-9082.
[11] M S, R J, P RN. Effect of change in the silica modulus of sodium silicate solution on the microstructure of fly ash geopolymers. J Build Eng. **2021**;44:102939.

Therefore, the FTIR spectra of the hybrid geopolymer activated with 6 % Na_2SiO_3 and water (A.A.P.) reveal similar structural modifications to those observed in the hybrid geopolymer activated with A.A.L. when we added PDMS.

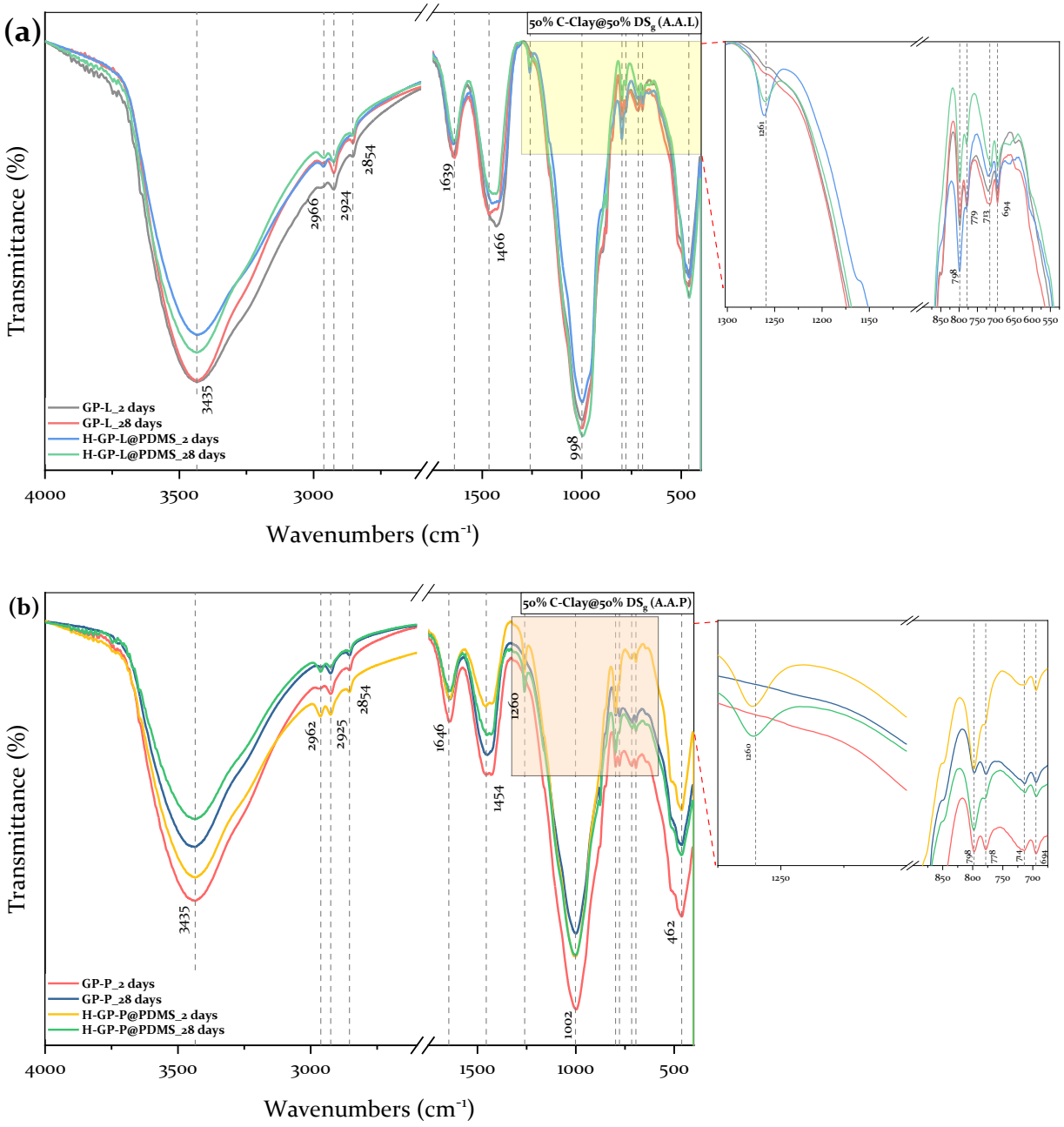

Figure 3.7. FTIR spectra of C-Clay @ DS_g geopolymers (GP) and hybrid geopolymers (H-GP) with 3 wt.% PDMS, prepared with (a) A.A.L and (b) A.A.P after 28 days.

3.2.3.4. Mineralogical characterization of 50 % C-Clay @ 50 % DS_g (H-GP @ PDMS)

The XRD graphs of the geopolymer and hybrid geopolymer (with 3 wt.% PDMS) activated with A.A.L. and A.A.P. are shown in Figure 3.8. Generally, geopolymer materials consist of a mixture of crystalline phases, such as quartz, and amorphous phases. In the XRD patterns (Figures 3.8a and 3.8b), several distinct peaks corresponding to crystalline

phases, including quartz (Qz) and muscovite (Mu), are evident in both the geopolymer and hybrid geopolymer pastes. The presence of these crystalline phases confirms that some of the starting materials were not fully ground, compaction issues occurred during sample preparation, and/or some materials remained unreacted within the geopolymer matrix. In the samples activated with A.A.L. (Figure 3.8a), the intensity of the quartz peaks is notably higher compared to those in samples activated with A.A.P. (Figure 3.8b), suggesting a more pronounced crystalline structure in the A.A.L. samples. Specifically, the quartz peaks are observed around 26.6° 2θ, while muscovite peaks appear around 8.8° and 28.3° 2θ.

Additionally, the XRD patterns show that the hybrid geopolymer (H-GP-L @ PDMS) exhibits a slightly more intense peak around 26.6° 2θ for quartz compared to GP-L, which may indicate that the addition of PDMS affects the degree of crystallinity or enhances the visibility of existing crystalline phases. This effect is consistent in both activation methods, but more pronounced in samples activated with the liquid activator (A.A.L.). Thus, the XRD analysis suggests that the incorporation of PDMS does not disrupt the existing crystalline phases in the geopolymer but may enhance the crystalline nature of certain phases.

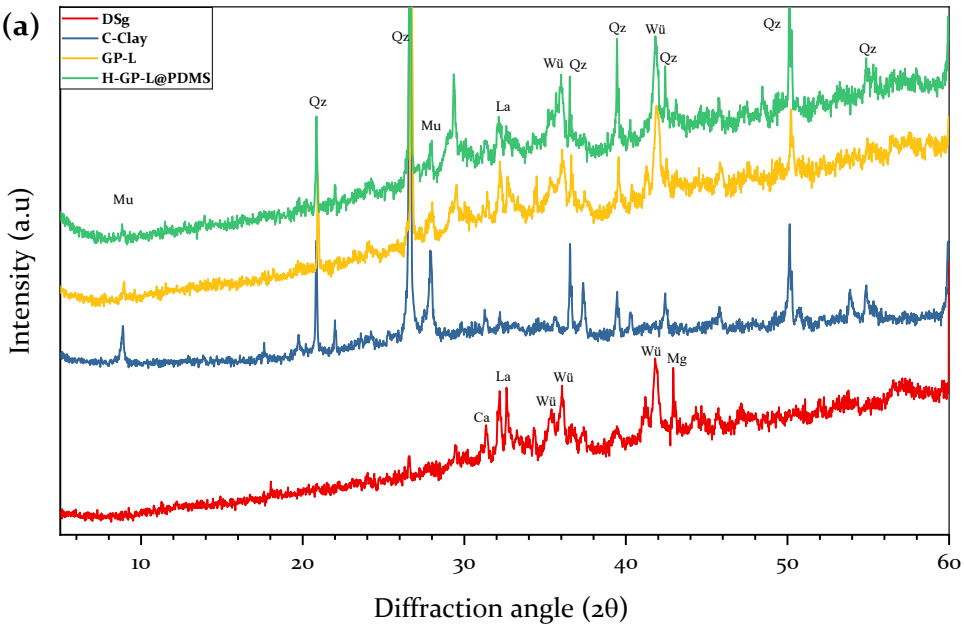

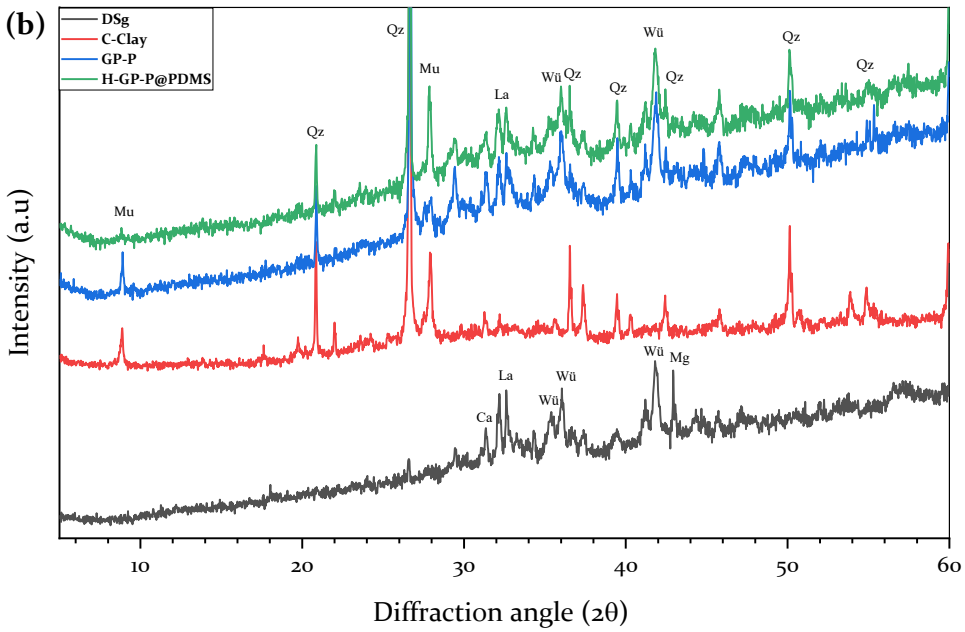

Figure 3.8. XRD patterns of the C-Clay, DS_g raw materials, base geopolymer (GP) and hybrid geopolymer (H-GP @ PDMS) made with (a) A.A.L. and (b) A.A.P. after 28 days.

3.2.3.5. Thermal analysis of 50 % C-Clay @ 50 % DS_g (GP and H-GP @ PDMS) after 28 days

Thermogravimetric (TG), differential thermal (DTA), and differential scanning calorimetry (DSC) analyses were used in order to study the physical and chemical transformations of the different geopolymer samples: GP-L, GP-P, H-GP-L @ PDMS, and H-GP-P @ PDMS after 28 days of curing, and the results are presented in Figure 3.9. It is clear that in all four samples, an exothermic peak of DTG (red line) appears between room temperature and 200 °C, which is associated with the evaporation of water [12].

In the last stage, the DTG curve shows exothermic peaks at temperatures between 500 to 700 °C (e.g., 630.47 °C for GP-L, 649.88 °C for GP-P, 655.92 °C for H-GP-L @ PDMS, and 643.88 °C for H-GP-P @ PDMS) because of the burning of exposed carbon obtaining CO_2 release due to chemical reaction [13]. The total weight losses for GP-L, GP-P, H-GP-L @ PDMS and H-GP-P @ PDMS are 10.98 % (3.4 mg), 9.43 % (2.85 mg), 12.02 % (3.78 mg) and 10.15 % (2.95 mg), respectively. The DTA confirms that the geopolymers activated with A.A.P. have more thermal stability compared to the geopolymers activated with A.A.L.

[12] Cong P, Mei L. Using silica fume for improvement of fly ash/slag based geopolymer activated with calcium carbide residue and gypsum. *Constr Build Mater*. **2021**;275:122171.
[13] Ul Haq E, Padmanabhan SK, Licciulli A. In-situ carbonation of alkali activated fly ash geopolymer. Constr Build Mater. **2014**;66:781-786.

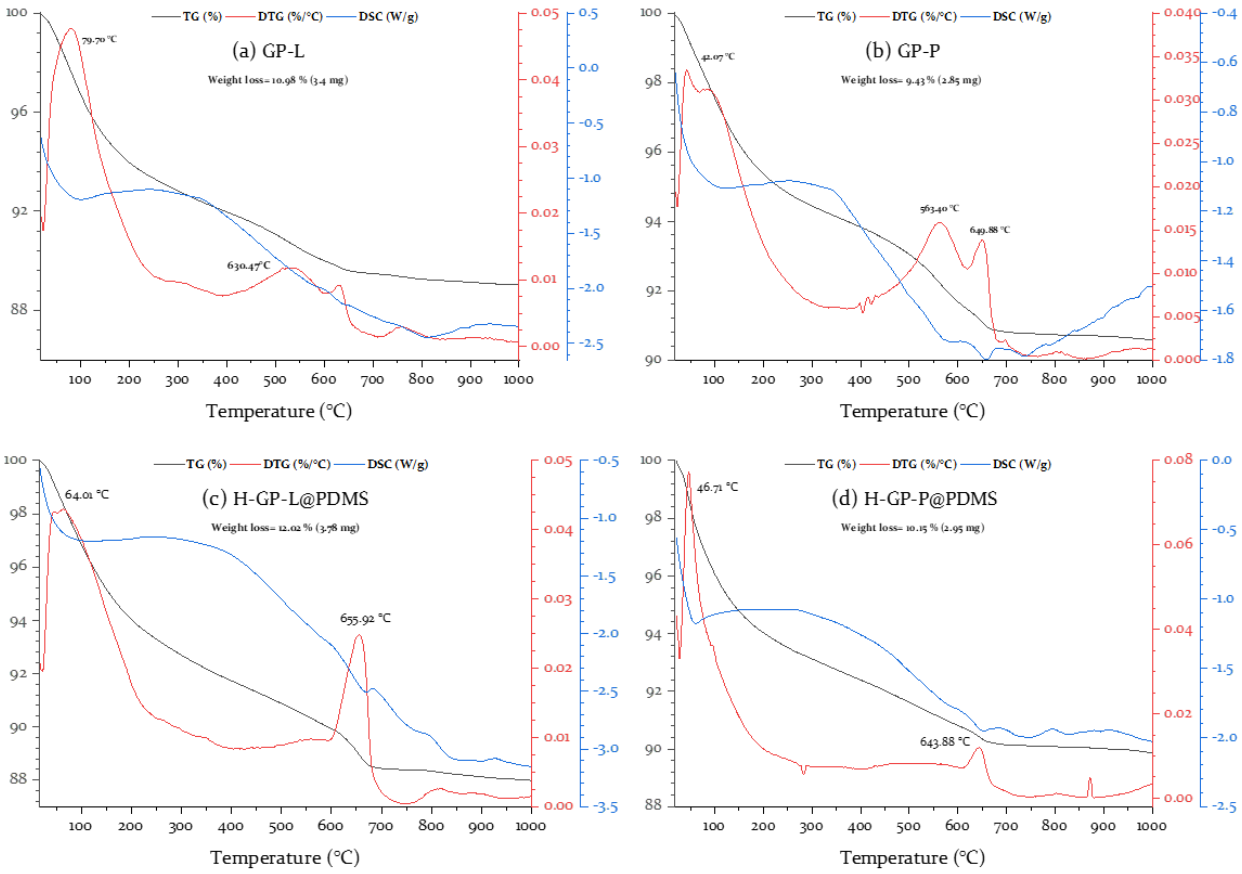

Figure 3.9. TG/DTG/DSC of (a) GP-L, (b) GP-P geopolymers, and (c) H-GP-L @ PDMS and (d), H-GP-P @ PDMS hybrid geopolymers made with A.A.L. and A.A.P. after 28 days.

3.2.3.6. Morphological study of 50 % C-Clay @ 50 % DS_g geopolymers activated with (A.A.L and A.A.P)

The microstructure of 50 % C-Clay @ 50 % DS_g hybrid geopolymers (H-GP-L @ PDMS) was examined through SEM, providing valuable insights (Figure 3.10). The SEM images show a heterogeneous surface with visible cracks as shown in Figure 3.10 a, while Figure 3.10 b shows spherical particles from the DS_g possibly due to the unreacted DS_g particles mixed with C-Clay particles resulting from the ground process. In addition, from Figure 3.10 c, pores and crystals can be observed within the geopolymer matrix. These crystals can improve compressive strength and durability. Furthermore, very high magnifications show a dense material with finely dispersed particles possibly due to the incorporation of PDMS (Figure 3.10 d). Microcracks are present, which are responsible for the lower strength compared to the base geopolymer (GP-L). Despite this, the results show that PDMS significantly enhances the water resistance and hydrophobicity of the hybrid geopolymer.

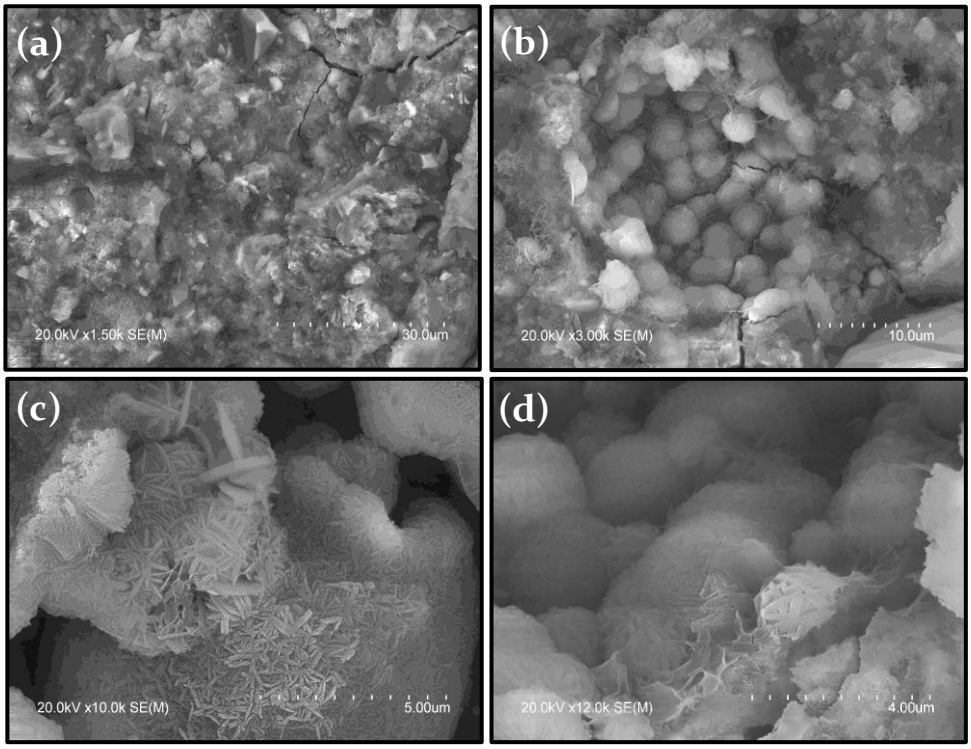

Figure 3.10. SEM Images of 50 % C-Clay @ 50 % DS_g hybrid geopolymers activated with A.A.L. (H-GP-L @ PDMS).

The SEM images shown in Figure 3.11 (at ×2.00K magnification) correspond to the 50 % C-Clay @ 50 % DS_g hybrid geopolymers (H-GP-P @ PDMS) activated with A.A.P. Figures 3.11 a and 3.11 b, reveal a rough and heterogeneous surface with visible microcracks and porosity. Compressive strength results are in accordance with this evidence (see Figure 3.4).

At higher magnifications ×6.00K (Figures 3.11 c and d), it is possible to observe crystalline phases within the geopolymer matrix. This indicates that PDMS helped to form a strong network. However, there are many microcracks which have reduced the compressive strength of the final product compared to the hybrid geopolymer made by A.A.L. (H-GP-L @ PDMS).

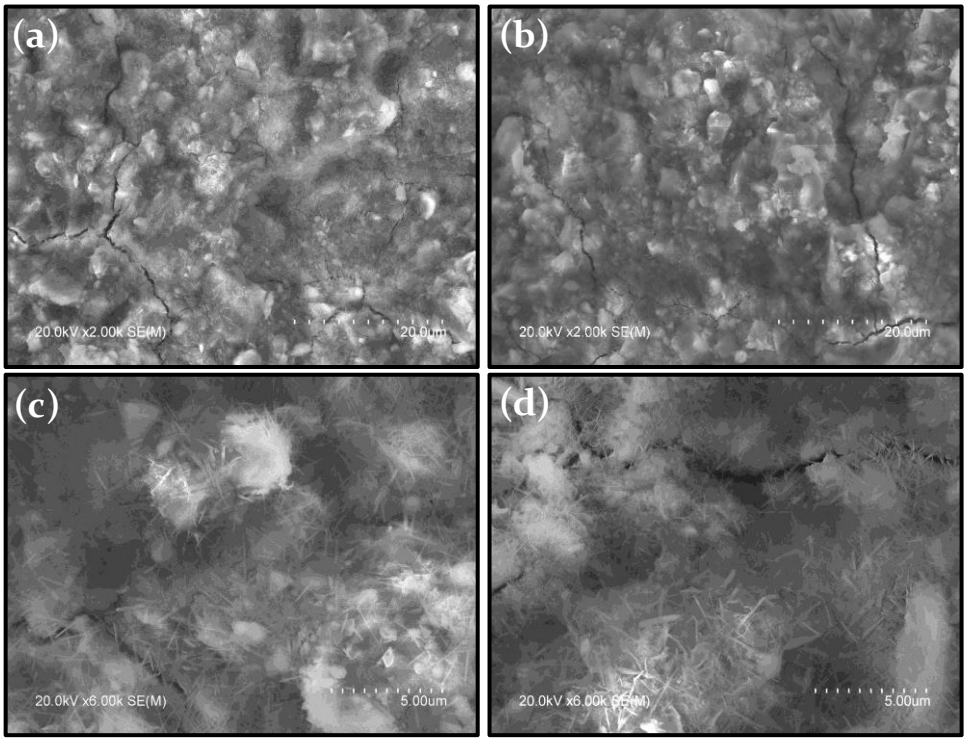

Figure 3.11. SEM Images of 50 % C-Clay @ 50 % DS_g hybrid geopolymers activated with A.A.P (H-GP-P @ PDMS).

3.2.3.7. Pore size distribution for the base and hybrid geopolymers (GP and H-GP @ PDMS)

The porosity data for the base geopolymer (GP) and hybrid geopolymers (H-GP) composed of the mixture of (50 % C-Clay and 50 % DS_g) are presented in Table 3.3. Figure 3.12 shows the pore size distribution of the hybrid geopolymer at curing age of 2 and 28 days. The results indicate the differences in porosity and bulk density between the different samples activated with Alkaline Activator Liquid (A.A.L.) and Alkaline Activator Powder (A.A.P.).

Table 3.3. Total porosity (%) and bulk density (g/cm³) for base (GP) and hybrid (H-GP) geopolymers.

Samples	**Total porosity (%)**		**Bulk Density (g/cm³)**	
	2 days	28 days	2 days	28 days
Base geopolymer (GP-L)	24.41	22.72	2.54	2.34
Hybrid geopolymer (H-GP-L @ PDMS)	22.66	24.37	1.98	1.76
Base geopolymer (GP-P)	30.12	29.13	1.78	1.78
Hybrid geopolymer (H-GP-P @ PDMS)	24.69	19.31	1.86	1.93

Hybrid geopolymers activated with A.A.L. (H-GP-L @ PDMS) show an increase of about 7.5 % in the porosity, from 22.66 % to 24.37 %, between 2 days to 28 days. Additionally, the bulk density decreases from 1.98 g/cm³ to 1.76 g/cm³ due to the

formation of additional pores of the geopolymer matrix. In contrast, the base geopolymers (GP-L) show a decrease in both porosity and bulk density.

In contrast, hybrid geopolymers activated with A.A.P. (H-GP-P @ PDMS) show a 22 % decrease in porosity, from 24.69 % to 19.31 %, and an increase in bulk density from 1.86 g/cm³ to 1.93 g/cm³ at 2 days and 28 days, respectively. Generally, extended curing period results a reduction of porosity within the material [14]. The base geopolymers (GP-P) show a high porosity, which correlates with a reduction in compressive strength (see Chapter 2, Figure 2.11 c), as denser materials typically exhibit lower porosity [15].

Higher porosity, it means that there are more empty spaces in materials structure, which can reduce its strength. On the other hand, lower porosity indicates that there are fewer gaps, leading to a denser structure and resulting in higher compressive strength for the material [16].

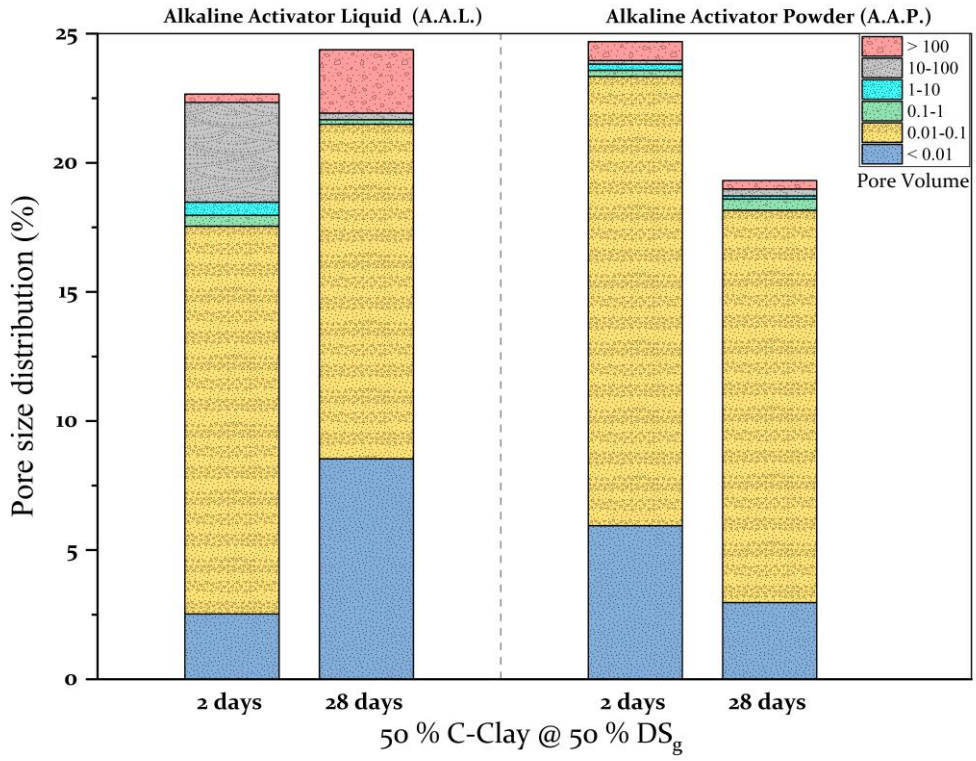

Figure 3.12. Porosity and pore size distribution of hybrid geopolymers samples with 3 wt.% PDMS, activated with A.A.L and A.A.P after 2 and 28 days of curing.

[14] Mo Z, Gao X, Su A. Mechanical performances and microstructures of metakaolin contained UHPC matrix under steam curing conditions. *Constr Build Mater*. **2021**;268:121112.
[15] Jaya NA, Yun-Ming L, Cheng-Yong H, Abdullah MMAB, Hussin K. Correlation between pore structure, compressive strength and thermal conductivity of porous metakaolin geopolymer. *Constr Build Mater*. **2020**;247:118641.
[16] Chen S, Ruan S, Zeng Q, et al. Pore structure of geopolymer materials and its correlations to engineering properties: A review. *Constr Build Mater*. **2022**;328:127064.

3.2.3.8. Water absorption for the base and hybrid geopolymers (GP and H-GP @ PDMS)

Water absorption (WA) is a crucial property of the geopolymer which can significantly impact their durability [17]. It is important to note that water absorption increases as the defect in surface porosity increases [18]. Figure 3.13 a illustrates the amount of water absorption by the test area of four (04) materials: geopolymers (GP-L and GP-P) and hybrid geopolymers (H-GP-L @ PDMS and H-GP-P @ PDMS) specimens after 28 days of curing. The results of water absorption are summarized in Table 3.4. The Figure shows that the results of WA were affected by the type of alkaline activator used and the incorporation of PDMS. It can be seen that all geopolymer specimens manufactured with A.A.P. (6 % Na_2SiO_3 and water) have lower water absorption values compared to those produced with A.A.L. as in the case of GP-L and H-GP-L @ PDMS. Figure 3.13 b shows that the GP-L sample has rapid water absorption within the first 3 minutes, which absorbed the entire quantity in the column (~ 5 ml). This increment in water absorption may be attributed to the presence of microcracks in the sample. In contrast, the GP-P sample absorbed the full amount in the column (~ 5 ml) after 24 hours, which indicates a high capacity for long-term water absorption.

The amount of water absorbed per unit area in the GP-P geopolymer decreased after 24 hours compared to H-GP-P @ PDMS, which reduced from 0.96 ± 0.07 to 0.09 ± 0.01 ml/cm² (91 % reduction) when adding 3 wt.% PDMS. Furthermore, both H-GP-L @ PDMS and H-GP-P @ PDMS, exhibited significantly reduced water absorption (WA), with H-GP-P @ PDMS absorbing the least amount of water. After 24 hours, the water absorption values for the hybrid geopolymers (H-GP-P @ PDMS and H-GP-L @ PDMS) were 0.09 ± 0.014 and 0.56 ± 0.09, respectively. This decrease in water absorption is due to the reduction in the porosity (Figure 3.12) and the nature of the organic modifier (PDMS) which exhibits hydrophobicity due to the presence of methyl ($-CH_3$) groups in its molecular structure. These groups, with their low surface energy, make the surface energetically unfavorable for interactions with polar water molecules [19].

[17] Niveditha M, Koniki S. Effect of Durability properties on Geopolymer concrete – A Review. E3S Web Conf. **2020**;184:01092.
[18] Rashad AM, Khafaga SA, Gharieb M. Valorization of fly ash as an additive for electric arc furnace slag geopolymer cement. *Constr Build Mater*. **2021**;294:123570.
[19] Tang D, Yang C, Shen C, Yu L, Tian Y, Zhu X. Preparing hydrophobic alkali-activated slag mortar with lotus-leaf-like microstructure by adding polydimethylsiloxane (PDMS). *Constr Build Mater*. **2023**;409:134148.

Table 3.4 The amount of water absorbed (W_i) by the test area (Q_i) [ml/cm^2] at the time (t_i).

Time (min)	The amount of water absorbed W_i (ml/cm^2)			
	GP-L	H-GP-L @ PDMS	GP-P	H-GP-P @ PDMS
1	0.57602 ± 0.04145	0	0.03289 ± 0.01104	0
2	0.82456 ± 0.01754	0	0.05263 ± 0.01432	0
3	0.91813 ± 0.04415	0	0.07237 ± 0.00439	0
4	/	0	0.08772 ± 0.00716	0
5	/	0.00292 ± 0.00506	0.10088 ± 0.00877	0
10	/	0.01462 ± 0.00506	0.15132 ± 0.0084	0
15	/	0.02339 ± 0.00506	0.1886 ± 0.00877	0
20	/	0.03041 ± 0.00442	0.22281 ± 0.01425	0
25	/	0.04386 ± 0.00877	0.25 ± 0.01519	0
30	/	0.04795 ± 0.00442	0.27632 ± 0.02208	0
35	/	0.05556 ± 0.00506	0.30263 ± 0.02532	0
40	/	0.06608 ± 0.00709	0.32895 ± 0.02996	0
45	/	0.0731 ± 0.0134	0.34649 ± 0.02996	0
50	/	0.08187 ± 0.0134	0.37193 ± 0.04011	0
55	/	0.09064 ± 0.02026	0.39035 ± 0.04558	0.00234 ± 0.00405
60	/	0.09942 ± 0.0282	0.41447 ± 0.04717	0.00234 ± 0.00405
120	/	0.15497 ± 0.01826	0.61184 ± 0.06958	0.00994 ± 0.00664
180	/	0.21053 ± 0.03039	0.77632 ± 0.08989	0.00994 ± 0.00664
24 h	/	0.5614 ± 0.08745	0.96491 ± 0.07162	0.08538 ± 0.01418

3.2.3.9. Contact angle test for the base and hybrid geopolymers (GP and H-GP @ PDMS)

The contact angle (CA) test was employed to evaluate the wettability of the surface of the geopolymer materials: GP-L, GP-P, H-GP-L @ PDMS, and H-GP-P @ PDMS to understand the behaviors of surfaces in contact with water and their ability to resist water-induced damage. Materials with contact angles less than 90° are classified as hydrophilic, while those with contact angles above 90° are known as hydrophobic. Furthermore, materials with contact angles greater than 120° are classified as over-hydrophobic, and those with contact angles exceeding 150° are deemed superhydrophobic [20,21].

Figure 3.13 a illustrates the effect of PDMS on the surface wettability of different geopolymer samples. The surface of GP-P is hydrophilic, with a CA of 90°, while GP-L with a CA of 35°, indicates rapid water absorption, and this correlates with porosity

[20] Zhong WL, Zhang YH, Fan LF, Li PF. Effect of PDMS content on waterproofing and mechanical properties of geopolymer composites. *Ceram Int*. **2022**;48(18):26248-26257.
[21] Ruan S, Chen S, Liu Y, Zhang Y, Yan D, Zhang M. Early-age deformation of hydrophobized metakaolin-based geopolymers. *Cem Concr Res*. **2023**;169:107168.

results, and the presence of microcracks observed in the SEM images (Figures 3.10 and 3.11). The addition of 3 % PDMS to the base geopolymer (GP-P) increased the contact angle by 42.33 %, which means that the surface became more hydrophobic and stable for water droplets. However, the CA of H-GP-L @ PDMS is 108.5°, which increased compared to the base geopolymer without PDMS (GP-L). Despite this, H-GP-L @ PDMS is slightly less hydrophobic than H-GP-P @ PDMS.

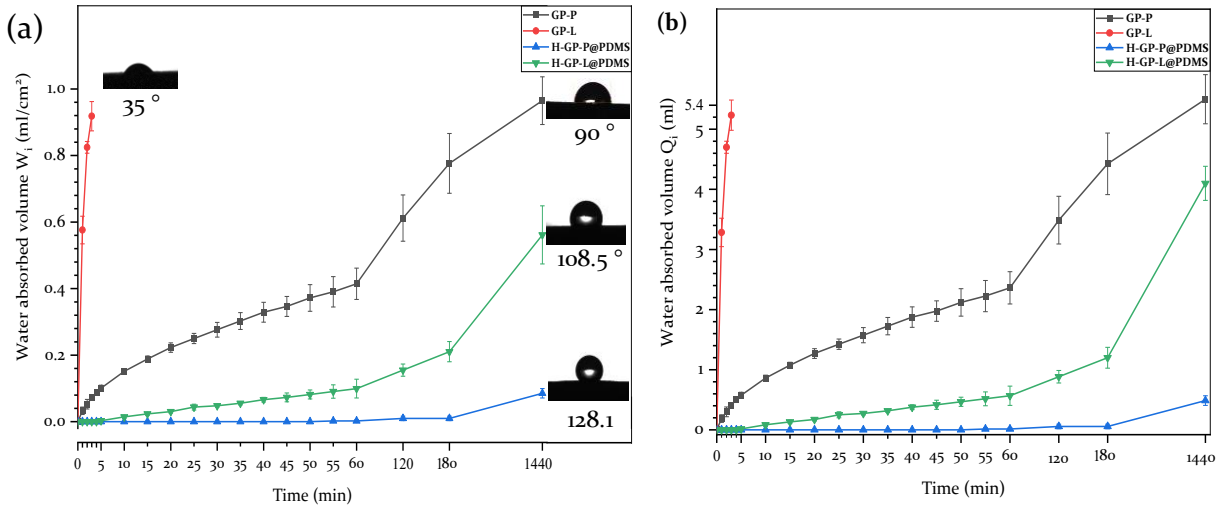

Figure 3.13. Water absorption test of the base geopolymers (GP-P and GP-L) and hybrid geopolymers (H-GP-P @ PDMS and H-GP-L @ PDMS) at 28 days of curing.

3.3. Conclusions

In this chapter, we investigated the preparation of two hybrid geopolymers based on two distinct base matrices; one composed of calcined clay mixed with electric arc furnace slag (50 % C-Clay @ 50 % DS_g) and the other composed of calcined clay mixed with brick waste (50 % C-Clay @ 50 % BW). Both matrices were activated using either A.A.L. or A.A.P. With a rational design and development approach, different hybrid geopolymers were synthesized using the 50 % C-Clay @ 50 % DS_g blend, which was functionalized separately with 3 wt.% of four (04) functional agents: PDMS, TEOS, acrylic resin, and TP56. Meanwhile, 50 % C-Clay @ 50 % BW was functionalized only with PDMS, and TP56 separately.

In general, the results demonstrated a consistent increase in compressive strength from 2 to 28 days of curing. For both hybrid geopolymers (50 % C-Clay @ 50 % DS_g and 50 % C-Clay @ 50 % BW), the samples activated with A.A.L. showed significantly higher compressive strength compared to those activated with A.A.P. In the case of 50 % C-Clay @ 50 % DS_g activated with A.A.L., the addition of acrylic resin resulted the highest strength, followed closely by PDMS. Meanwhile, in the samples activated with A.A.P., PDMS showed better compressive strength compared to other functional agents. For the hybrid geopolymer based on 50 % C-Clay @ 50 % BW, the addition of TP56 has no effect in improving the compressive strength of geopolymers.

The FTIR spectra of the hybrid geopolymer activated by A.A.P. displayed similar modifications to the hybrid geopolymer activated with A.A.L. The XRD analysis indicates that the incorporation of PDMS does not change the phases in the geopolymer. Additionally, the DTG analysis confirmed that geopolymers activated with A.A.P. exhibit slightly greater thermal stability compared to those activated with A.A.L. The morphological study of 50 % C-Clay @ 50 % DS_g-based hybrid geopolymers, conducted through the SEM, indicates the presence of microcracks in both samples activated with A.A.L. and A.A.P.

The porosity results showed that in the sample activated with A.A.L., total porosity increased, and bulk density decreased. In contrast, hybrid geopolymers activated with A.A.P. exhibited a decrease in porosity and an increase in bulk density. Regarding water absorption (WA), hybrid geopolymer samples produced with A.A.P. have lower water absorption values compared to those produced with A.A.L. likely due to the increased porosity in the A.A.L.- activated samples. The contact angle (CA) measurement showed that GP-P is hydrophilic (rapid water absorption), while H-GP-P @ PDMS is highly hydrophobic (resistant to water absorption). The hybrid geopolymer made with A.A.L. (H-GP-L @ PDMS) is less hydrophobic than hybrid geopolymer made with A.A.P. (H-GP-P @ PDMS), which is consistent with contact angle results.

The results show that PDMS enhances slightly the mechanical properties, and significantly improve the water absorption resistance of the hybrid geopolymers. Future experiments will focus on optimization the hybrid geopolymer formulation by the addition of other and different amounts of functional agents that can act in synergy with PDMS to enhance the consolidation properties of the final material, while preserving its excellent water resistance and hydrophobic characteristics.

CHAPTER 4

LIFE CYCLE ASSESSMENT (LCA)

This chapter provides a concise overview of the life cycle analysis of building materials, with a focus on evaluating their environmental contributions. By emphasizing previous research and theoretical developments, it underscores the need to integrate advanced materials and innovative technologies into construction practices to foster a more ecologically conscious economy. The chapter highlights the potential of geopolymers as a sustainable alternative to conventional materials, stressing the importance of impact assessment through life cycle analysis (LCA) and life cycle cost analyses to optimize the production processes of geopolymers and hybrid geopolymers. It concludes by outlining the methods that will be employed in future research, focusing on the use of LCA and cost analyses to assess the environmental and economic performance of these materials, with the aim of driving greener and more sustainable production practices.

4.1. Sustainable development

Currently and internationally, several steps have been taken to protect the environment and preserve biota, in order to reduce or eliminate all sources and types of pollution caused by the related economic sector, while thinking about both economic gain and social happiness [1]. Indeed, we are talking about sustainable development, a concept of development that fits into a long-term perspective and integrates environmental and social constraints into the economy, while meeting current needs and preserving the right of future generations to use their wealth wisely.

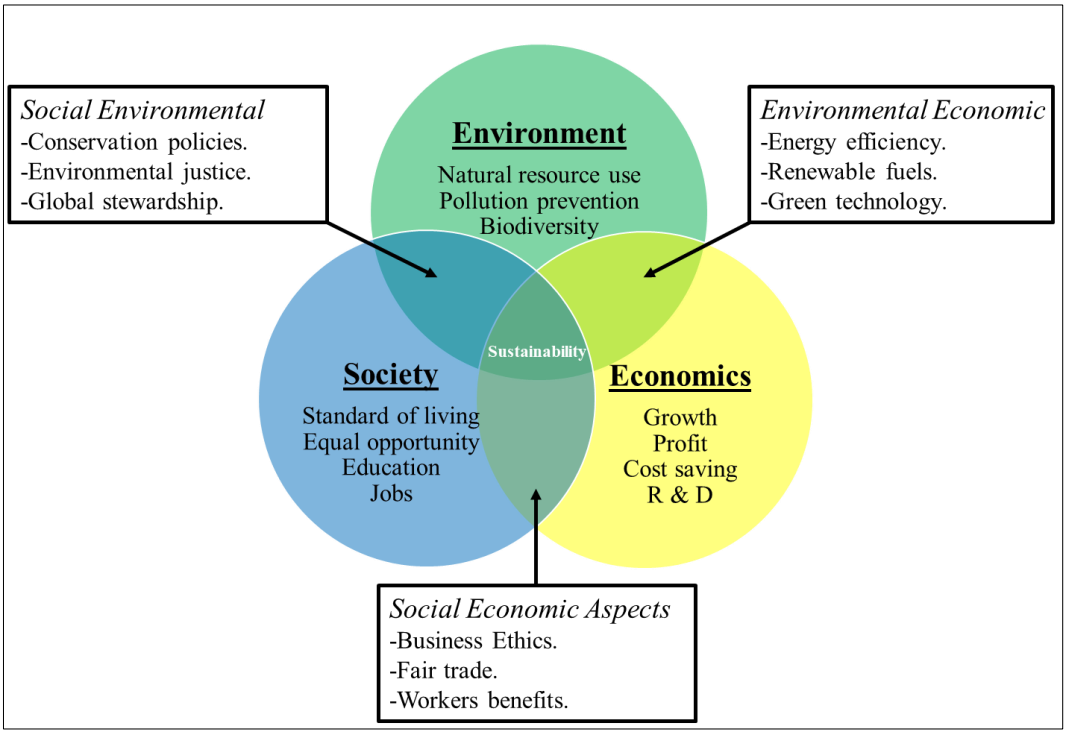

Figure 4.1. Interplay of the environmental, economic, and social aspects of sustainable development [2].

Following this new international policy, the building sector, like any other economic sector, is faced with an obligation to adapt to the main criteria and approaches [3]:

- Think globally, act locally.
- Respect the principles of solidarity, precaution, responsibility and participation.
- Maintain the three pillars: environmental, social and economic.

The use of locally recyclable biomaterials to produce building materials and/or the proposal of less toxic and polluting synthesis protocols have therefore become the focus of an increasing amount of scientific research, which lowers the global carbon footprint and, in the meantime, affirms responsibility and individual and/or collective involvement

[1] Maqbool R, Arul T, Ashfaq S. A mixed-methods study of sustainable construction practices in the UK. *J Clean Prod*. **2023**;430.
[2] Fedkin MR et al. Adopted from the University of Michigan Sustainability Assessment. Published online **2002**.
[3] Wang M, Pan X, Shen Y, Xu H, Tian L. Construction and evolutionary pattern of the coupling relationship network of regional sustainable development in China. *J Clean Prod*. **2024**;445.

within a framework of global solidarity. Sustainable building goods, also known as eco-construction products, include green concrete, biocomposites, and geopolymers, among others, without forgetting a thought to ensure optimal energy performance [4,5,6]. Each of these systems has benefits and limitations in terms of applicability such as the product to be synthesized, cost, sustainability, legislation, etc [7].

4.2 . Eco-construction

In order to respect the principles of sustainable development, housing is built or renovated using less polluting and less toxic materials, most often organic materials, with a design that employs a minimum number of machines, a water recovery system and while rationing energy consumption, representing in this way an eco-construction philosophy.

Indeed, as soon as a building is used for several decades, it is necessary to be interested in its impact on the environment, both in terms of the construction itself and in terms of the elements that constitute it and which we call "materials and building components".

This can only be done using a "life cycle" approach. Most studies show that the phases of use and end of life of a building and/or its construction materials are important or even predominant in terms of environmental impacts [8].

Reducing these environmental repercussions is really the primary goal of eco-conception, also known as eco-design, which sits at the core of a company's sustainable growth strategy. Therefore, eco-conception simply consists of integrating a fourth criterion (environment) into the three criteria used in conception (technical reliability, cost control and customer expectation).

It is believed that about 80 % of the costs of a product over its entire life cycle are a direct consequence of the choices made during the design phase. Since only 10 % of total product development costs are devoted to the conception (design) phase, it is reasonable to believe that good control of impacts from the conception (design) stage will hardly increase the overall cost of product [8]. Figure 4.2 shows the cost/impact ratio in the conception (design) process.

Therefore, the synthesis of geomaterials, as building materials, has been included in an eco-design approach that must be done by keeping a life cycle thinking (multi-stage approach) and by focusing on several environmental impacts (multi-criteria approach).

[4] Rajesh Antony M, Raj Rajendran R, Al- Khazaleh M, Joe A, prince S. Thermal insulation performance of green concrete using bio and industrial wastes: An experimental approach. *Mater Today Proc*. Published online **2023**.

[5] Ren Y, Zhong Y, Yang Y, et al. Green recyclable biocomposite prepared from lignin and bamboo. *J Clean Prod*. **2024**;449.

[6] Çelikten S, Sarıdemir M, Soloğlu M. Effects of elevated temperatures and cooling regimes on the waste andesite dust-based geopolymer mortars. *Constr Build Mater*. **2024**;422.

[7] Aïdo. Revue Internationale de recherche et de développement. *Rev Int Rech Jurid Polit*. **2020**;5:512-529.

[8] Menet JL, Gruescu IC. *L'éco-Conception Dans Le Bâtiment En 37 Fiches-Outils*. Dunod; **2014**.

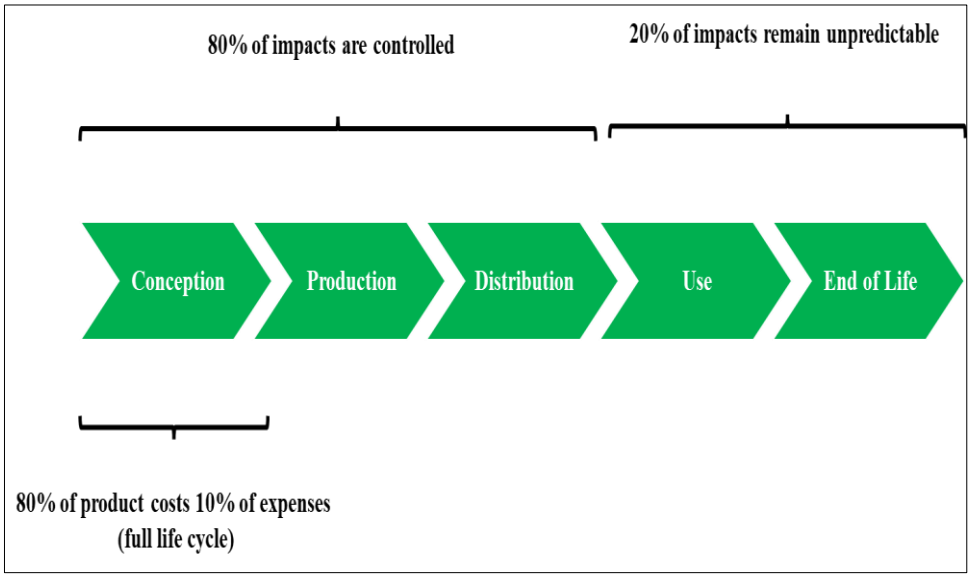

Figure 4.2. Cost/impact ratio in the conception (design) process.

Like the quality approach described by ISO 9 001 and later, environmental management, defined by ISO 14 001 and later, is based on continuous improvement. Thus, an eco-designed product must have a lower environmental impact than the product it replaces, and so on.

The Continuous Improvement approach is very well known in the industrial world. It is based on the Deming principle, also called PDCA (Plan Do Check Act) [9,10]. This method takes place in four successive stages aimed at establishing a virtuous circle, allowing them to constantly improve the quality of a product or activity (table 4.1).

In the case of eco-design, we speak of the POEMS (Product Oriented Environmental Management System) approach [11], a continuous improvement that allows them to [8]:

- Compare different design alternatives from an environmental perspective.
- Measure the environmental inputs generated.
- Identify opportunities for environmental innovation (eco-innovation).

Therefore, research on geopolymer materials in eco-construction follows the next methodological steps: Planning, preliminary and detailed design, testing and prototyping, production and finally product review. However, it remains very important to think about the Life Cycle Assessment (LCA).

[9] Jovanović B, Filipović J, Bakić V. Energy management system implementation in Serbian manufacturing – Plan-Do-Check-Act cycle approach. *J Clean Prod*. **2017**;162:1144-1156.
[10] Energy Management Systems - Requirements and Recommendations for Implementation. Published online **2018**.
[11] Van Berkel R, Van Kampen M, Kortman J. Opportunities and constraints for Product-oriented Environmental Management Systems (P-EMS). *J Clean Prod*. **1999**;7(6):447-455.

Table 4.1: Continuous improvement approach applied to eco-design [8, 9].

Plan	Do	Check	Act
• **Definition of the methodology.** • **Eco-design policy.** • **Regulatory watch.** • **Identification of the texts to be applied.** • **Identification of strategic study axes(s).**	• Environmental Impact Assessment • Design and/or redesign • Regulatory compliance	• Assessment of regulatory compliance • Technical improvement assessment • Environmental impact reduction assessment	• Product innovation • Improved product environmental performance • Taking into account regulatory developments

The following figure 4.3. details the life cycle of a fictitious product, from the reception of the raw material to the finished reusable product, with the emission of industrial waste. Therefore, life cycle assessment (LCA) shows in which stage of production the environmental impact is high, which facilitates decision-making in this stage for a more ecological industry.

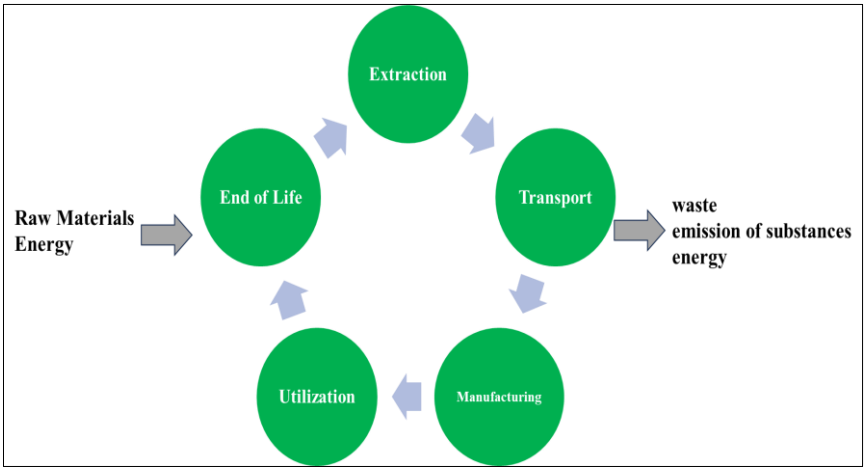

Figure 4.3. Life cycle thinking for a fictitious product [8].

4.3 . Life Cycle Assessment

Sustainable development remains a very complex concept, which explains the extreme difficulty of building a global system of indicators that can describe it in a relevant way for all sectors. The International Organization for Standardization (ISO) proposes the Life Cycle Assessment (LCA) as a technique for assessing the environmental aspects and potential environmental impacts associated with a product or product system over its entire life cycle, with a multi-criteria approach [12,13].

[12] ISO. Environmental management. Life cycle assessment. Principles and framework. Amendment. *Eur Stand*. **2020**;1(4):20.
[13] ISO 14044:2006(en), Environmental management — Life cycle assessment — Requirements and guidelines

Indeed, this initiative comes from the first discussions on pollution in the second part of the 20th century:

- 1960-1970: Midwest Research Institute (MRI) is interested in the need for a life cycle analysis system that addresses environmental issues through Resource and Environmental Profile Analysis (REPA)[14].
- 1970-1990: Following the 1st oil shock, the European interest in a circulatory economy and energy clean and independent increases. Design of the term "*Life Cycle Assessment*" following some scientific works and providing a list of data that may be required in LCA studies [14].
- 1990-2000: Standardization of LCA methodology by the Society of Environmental Toxicology and Chemistry (SETAC), then by the International Organization for Standardization (ISO) which developed methods and procedures (dar 14040: 2006 - Environmental Management - Life Cycle Assessment - Principles and Framework" and ISO 14044: 2006 - Environmental Management - Life Cycle Assessment - Requirements and Guidelines) [12,14].
- Since 2000: Elaboration and development of life cycle analysis technique, by monitoring the United Nations Environment Programme (UNEP) and SETAC covering environmental, economic and social dimensions, within the framework of sustainable development [14].

In fact, Life Cycle Assessment refers to the evaluation of all environmental, economic and social negative impacts and benefits in decision-making processes in order to have more sustainable products throughout their life cycle [14, 15]. For this purpose, the inflows (energy, water, materials) and outflows (greenhouse gas emissions, liquid wastes, solid wastes) of the product or service under study, for each of its life stages, are recorded and associated with environmental impacts (climate change, eutrophication, scarcity of resources, among others).

[14] Curran MA. Life Cycle Assessment: Principles and Practice. **2006**;(May):80.
[15] United Nations Environmental Program (UNEP). Towards a Life Cycle Sustainability A ssessment: Making informed choices on products. Published online **2011**:25.

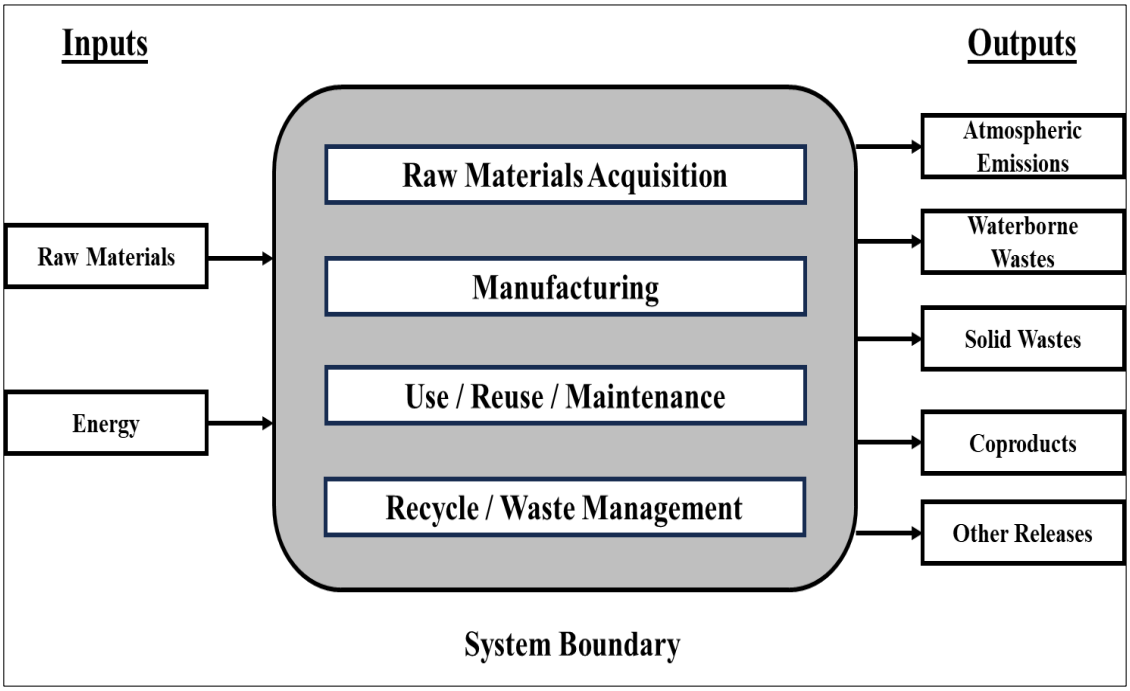

Figure 4.4. Life Cycle stages [16].

This technique presents some benefits for governors, enterprises and/or consumers [15]:

- Organizing complex environmental, economic and social information and data in structured form.
- Providing a comprehensive picture of both positive and negative impacts along the product life cycle by clarifying the trade-offs between the three sustainability pillars.
- Helping for a better decision-making by taking into consideration the impacts associated with the products and/or services.
- Encouraging smart investment, having a better SWOT analysis and improving Research and Development.

LCA is presented as an iterative process consisting of four steps [13, 15]:

4.3.1 State goal and scope of the study

In this step, we intend to frame the life cycle assessment study of the system into consideration. Therefore, the objectives, scope of the analysis, a general life cycle description, details of functional unit, system boundaries, allocation methods, limitations of the study, quality of data required, and intended audience should be determined. This stage also defines the fundamental assumptions, as well as the reference flow and effect categories [15].

[16] Du P. Life cycle assessment of urvan vs. suburban residential mobility in Chicago. In: *Proceedings of the ARCC 2015 Conference*. ; **2015**.

Table 4.2. Main impact categories.

Impact category	Effects and/or estimations	Main chemical substances	Impact indicators
Global Warming Potential (GWP)	Global warming and climate change	CO_2 CH_4 N_2O O_3 H_2O CFC	Kg CO_2-eq
Ozone layer depletion (ODP)	High UV radiation levels	CFC-11 CFC-12 HCFC-22 Halon 1301	Kg CFC 11-eq
Human toxicity (HP)	Impact on human health which can be non-cancer and cancer-related toxic substances	Arsenic (As) Cadmium (Cd) Chromium (Cr) Lead (Pb) Zinc (Zn) Dioxins, Formaldehyde Benzene	CTUh, kg Benzene-eq, Kg Toluene-eq
Particulate Matter (PM)	Impact on human health due to the respiration of very small particles	PM2.5 PM10 NOx SO_x	Kg PM2.5-eq Kg PM10-eq Disability-Adjusted Life Year
Eutrophication	Biological activity of organisms in excess due to over-nutrition	NO_X Ammonia (NH_3) Nitrogen (N) Phosphorus (P)	Kg NO_3-eq Kg PO_4-eq Kg P-eq Kg N-eq
Land use	Occupying, reshaping and managing land for human purposes	/	Kg C deficit
Water scarcity	Water deficiency or a lack of safe water supplies	/	m^3 eq
Ionizing radiation (HH)	Human health and ecosystems linked to the emissions of radionuclides	/	kBq U-235

Freshwater ecotoxicity	Impact on freshwater organisms of toxic substances emitted into the environment	Heavy metals Organic solvents	CTUe
Abiotic depletion (Fossil fuels)	The depletion of natural fossil fuel resources	/	MJ net calorific value
Abiotic depletion (elem., econ. reserve)	The depletion of natural non-fossil fuel resources	/	Kg Sb-eq
Acidification	Potential acidification of soils and water	NOx SOx	Kg SO_2-eq

4.3.2 Inventory of resources use and emissions

Also called Life Cycle Inventory (LCI) Analysis, this phase defines the inputs and outputs of each elementary process in the system. Here, we have a global view of the resources used and the outgoing flows of our product/service. It is at this stage that the scope of the study, the cut-off and allocation rules, and the various collection methods chosen are specified. It may also be necessary to make more precise assumptions to complete the life cycle information [14,17].

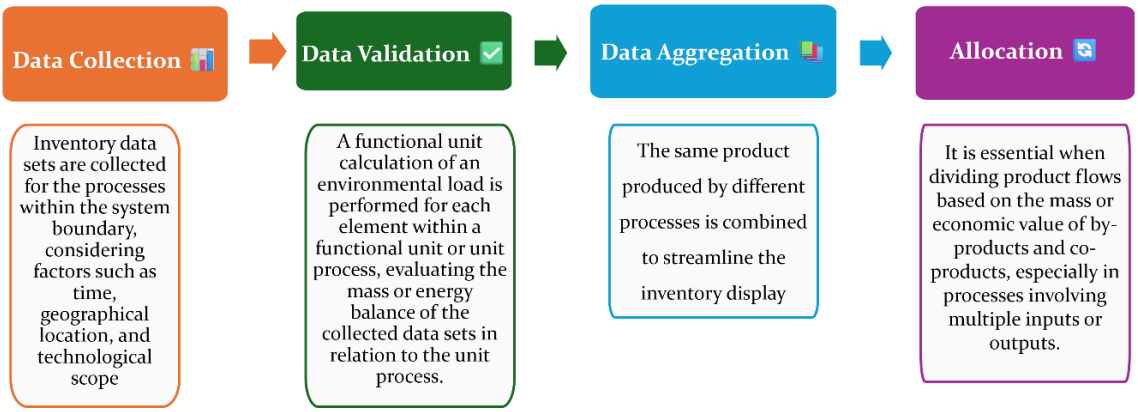

Figure 4.5. Life Cycle Inventory (LCI) analysis procedure.

[17] Jensen AA, Hoffman L, Moller BT, Schmidt A. *Life Cycle Assessment. A Guide to Apporaches, Experiences and Information Sources. EEA Environemntal Issues Series, No.6.* European Environment Agency; 1997.

4.3.3 Impact assessment

In this step, we translate the inventory of flows into environmental impacts through modeling on LCA software. In detail, a first "gross" result of the analysis on all the selected environmental indicators is obtained. It evaluates the impacts of inputs and outputs of the system by focusing human health, environment and natural resource utilization. Therefore, the selection and definition of impact categories are mandatory. Note that at this step, two approaches, namely the midpoint and the endpoint, are used when characterizing and normalizing the inventory data: the midpoint is considered to be an impact category indicator in between life cycle inventory results and endpoints in a cause effect diagram or environmental system. On the other hand, the endpoint approach is used to demonstrate the final effects [14,18]

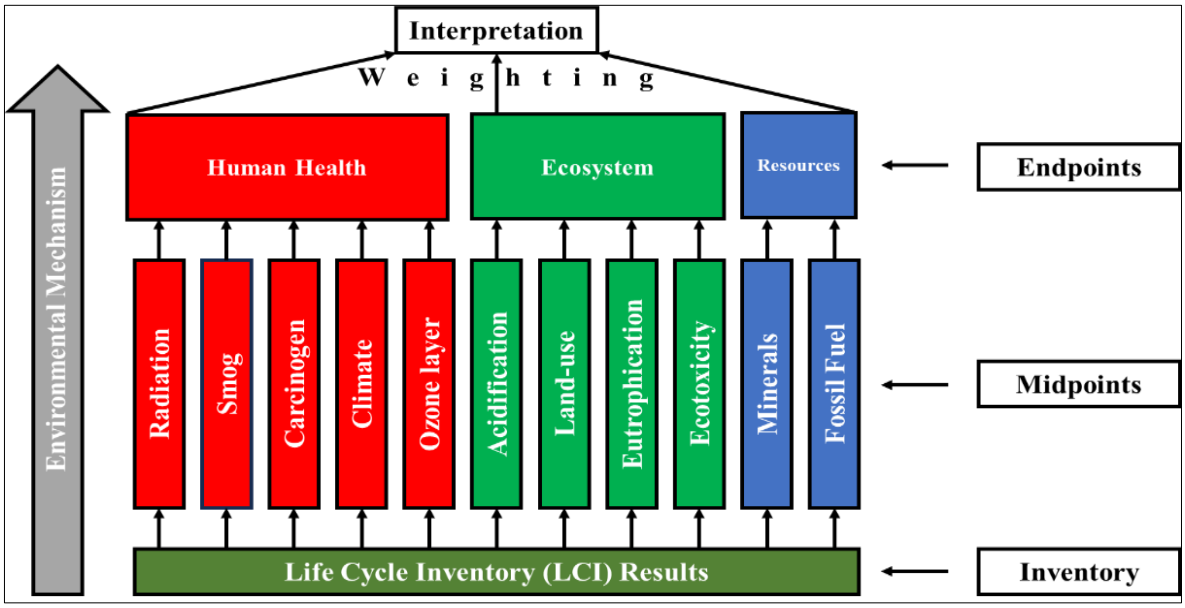

Figure 4.6. Relationship between midpoint and endpoint [19].

4.3.4 Interpretation

In this step, the results obtained are interpreted. The objective is to identify the main sources of impact between and within the life cycle phases. In the case of a comparative LCA, the interpretation is also the moment to present the differences in impact between the solutions studied. Sometimes it is necessary to perform one or more sensitivity studies to refine its interpretation.

[18] simapro manual PRe Consultants. Introduction to LCA with SimaPro 7. *PRé Consult Netherlands Version*. Published online **2008**:1-88.
[19] Chen G, Wang X, Li J, et al. Environmental, energy, and economic analysis of integrated treatment of municipal solid waste and sewage sludge: A case study in China. *Sci Total Environ*. 2019;647:1433-1443.

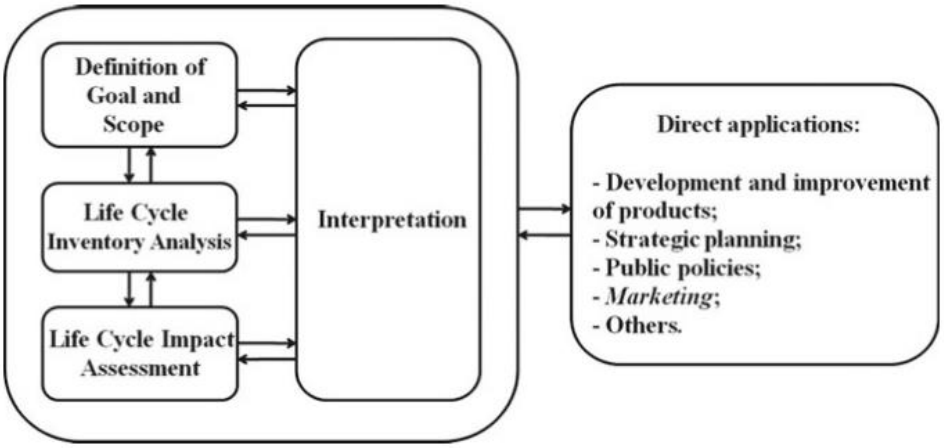

Figure 4.7. Phases of life cycle assessment (LCA) and their direct applications [20].

The methodological path of the LCA may lead, at any moment of the study, to review the previous step, for reasons of technical difficulties, collection of information, unsatisfactory results, poorly defined assumptions, or due to the temporal drift in the LCA analysis.

Although LCA is a very powerful tool, it faces some limitations that are important to note before undertaking a project and also when interpreting the results [16,21]:

- Modelling can be complicated due to lack of data available in databases, especially for underdeveloped countries.
- Difficulty in accurately collecting the entire life cycle input and output of the product and/or system studied, which makes a comparative study more difficult.
- Impossibility of studying all environmental impacts: It is not yet possible to calculate the impact of a product in terms of microplastic generation, toxicity of nanomaterials, influence on the landscape, light, visual and/or sound pollution, impact of waves, among other things, but these aspects can be addressed through complementary tools.

LCA, in fact, is only one of the many possible tools in the eco-design approach. LCA is not the most appropriate technique for all situations. In addition, LCA depends on working hypotheses, sometimes making the approach subjective. Bringezu et al. propose different methods for different objects of interest, in order to discuss the current state of assessment methods integrating economic and environmental goals (table 4.3).

[20] Poltronieri CF, Leite LR, Sousa SR. *Environmental Management Systems and Performance Measurement*.; 2021.
[21] W. Klöpffer and B. Grahl, *Life Cycle Assessment (LCA),* Weinheim, Germany: Wiley-VCH Verlag GmbH & Co. KGaA, (**2014**).

Table 4.3. Types of analysis and associated issues of concern [22,23].

Issue of concern	**Environmental impacts, supply security, technology development within businesses, countries, regions**			**General environmental and economic impacts of materials and goods**		
Objects of interest	Substances	Materials	Products	Businesses	Economic activities	Countries and regions
Type of analysis	Substance Flow Analysis (SFA)	Material Flow Analysis (MFA)	Life Cycle Assessment (LCA)	Business level MFA	Input-Output Analysis (IOA)	Economy-wide MFA

According to the work of Hawkins et *al.* [24], Bovea et *al.* [25], Moriguchi et *al.*[26] and Dossche et *al.*[27], Material Flow Analysis (MFA), Input-Output Analysis (IOA), and Life Cycle Assessment (LCA) have proven to be the most appropriate methods for conducting an environmental and economic assessment of products and systems, but none of these methods can provide a complete economic and ecological evaluation of a complex system within the framework of a circular economy (CE) in isolation: each method has different system limitations, benchmarks, calculation techniques and scopes (Table 4.4) [28,29,30].

It is very important to be able to explain the results of this tool. However, the LCA of a product sometimes presents complex and often relative conclusions, because the realization of the LCA can be influenced, voluntarily or not, by the choices made by those who conducted the study and proposed the working hypotheses. A simple and understandable presentation of the results of an LCA and decision criteria is not easy [14].

[22] Bringezu S, Moriguchi Y. Material flow analysis. In: Ayres L, Ayres RU, eds. *A Handbook of Industrial Ecology*. ; **2015**

[23] OECD. Measuring Material Flows and Resource Productivity. *Vol 1*. **2008**;III:1-164.

[24] Hawkins T, Hendrickson C, Higgins C, Matthews HS, Suh S. A mixed-unit input-output model for environmental life-cycle assessment and material flow analysis. *Environ Sci Technol*. **2007**;41(3):1024-1031.

[25] Bovea MD, Powell JC. Developments in life cycle assessment applied to evaluate the environmental performance of construction and demolition wastes. *Waste Manag*. **2016**;50:151-172.

[26] Moriguchi Y, Hashimoto S. *Material Flow Analysis and Waste Management*. Springer International Publishing; **2015**.

[27] Dossche C, Boel V, De Corte W. Use of Life Cycle Assessments in the Construction Sector: Critical Review. *Procedia Eng*. **2017**;171:302-311.

[28] Joshi S. Product environmental life-cycle assessment using input-output techniques. *J Ind Ecol*. **1999**;3(2-3):95-120.

[29] Nakamura S, Nakajima K, Kondo Y, Nagasaka T. The waste input-output approach to materials flow analysis: Concepts and application to base metals. *J Ind Ecol*. **2007**;11(4):50-63.

[30] Haas W, Krausmann F, Wiedenhofer D, Heinz M. How Circular Is the Global Economy? A Sociometabolic Analysis. In: *Social Ecology*. ; **2016**:259-275.

Table 4.4. Comparison of methods.

	MFA	IOA	LCA
Description	-Methods to investigate the technical processes of a socioeconomic system and its dependencies in a defined boundary (space and time) -Is performed according to the first law of thermodynamics; the basic condition is that the input must always equal the output including all stock changes	-Top-down economic tool for analyzing inter industrial interdependencies in an economy -Describes the distribution of goods and services by using a system of linear equations	-Bottom-up methodological framework encompassing all the impacts of a product system from cradle to grave -A decision-support tool used to promote sustainable management as well as sustainable construction and to assess and plan CE strategies
System definition	Functional or geographical	Geographical or political	Functional Regionalization possible
Advantage	Flexibility regarding model assumptions, mass balancing (filling data gaps), basis for impact assessment methods	Public data available (on nationwide level), possibility to extend to broaden the scope (multiple regions MRIO or environmental extensions EEIO)	Detailed evaluation of a product, product comparisons, multi-dimensional
Possible problems/Disadvantage	Availability of data, one-dimensional monetary flows are not represented	Low resolution due to high aggregation, partial simplifications and assumptions, spatial boundaries	Truncation error; subjective definition of the system boundary, choice of allocation

In the building materials sector, LCA normally includes raw material extraction, selection, locations, transportation, design process, construction system and service life. The operating principle of the software is based on taking inputs in the form of material take-offs, converting them to mass and attaching this mass value to the LCI data available from an LCI database. Therefore, it is mandatory that recycled materials, for example, are sent to the nearest recycling center using a transport sensitivity analysis for the specific context, in order to have a more accurate analysis.

Obviously, in this work, we are interested in studying the economic and environmental impact of geopolymer materials through Life Cycle Assessment (LCA), while continuing previous research work on the synthesis of advanced, less expensive and more sustainable geopolymers, proposing less toxic synthesis protocols, resulting from materials with desired physico-chemical properties, taking into consideration the methodology and limitation of LCA study [11,13].

4.4 . Life Cycle Assessment of geopolymers

Geopolymer materials were invented in 1979 by J. Davidovits in response to a fire between 1970 and 1973 in France. He found a way to replace flammable plastics with non-flammable alternatives using inorganic polymers, so called geopolymers, obtained by alkaline activation of a solid inorganic aluminosilicate [31]. These materials have a high mechanical performance and harden rapidly at room temperature and are able to withstand fire, heat and aggressive attacks (acid or atmospheric) [32,33,34,35,36]. They also have the ability to be formulated from a wide range of minerals such as fly ash [37], blast furnace slag [38], metakaolin[39] or other natural minerals[40,41].

---

[31] Davidovits J. Geopolymer Cement a review. *Geopolymer Sci Tech*. **2013**;(0):1-11.
[32] J D. Properties of Geopolymer Cements. *First Int Conf Alkaline Cem Concr*. **1994**;(October 1994):131-149.
[33] Elgarahy AM, Maged A, Eloffy MG, et al. Geopolymers as sustainable eco-friendly materials: Classification, synthesis routes, and applications in wastewater treatment. *Sep Purif Technol*. **2023**;324.
[34] Chen Z, Yu J, Nong Y, Yang Y, Zhang H, Tang Y. Beyond time: Enhancing corrosion resistance of geopolymer concrete and BFRP bars in seawater. *Compos Struct*. **2023**;322.
[35] Wang J, Chen X, Li C, Zhou Z, Du P, Zhang X. Evaluating the effect of kaliophilite on the fire resistance of geopolymer concrete. *J Build Eng*. **2023**;75.
[36] Sukontasukkul P, Intarabut D, Phoo-ngernkham T, Suksiripattanapong C, Zhang H, Chindaprasirt P. Self-compacting steel fibers reinforced geopolymer: Study on mechanical properties and durability against acid and chloride attacks. *Case Stud Constr Mater*. **2023**;19.
[37] Sathsarani HBS, Sampath KHSM, Ranathunga AS. Utilization of fly ash-based geopolymer for well cement during CO_2 sequestration: A comprehensive review and a meta-analysis. Gas Sci Eng. **2023**;113.
[38] Humberto Tommasini Vieira Ramos FJ, Vieira Marques M de F, de Oliveira Aguiar V, Jorge FE. Performance of geopolymer foams of blast furnace slag covered with poly(lactic acid) for wastewater treatment. *Ceram Int*. **2022**;48(1):732-743.
[39] Mehmood A, Irfan-ul-Hassan M, Yaseen N. Role of industrial by-products and metakaolin in the development of sustainable geopolymer blends: Upscaling from laboratory-scale to pilot-scale. *J Build Eng*. **2022**;62.
[40] Kumar YN, Dean Kumar B, Swami BLP. *Mechanical Properties of Geopolymer Concrete Reinforced with Steel and Glass Fibers with Various Mineral Admixtures*. Vol 52.; **2022**.
[41] Martin PB, Medri V, Papa E, Vaccari A. From clays and clay minerals to geopolymers: Looking to the future. *Appl Clay Sci*. **2024**;251.

This definition and description of the properties of geopolymers confirms the judicious choice to focus more and more on their use in the eco-construction sector, and therefore the need for a life cycle assessment.

Most of the environmental impacts of the construction sector are related to the three phases of the building life cycle: construction materials manufacturing, building operations (use phase) and end-of-life [8].

4.4.1 Raw materials and resources

The geopolymer binder is described as an inorganic material rich in silicon (Si) and aluminium (Al) deriving from the activation through alkaline solutions of certain types of clays such as fly ash, blast furnace slag and metakaolin, or from industrial waste and sub-clay products [42]. These raw materials are available worldwide and are extracted from natural deposits or obtained as components of tailings or waste from other industries. As a result, geopolymers meet the requirements of the United Nations Environment Program for the use of local, less expensive and less toxic materials [43].

The figure 4.8 shows the percentage of different syntheses of geopolymers from raw materials cited in scientific journals.

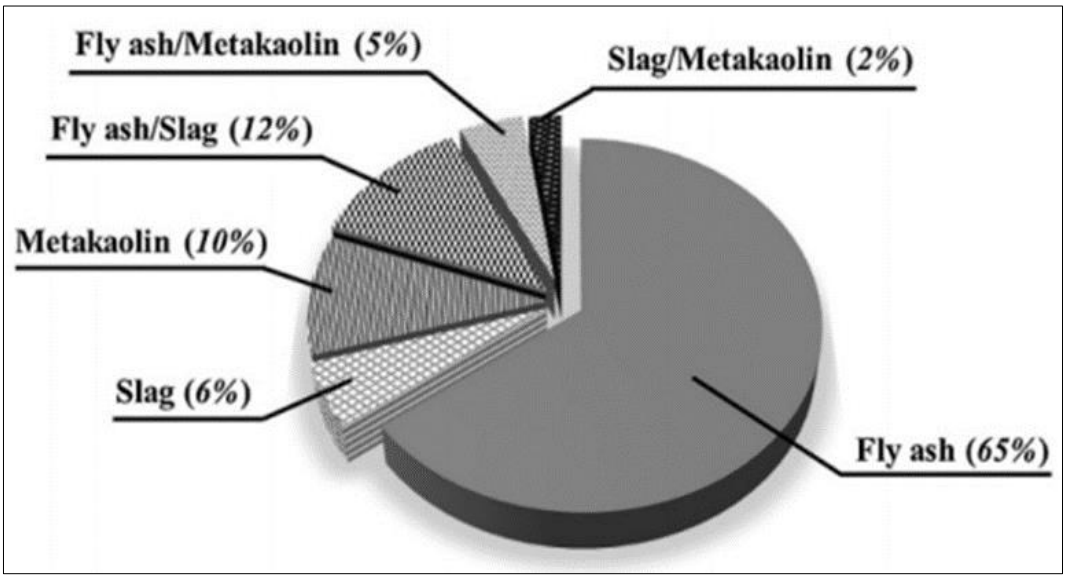

Figure 4.8. Geopolymer materials based on fly ash, blast furnace slag and metakaolin mentioned in scientific journals [44].

The necessity for a database including process information for the raw materials utilized remains required, by determining the impact values for the manufacture of one ton of the raw material, and subsequently the consideration of the production phase of

[42] Call RE. The chemistry of soils. *Science (80-)*. 1892;20(493):29-30.
[43] Building Material and the Climate: Constructing a New Future. *Build Mater Clim Constr a New Futur*. Published online **2023**.
[44] Hasnaoui A, Ghorbel E, Wardeh G. Optimization approach of granulated blast furnace slag and metakaolin based geopolymer mortars. *Constr Build Mater*. **2019**;198:10-26.

geopolymers from the extraction of raw materials to the finished product. For example, the Diogen data (developed by a working group of the Association franaçise du génie civile) are calculated according to NF EN 15804+A1 [45] [46]. Life cycle analysis methods should therefore be compatible with the indicators provided by the standard.

Table 4.5 shows the metakaolin (MK) and ground granulated blast-furnace slag (GGBFS) values. The MK data correspond to the production of the MK flash rose produced in Flumel in France by Argeco. The GGBFS data correspond to the production of Ecocem slag composed of 100 % granulated blast furnace slag manufactured in Fos-sur-Mer in France.

Dredging sediments are considered waste from the water. It is therefore important to take into consideration all the stages of dredging and treatment (displacement, dredging by hydraulic suction, natural drying for one and two months, and leaching of heavy metals) to have the most accurate results.

Table 4.5. Environmental impacts of MK and GGBFS from the Diogen database.

Diogen Data	Unit	MK	GGBFS
Acidification (A)	kg.SO_2.eq.	1,87E-01	7,08E-02
Ozone Layer Depletion (OLD)	kg.CFC-11.eq.	2,74E-05	5,02E-06
Eutrophication (E)	kg.PO_4.eq.	1,70E-02	7,05E-03
Photochemical ozone formation (POF)	kg.ethylene.eq.	1,06E-02	4,01E-03
Water pollution (WP)	m^3	12,7	-
Climate Change (CC)	kg.CO_2.eq.	129	15,7
Resource Utilization, Fossil (RUF)	MJ	2,45E+03	2,27E+02
Resource Utilization, Minerals and Metals (RUM)	kg.Sb.eq.	3,77E-06	8,82E-02

4.4.2 Energy

The building sector, which represents 40 % of global energy consumption and 30 % of greenhouse gas emissions (GHG), is identified as the most consumer sector, ahead of transport, industry, etc [47]. Research indicates that energy consumption in this sector will continue to increase by 50 % until 2030 [48].

Cement or concrete is considered one of the most used building materials in the world. About 5 % of anthropogenic CO_2 emissions and 14 % of the total global energy

[45] Nikravan M, Firdous R, Stephan D. Life cycle assessment of alkali-activated materials: a systematic literature review. *Low-carbon Mater Green Constr*. **2023**;1(1).
[46] DIOGEN - AFGC. Accessed May 10, **2024**. https://www.afgc.asso.fr/ressources/diogen/
[47] Nejat P, Jomehzadeh F, Taheri MM, Gohari M, Muhd MZ. A global review of energy consumption, CO2 emissions and policy in the residential sector (with an overview of the top ten CO2 emitting countries). *Renew Sustain Energy Rev*. **2015**;43:843-862
[48] Hassan JS, Zin RM, Majid MZA, Balubaid S, Hainin MR. Building energy consumption in Malaysia: An overview. *J Teknol*. **2014**;70(7):33-38.

consumption of the industrial sector are attributed to the manufacture of cement to produce concrete [49].

It is therefore essential to choose construction materials with low environmental impact and whose manufacture or extraction does not require a lot of energy.

4.4.3 Transport and distribution

In some cases, there is no implementation of channels or companies that value sediment dredging, hence the need to take into account the environmental costs of transporting and exporting materials. The comparison between the use of cement, whose factories are numerous and whose market is old, and that of alkaline reagents and geopolymerization is flawed by their limited use on the market today. Thus, in the second step, a sensitivity analysis must be carried out taking into account similar transport distances for cement and alkali. The unit used for this calculation is ton per km. An inventory of transport and geographical location must be established.

4.4.4 Transformation and manufacturing

The manufacturing scenarios for the different geopolymers can be established according to the standards NF EN ISO 14040 and NF EN ISO 14044 and subsequently be modeled on the LCA software using a database [50] [51].

4.4.5 Retail and utilization

During the operating phase, the building requires energy for lighting, heating, air conditioning and the production of domestic hot water. 80 % of GHG emissions throughout the life cycle of the building are related to this phase of use when electricity is used for the needs of the building [52]. Most of the energy consumed during this phase is reserved for thermal comfort, such as heating in winter and air conditioning in summer.

Energy efficiency is a major concern in energy strategies in many countries. New policy constraints have been put in place to address this issue in order to improve the thermal performance of buildings and ensure better control and rationalization of energy consumption in this industry.

Increasing the energy efficiency of a building can be a real challenge. The use of conventional building materials is sometimes unsuited for the need to allow the emergence of an autonomous path towards future structures that we want to be less energy-consuming and more user-friendly for man and his environment.

---

[49] Alsalman A, Assi LN, Kareem RS, Carter K, Ziehl P. Energy and CO_2 emission assessments of alkali-activated concrete and Ordinary Portland Cement concrete: A comparative analysis of different grades of concrete. *Clean Environ Syst*. **2021**;3.

[50] ISO. Environmental management. Life cycle assessment. Principles and framework. Amendment. *Eur Stand*. **2020**;1(4):20.

[51] ISO 14044:**2006**(en), Environmental management — Life cycle assessment — Requirements and guidelines.

[52] Huguet JR. *PhD Thesis*. La Rochelle; **2019**. Available from: https://www.theses.fr/2019LAROS034

4.4.6 End of life and waste

In general, one ton of manufactured Portland cement releases one ton of CO_2 into the atmosphere [53]. This huge CO_2 emission is due to a number of factors, including the energy required for the production process and the necessary calcination of limestone at a temperature of 1450°C. It should be kept in mind that limestone represents 80 % of the components of cement while the rest is made up of clay and gypsum.

The significant environmental and energy benefits of geopolymers are an important factor in researchers' increased interest in geopolymer science. Geopolymer cement, called "green cement", can provide a good environmental solution to the problem of greenhouse gas emissions. Indeed, compared to Portland cement, which emit about one ton of carbon dioxide for each ton manufactured, a significant reduction of 40-80 % of CO_2 emissions can be achieved in the manufacture of geopolymers [54].

In addition, compared to the energy required to manufacture geopolymer cement, the amount of energy used to produce Portland cement, which is about 4700MJ/t, is substantially higher. Metakaolin-based geopolymers require an average amount of energy of about 2715MJ/t, mainly used for the calcination of natural aluminosilicates (Kaolinite).

The figure 4.9 shows the comparison of total carbon emissions between Portland concretes (OPC) without and with mineral additives (SCM) and geopolymer concretes based on slag (GBFS), fly ash (FA) or metakaolin (MK), for the same mechanical strength class. It should be noted that the carbon footprint of geopolymer concrete is significantly lower than that of Portland concrete. Geopolymer concretes based on blast furnace slag or fly ash showed a very small footprint compared to OPC. Indeed, this footprint can increase significantly, especially when metakaolin is used only as an aluminosilicate precursor [55].

[53] Yang K-H, Song J-K, Song K-I. Assessment of CO_2 reduction of alkali-activated concrete. *J Clean Prod*. **2013**;39:265-272.
[54] Ohunakin OS, Leramo OR, Abidakun OA, Odunfa MK, Bafuwa OB. Energy and Cost Analysis of Cement Production Using the Wet and Dry Processes in Nigeria. *Energy Power Eng*. **2013**;05(09):537-550.
[55] Nazari A, Sanjayan JG. *Handbook of Low Carbon Concrete*. Butterworth-Heinemann; **2016**.

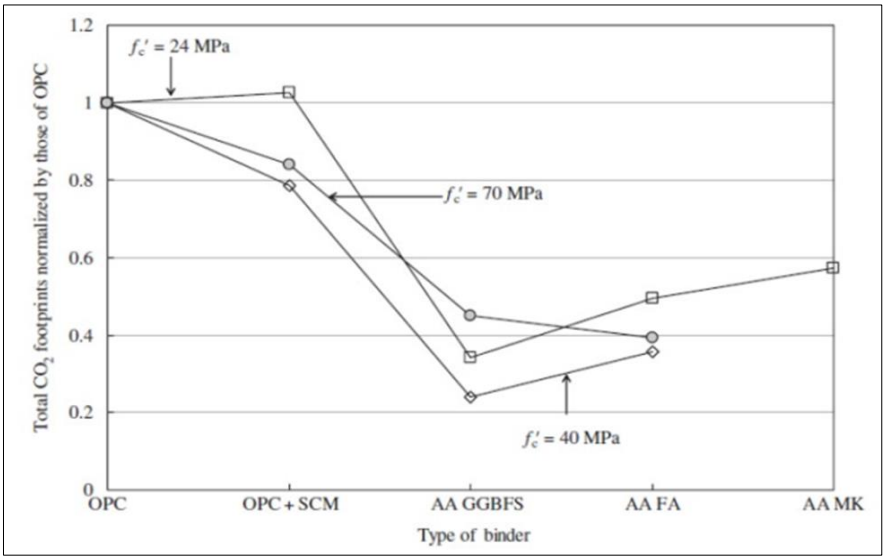

Figure 4.9. Comparison of total carbon emissions between Portland concretes (OPC) without and with mineral additives (SCM) and geopolymer concretes based on slag (GBFS), fly ash (FA) or metakaolin (MK), for the same mechanical strength class [53].

It is clear from all the information reported in the previous paragraphs that the building sector is an energy intensive industry. It is an industry responsible for producing a large amount of CO_2 emissions that threaten the continuation of life on the planet.

It was mentioned that the origin of this large amount of CO_2 emissions is caused during the use phase of the building to improve thermal comfort and the manufacturing phase.

However, the use of other alternative solutions developed recently such as the use of phase change materials and geopolymers may be a solution to limit the negative influence of the building sector on the environment. This essential solution is integrated in the field of eco-construction and sustainable construction, which uses materials with a low environmental impact and does not require much energy to be produced or extracted.

The table 4.6 presents the state of the art on the different works of life cycle analysis of geopolymer materials with different precursors from industry.

Table 4.6. LCA studies with different waste materials.

Ref	Geography	System Boundary	Alternative Concrete Components	Impact Assessment Method
[56]	USA	Cradle to gate	Fly ash and Limestone	/

[56] Celik K, Meral C, Petek Gursel A, Mehta PK, Horvath A, Monteiro PJM. Mechanical properties, durability, and life-cycle assessment of self-consolidating concrete mixtures made with blended portland cements containing fly ash and limestone powder. *Cem Concr Compos*. **2015**;56:59-72.

[57]	Europe	Cradle to gate	Blast furnace slag and fly ash	CML
[58]	Italy	Cradle to gate	incinerator ashes, blast furnace slag, marble sludge and CDW	Ecoindicator 99
[59]	Spain	Cradle to grave	Fly ash and blast furnace slag	/
[60]	France	Cradle to grave	Traditional vs. Geopolymer concrete consisting of fly ash, GGBFS, metakaolin	CML 2001
[61]	Serbia	Cradle to gate	Fly ash and recycled aggregate	CML baseline
[62]	Australia	Cradle to gate	Waste plastic fiber virgin plastic fiber	Australian Indicator set V3.00
[63]	Norway	Cradle to gate	Plastic aggregate	ILCD 2011 Midpoint+
[64]	Italy	Cradle to cradle	Expanded polystyrene	COMFEN version 5
[65]	Australia	Cradle to cradle	HDPE and PET	/
[59]	Serbia	Cradle to gate	Recycled aggregate concrete	CML

[57] Chen C, Habert G, Bouzidi Y, Jullien A, Ventura A. LCA allocation procedure used as an incitative method for waste recycling: An application to mineral additions in concrete. *Resour Conserv Recycl*. **2010**;54(12):1231-1240.
[58] Colangelo F, Navarro TG, Farina I, Petrillo A. Comparative LCA of concrete with recycled aggregates: a circular economy mindset in Europe. *Int J Life Cycle Assess*. **2020**;25(9):1790-1804.
[59] García-Gusano D, Garraín D, Herrera I, Cabal H, Lechón Y. Life Cycle Assessment of applying CO2 post-combustion capture to the Spanish cement production. *J Clean Prod*. **2015**;104:328-338.
[60] Habert G, Roussel N. Study of two concrete mix-design strategies to reach carbon mitigation objectives. *Cem Concr Compos*. **2009**;31(6):397-402.
[61] Marinković SB, Ignjatović I, Radonjanin V. Life-cycle assessment (LCA) of concrete with recycled aggregates (RAs). *Handb Recycl Concr Demolition Waste*. Published online January 1, **2013**:569-604.
[62] Yina S, Tuladhar R, Sheehan M, Combe M, Collister T. A life cycle assessment of recycled polypropylene fibre in concrete footpaths. *J Clean Prod*. **2016**;112:2231-2242.
[63] Javadabadi MT. *Master's Thesis*. NTNU; **2019**.
[64] Hay R, Ostertag CP. Life cycle assessment (LCA) of double-skin façade (DSF) system with fiber-reinforced concrete for sustainable and energy-efficient buildings in the tropics. *Build Environ*. **2018**;142:327-341.
[65] Grant T. AusLCI database manual. **2022**;(October):35.

[66]	Switzerland	Cradle to gate	Recycled concrete	Eco-indicator 99 and Ecological Scarcity 2006
[67]	Europe	Cradle to gate	Fly ash, foundry sand, steel slag and recycled aggregate	CML 2001
[68]	Belgium	Cradle to gate	Fly ash and blast furnace slag	CML 2002 and Eco-indicator 99

4.5 . Case of study

The objective of this work is to use local waste to produce sustainable building materials through the study of the synthesis of green geopolymer materials from industrial by-products Electric Arc Furnace Slag (DS), Calcined Clay (C-Clay), Metakaolin (MK_T), Brick waste (BW) and different alkaline activators solid (A.A.L) and liquid (A.A.L), as well as evaluating the environmental and economic impacts. Indeed, a Life Cycle Analysis will be conducted using SimaPro 9.5 LCA software (table 4.7), as per ISO 14040/14044. This software was launched in 1990 by PRé Consultants providing Ecoinvent 3.9.1 database as well as details of life cycle analyses [69]. Characterization, damage assessment, normalization and weighting are the basic impact assessment steps that are available under SimaPro, which are optional steps for ISO standards [70].

Table 4.7. General characteristics of SimaPro 8.4.1.0 LCA software.

Key elements	General Characteristics of PRé - SimaPro
Level of analysis	Product analysis tool
LCA stages	Cradle to grave, gate to gate
Data locations	Global
LCI libraries	• Agri-footprint – economic allocation • Agri-footprint – gross energy allocation • Agri-footprint – mass allocation • Ecoinvent v3 – allocation, default – system • Ecoinvent v3 – allocation, default – unit • Ecoinvent v3 – allocation, recycled content – system

[66] Knoeri C, Sanyé-Mengual E, Althaus HJ. Comparative LCA of recycled and conventional concrete for structural applications. *Int J Life Cycle Assess*. **2013**;18(5):909-918.
[67] Turk J, Cotič Z, Mladenovič A, Šajna A. Environmental evaluation of green concretes versus conventional concrete by means of LCA. *Waste Manag*. **2015**;45:194-205.
[68] Van Den Heede P, De Belie N. Environmental impact and life cycle assessment (LCA) of traditional and 'green' concretes: Literature review and theoretical calculations. *Cem Concr Compos*. **2012**;34(4):431-442.
[69] Goedkoop M, Oele M, Leijting J, Ponsioen T, Meijer E. Introduction to LCA with SimaPro. PRé Consultants; **2016**.
[70] Goedkoop M, Oele M, de Schryver A, Vieira M, Ponsioen T. Introduction to LCA with SimaPro 7. PRé Consultants; **2008**.

	• Ecoinvent v3 – allocation, recycled content – unit • Ecoinvent v3 – consequential – system • Ecoinvent v3 – consequential – unit • ELCD • EU&DK Input Output Database • Industry data 2.0 • Methods • Swiss Input Output Database • USLCI
LCIA methods	• BEES+ • TRACI 2.1 • CML-1A (baseline and non-baseline) • Ecological Scarcity 2013 • EDIP 2003 • EPD 2013 • EPS (2015d and 2015dx) • ILCD 2011 Midpoint+ • IMPACT 2002+ • ReCiPe 2016 • Cumulative Energy Demand • Ecosystem Damage Potential • Greenhouse Gas Protocol • IPCC 2013 GWP 100a • IPCC 2016 GWP 20a • Selected LCI Results • Selected LCI Results, additional • USEtox 2 (recommended + interim) • USEtox (recommended only) • CML 1992 • CML 2 baseline • CML 2001 (all impact categories) • Eco-Indicator 95 • Eco-Indicator 99 • Ecological Footprint • Ecopoints 97 (CH) • EDIP / UMIP 97 • IPCC 2001 GWP

CHAPTER 5

CONCLUSIONS AND FINAL REMARKS

To conclude, this doctoral dissertation presents novel synthesis and evaluation of the performance of geopolymeric and hybrid geopolymeric materials using local precursors.

First of all, an introduction (Chapter 1) presents a background overview of geopolymer materials, focusing on their composition, and properties, as a sustainable alternative to Ordinary Portland Cement concrete (OPC). The different raw materials that were employed to produce geopolymers (i.e., clay and kaolin) and industrial by-products (i.e., electric arc furnace slag and brick waste) were fully studied and their properties were reported. This chapter also highlights the role of alkaline activation solutions, including sodium hydroxide and sodium silicate for the synthesis of geopolymers. Thereafter, the development of sustainable hybrid geopolymers produced by combining secondary raw materials and functional agents in order to enhance the properties of geopolymers is discussed. A brief introduction to Life Cycle Assessment was also presented to further assess the sustainability of these materials in the future.

In Chapter 2, is reported the synthesis and evaluation of geopolymeric materials using different local raw materials from Sicily (southern Italy), including arc furnace slag (DS), clay, brick waste (BW), kaolin (K), and volcanic rock (slag). The chemical and physical properties of these raw materials were investigated as well as their reactivity optimization through thermal and mechanical treatments. For this purpose, thermal (for clay and kaolin) and mechanical treatments (for DS, calcined clay and metakaolin) were evaluated. Various geopolymers activated with sodium hydroxide solution, alkaline activated liquid (A.A.L.) and powder (A.A.P.) were prepared and experimentally characterized. Afterward, the effects of the combination of different raw materials in equal proportion 50/50 (i.e., MK_T + DS_g, MK_T + BW, C-Clay + DS_g, C-Clay + BW) were studied under different temperatures as well as their mechanical properties. The key findings presented in this chapter are as follows:

1- Thermal treatment for Clay, K as well as mechanical treatments for DS, C-Clay and MK significantly improved the compressive strength in the geopolymeric materials;

2- The optimal conditions found for the synthesis of high-performant geopolymers with good mechanical properties was a combining 50 % of C-Clay and 50 % of DS_g activated with 8 M NaOH solution and cured at 65 °C;
3- The mixtures activated with A.A.L have higher compressive strengths than the geopolymer activated with A.A.P.

In Chapter 3, the development and characterization of hybrid organic-inorganic geopolymers by introducing different functional agents into two matrices (i.e., 50 % of C-Clay and 50 % of DS_g and 50 % of C-Clay and 50 % of BW) is reported. These functional agents were: PDMS, TEOS, acrylic resin, and TP56. Thus, with the aim to enhance the properties of geopolymers the effect on the physic-chemical properties of the obtained material integrating the functional agents was described. Therefore, were developed different hybrid geopolymers with two alkaline activators (A.A.L. and A.A.P.) and then studied the compressive strength, mineralogical, morphological, thermal, surface wettability, water absorption, and porosity properties to identify the optimal mixture. The key conclusions of this chapter are the following:

1- The compressive strength increased over the curing age for all samples;
2- The addition of PDMS showed better mechanical properties compared to TEOS, Resin, and TP5;
3- The SEM Analysis revealed microcracks in C-Clay @ DS_g samples activated with both A.A.L. and A.A.P.;
4- Porosity and water absorption tests showed that samples activated with A.A.P. showed lower porosity which improved the water absorption resistance;
5- Contact Angle measurements indicated that hybrid geopolymer prepared with A.A.P. alkaline activator and functionalized with PDMS is the most hydrophobic.

In Chapter 4, the path for future research to carry out a life cycle assessment comparing the environmental and economic impacts of geopolymers with conventional materials is outlined. The findings will expect to prove the feasibility of geopolymers as an alternative to conventional materials. Therefore, it's important to perform LCA and life cycle cost to further optimize the manufacture process of the geopolymers and hybrid geopolymers towards a greener and more sustainable production.

CHAPTER 6

MATERIALS AND METHODS

This chapter outlines the analytical techniques used to characterize the starting materials and the synthesized products, focusing on determining their physico-chemical properties. A series of experiments were conducted to analyze both the raw materials and the geopolymer samples prepared from five industrial by-products and natural materials. Various experimental methods were employed to study the characteristics of the raw materials and the resulting geopolymer pastes. This section provides detailed descriptions of the sample preparation, the methodologies used, and the experimental procedures applied throughout the study.

6.1. Experimental section

6.1.1. Materials

Natural and by-products raw materials (Electric Arc Furnace Slag (DS), clay, brick waste (BW), kaolin (K), and Volcanic rock (slag)) were used in this work. The raw materials were sourced from various suppliers in Sicily. *Electric Arc Furnace Slag (DS):* is a by-product generated during the production of steel in electric arc furnaces, provided by Acciaierie di Sicilia located in Catania, Italy. *Clay:* is a fine-grained natural material provided by the Fauci Group, Palermo, Italy. *Brick Waste (BW):* is a red and fine-grained material collected from debris piles generated during the renovations of Messina University, Italy. *Kaolin (K):* is a white and highly pure clay mineral. *Volcanic rock (slag):* is a type of volcanic rock typically composed of various silicate minerals along with oxide minerals. Sodium hydroxide (NaOH) solution which is the most common activator was prepared with a commercial solid NaOH (from Panreac) and deionized water. Sodium silicate solution of natural origin (Bioki, Italy). Sodium metasilicate anhydrous powder (Na_2SiO_3) obtained from ThermoFisher GmbH, Germany which had SiO_2 and Na_2O concentrations ranging from 44.7 % to 47.6 % and 49.1 % to 51.7 %, respectively. 2-propanol known as isopropanol, is a high-grade reagent to stop a chemical reaction with 99.9 % purity supplied by GLR Labkem, Spain. For hybrid geopolymer we added four consolidants: Polydimethylsiloxane (PDMS) and Tetraethyl orthosilicate (TEOS) were purchased from Sigma Aldrich at a high purity, Acrylic Resin which is pure adhesive, milky white with medium viscosity (Sinopia) and TP56 mixture (56 wt.% of PDMS in combination with ethoxysilane and 0.05 % of n-octylamine). A solution of TP56 comprising TES40 and PDMS was prepared by mechanical mixing of the components for 5 minutes. Subsequently, N-octylamine was added and the solution vigorously stirred at 800 rpm for an additional 10 minutes and stored as described in the work of Garcia-Lodeiro et al. (2022).

6.1.2. Synthetic procedures for Chapter 2

6.1.2.1. Preparation of geopolymer pastes

Several trials were conducted to evaluate the influence of NaOH concentration and curing temperature on the properties of geopolymer pastes (Table 6.1). The following steps outline the experimental procedure:

Precursors: The starting materials used were Slag, DS, DS_g, K, MK_T, Clay, C-Clay and BW.
Alkaline Activator: NaOH solutions with concentrations of 4 M, 6 M, and 8 M were prepared by dissolving NaOH pellets with distilled water.
Mixing and casting: The precursors were dispersed into the sodium hydroxide solution under mechanical stirring for approximately 3 minutes, to ensure the formation of a homogeneous mixture. Then, the fresh paste was cast into stainless steel molds (10 mm ×10 mm ×60 mm), and then subjected to vibration under a shaking table for 1 minute.

Curing: After the casting, geopolymer specimens were cured immediately. Two types of curing were used in this work: oven curing (85 °C) and room temperature curing (23 ± 2 °C). The pre-curing process is described as follows:

At room temperature 23 °C: Specimens were initially stored with the molds in a climatic chamber at 22 ± 1 °C and 95 ± 3 % relative humidity (RH) for 20 hours. After this initial period, the specimens were removed from the molds and stored continually in the climatic chamber under the same conditions until they reached the testing age of 2, 7, and 28 days. The size of the samples produced was uniform.

At 85 °C (oven curing): The paste specimens were cast in molds then sealed with plastic film and placed in a closed plastic box with a little water under the molds (See Figure.6.1) in order to prevent extensive moisture loss during the heat curing stage. The plastic boxes containing the specimens were placed in an oven for the initial 20 hours at 85 °C. After this period, the boxes were removed from the oven and allowed to cool to room temperature to avoid a drastic change in the environmental conditions. Finally, the specimens were demolded and transferred to a climatic chamber set to a temperature of 22 ± 1 °C and 95 % relative humidity. The specimens were stored in the same chamber until the testing ages of 2, 7, and 28 days.

Table 6.1. Pastes elaboration information.

Materials	Liquid Activator	Paste Liquid/Solid	Curing
DS	NaOH (4 M and 6 M)	0.33	25 °C
DS_g	NaOH (4 M and 6 M)	0.35	25 °C
Clay	NaOH (6 M and 8 M)	0.58	85 °C
C-Clay	NaOH (4 M and 8 M)	0.60	85 °C
BW	NaOH (6 M and 8 M)	0.38	25 °C, 85 °C
MK	NaOH (6 M and 8 M)	0.75	85 °C
MK_T	NaOH (4 M and 8 M)	0.77	25 °C, 85 °C
Slag	NaOH (4 M and 6 M)	0.27	25 °C

6.1.2.2. Development of geopolymeric mix designs

The geopolymeric binder was prepared as follows: first, we manually mixed in a plastic bag the precursors in a 50/50 proportion. The resulting mixture was then dispersed into the NaOH solution (6 M and/or 8 M) under mechanical stirring for approximately 3 minutes, to ensure the formation of a homogeneous mixture. The pastes were cured at 65 °C for 24 hours. 65 °C was chosen as the curing temperature for the synthesis of all geopolymer mixtures due to its significant impact on strength (Chapter 2, section 2.2.3.1) without the need for higher energy input. After curing, the specimens were demolded and transferred to a climatic chamber set to a temperature of 22 ± 1 °C and 95 % relative humidity. The specimens were stored in the same chamber until they reached the testing age.

Table 6.2. Elaboration details for the geopolymers specimens.

Geopolymer paste	Liquid Activator	Paste Liquid/Solid	Curing
MK_T + DS_g	NaOH (6 M and 8 M)	0.58	65 °C
MK_T + BW	NaOH (6 M)	0.67	65 °C
BW + DS_g	NaOH (6 M and 8 M)	0.35	65 °C
C-Clay +BW	NaOH (6 M)	0.40	65 °C
C-Clay + DS_g	NaOH (6 M)	0.36	65 °C

6.1.2.3. Development of geopolymeric mixtures using various alkaline activators (Liquid and Solid)

The binders 50 % *C-Clay @ 50 % DS_g, 50 % C-Clay @ 50 % BW and 50 % MK_T @ 50 % DS_g* were selected and activated using two design methods:

1. **First Approach A.A.L:** (Chapter 2, Figure 2.1):
    - The binder was created by mixing the mixtures with the alkaline activator liquid.
    - The liquid/solid ratio was set around 0.38 (by mass) for all samples.
2. **Second Approach A.A.P:** (Chapter 2, Figure 2.1):
    - First, we mixed the mixtures and 6 wt.% of sodium metasilicate anhydrous powders (Na_2SiO_3) in plastic bag.
    - A measured amount of distilled water was then added to the powder mixture.
    - The water-to-binder ratio was fixed at 0.28 (by mass).

Table 6.3. Geopolymer elaboration information.

Mixtures	Activators		Curing
	Liquid (A.A.L)	Powder (A.A.P)	
C-Clay @ DS_g	NaOH (8 M)/Sodium Silicate (3:1)	6 % Na_2SiO_3 + water	65 °C
C-Clay @ BW	NaOH (8 M)/Sodium Silicate (3:1)	6 % Na_2SiO_3 + water	65°C
MK_T @ DS_g	NaOH (8 M)/Sodium Silicate (3:1)	6 % Na_2SiO_3 + water	65 °C

Key Observations

The effect of NaOH concentration showed that 4 M NaOH produced lower compressive strength, 6 M NaOH provided balanced improvement, and 8 M NaOH exhibited the highest initial strength. Curing at room temperature resulted in slower geopolymerization and lower early strength, while 85 °C enhanced the process, improving mechanical properties. BW samples remained too soft to test after 2 and 7 days of curing, and slag samples were not good after demolding (see figure 6.1).

Better compressive strengths were observed for: (a) 50 % C-Clay + 50 % DS_g (65 °C, 6 M NaOH); (b) 50 % C-Clay + 50 % BW (65 °C, 6 M NaOH) and (c) 50 % MK_T + 50% DS_g (65 °C, 8 M NaOH).

Figure 6.1. Slag-Based geopolymer after demolding.

6.1.3. Synthetic procedures for Chapter 3

The procedure started with the preparation of these precursors where the calcined clay was equally combined with electric arc furnace slag (50 % C-Clay @ 50 % DS_g) or waste bricks (50 % C-Clay @ 50 % BW) to produce the geopolymers. The choice of these combinations for geopolymer synthesis was based on their performance in preliminary compressive strength tests. Specifically, the mixture of C-Clay and DS_g demonstrated high compressive strengths with both activators, while BW was incorporated to explore whether the introduction of functional agents could further improve the mechanical properties.

Two types of alkaline activators were made: Liquid alkaline activator (A.A.L) which involved mixing 8 M sodium hydroxide solution with sodium silicate solution in a 3:1 ratio, and powder alkaline activator (A.A.P) which was created by dry mixing of sodium silicate powder with water. The hybrid geopolymers were then activated by combining each base matrix with either A.A.L or A.A.P. In the case of samples activated with A.A.L, the liquid activator was gradually added into the mixture of calcined clay and electric arc furnace slag or brick waste after mixing with them. On the other hand, for the A.A.P. activated samples, the activator powder was first mixed with the dry precursors before adding water and then the hybrid component.

To produce hybrid geopolymers, 3 % by weight of the functional agents (PDMS, TEOS, acrylic resin, and TP56) were added to a mixture. This mixture was initially stirred for 2 minutes and then mixed for an additional 1 minute. For the calcined clay and brick waste matrix, only PDMS and TP56 were used (chapter 3, Figure 3.1 and 3.2).

The obtained pastes were casted into steal mold after shaking for 1 minute to get rid of bubble. The samples were then removed from the molds after initial curing (1 day in the oven) and cured at 25 °C with 95 % relative humidity for 2, 7, and 28 days. Various tests were performed on the cured samples such as compressive strength test, FTIR, XRD, XRF, TGA, SEM, porosity as well as water absorption measurements.

6.2 . Instrumental techniques

This section presents the various instrumental techniques and equipment used in this Ph.D. thesis. All analyses were conducted at the Institute of Building Sciences Eduardo Torroja (CSIC, Madrid), where these instruments were employed to characterize the starting materials and the geopolymer products.

6.2.1. Sieve analysis

To obtain a general indication of the particle size range of the precursor materials, a sieve analysis was performed using sieves with mesh sizes of 63 µm and 45 µm. For the analysis, 10 grams of the sample were used. The sample was washed with water to pass through the sieves and then dried in an oven at 85 °C for 15 minutes. After drying, the raw materials were reweighed to determine the percentage of material passing through two sieves (Figure 6.2).

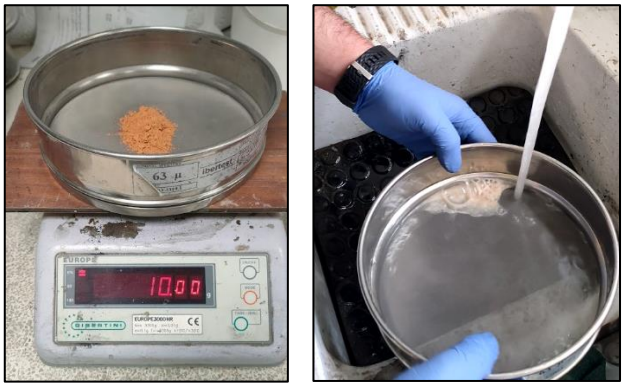

Figure 6.2. Sieve analysis for the raw materials using 63 µm and 45 µm.

6.2.2. Moisture determination

The moisture content of the raw materials was determined by drying the starting materials in an oven. The samples were initially weighed, then dried at 100 °C for 24 hours, and reweighed after cooling. The mass loss compared to the initial weight was used to calculate the moisture content.

Table 6.4. Moisture content of raw materials.

	Glass Weight P_v (g)	Sample Weight P_M (g)	Glass + Sample Weight $(P_v + P_M)_A$ (g)	Glass + Sample Weight $(P_v + P_M)_B$ (g)	Average Glass + Sample Weight $(P_v + P_M)$ (g)	Dried in oven at 100º c	Glass + Sample Weight After Drying $(P_v + P_M)_C$ (g)	Moisture (%)
DS	13.2624	5.5006	18.7630	18.7631	18.7631		18.7561	**0.1263**
Clay	25.1397	5.5004	30.6401	30.6402	30.6402		30.5808	**1.0790**
BW	27.0146	5.5000	32.5146	32.5146	32.5146		32.5111	**0.0636**
MK	24.0596	5.5004	29.5600	29.5597	29.5599		29.5517	**0.1482**
Slag	13.2512	5.5002	18.7514	18.7512	18.7513		18.7367	**0.2654**

6.2.3. Loss On Ignition (L.O.I)

The Loss on Ignition (LOI) method was employed to determine the amount of weight loss material undergoes at a high temperature in a muffle furnace (SATER). 1 gram of the raw materials was placed in crucibles and heated from 100 °C to a final temperature of 1000 °C for 1 hour (figure 6.3). The results are summarized in Table 6.5 below.

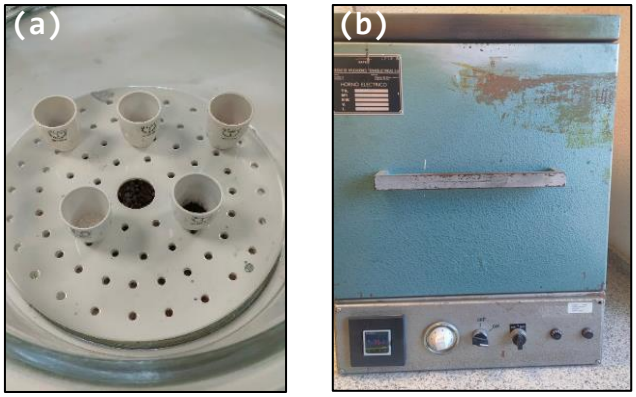

Figure 6.3. Loss on Ignition (LOI) process: (a) raw materials in crucibles, (b) muffle furnace setup.

Table 6.5. Loss on Ignition (LOI) analysis of raw materials.

	Crucible weight	Sample Weight	Crucible Weight + Sample Weight	Crucible Weight + Sample Weight	Average value Crucible + Sample weight	Crucible weight + Residue weight	Loss On Ignition
	P_C (g)	P_M (g)	$(P_C + P_M)_A$ (g)	$(P_C + P_M)_B$ (g)	$(P_C+P_M)_A$ + $(P_C+P_M)_B$ (g)	$(P_C + P_R)$ (g)	(%)
DS	23.1584	1.0004	24.1588	24.1589	24.1589	24.1558	**0.3049**
Clay	23.2677	1.0005	24.2682	24.2683	24.2683	24.1008	**16.7358**
BW	21.5362	1.0001	22.5363	22.5361	22.5362	22.5236	**1.2600**
MK	22.6052	1.0006	23.6058	23.6060	23.6059	23.5736	**3.2277**
Slag	23.7833	1.0001	24.7834	24.7834	24.7834	24.7401	**4.3296**

6.2.4. Chemical composition

The elemental composition of each starting material was determined using the instrumental technique of X-ray fluorescence (XRF). This technique offers both qualitative and quantitative information regarding the elemental composition of the sample and the concentrations of its elements, where the sample is bombarded with X-rays, causing its electrons to be excited. As the electrons return to their ground state, they emit characteristic X-rays, whose intensity and energy are measured to identify and quantify the elements present in the sample.

Table 6.6. Information on XRF analysis of starting materials.

Spectrometer	PHILIPS PW-1004 X-RAY
X-ray tube generator	Sc-Mo
Condition of analysis	After L.O.I of starting materials (Table 6.5)

6.2.5.Thermal and mechanical treatments of the precursors

In general, to increase the reactivity of the precursors, thermal and mechanical treatment are commonly used techniques.

6.2.5.1. Thermal treatment

For MK and Clay, calcination was used to transform it into a more reactive. Thermal activation, typically conducted at temperatures between 600-800 °C, dehydrates the kaolinite and disrupts its crystalline structure, converting it into a highly reactive amorphous aluminosilicate. MK and clay were calcined at 750 °C for 3 hours in a muffle furnace laboratory (figure 6.4).

Figure 6.4. Precursors: (a) clay before calcination and (b) calcined clay.

6.2.5.2. Mechanical treatment

The particle size reduction for DS and slag was carried out using Retsch Vibratory Disc Mill RS 200. The grinding was performed with a milling speed of 1200 rpm for 30 s at room temperature (Figure 6.5)

Figure 6.5. The vibratory disc mill Retsch adopted for the mechanical treatment.

6.2.6. Laser diffraction particle size analysis (PSD)

This analytical technique is called laser diffraction particle size analysis. It was used to study the particle size of starting materials (DS, Clay, K and BW). It is more accurate than the sieve particle size test, making it particularly suitable for various types of powders. The principle of laser diffraction is based on a laser beam that illuminates a particle, and diffraction fringes are observed. The intensity of the diffracted radiation and the diffraction angle depends on the particle size: the smaller the particles result in larger the diffraction angles. The ISO 13320 standard specifies the theory and optimal conditions for the use of laser diffraction particle size analyzers, also known as laser granulometry.

Table 6.7. Information on PSD analysis of starting materials.

Diffractometer	Sympatec
Measuring range	0.90-175 microns
Dispersion of samples by ultrasound	Propan-2-ol

6.2.7. Mechanical properties

The ultimate compressive strength of geopolymers was carried out under ambient air conditions after 2, 7, and 28 days of curing using an Ibertest Auto test 200-10 testing system (Figure 6.6), relied on this standard (UNE-EN 196-1). The values are an average of three samples, with errors reported as the standard deviation from the mean. Small pieces were taken from the crushed samples and immersed in isopropanol for several days to stop the geopolymerization reaction after the exactly testing age (2, 7 and 28 days). Afterward, the samples were removed from the isopropanol, dried, and then ground into a fine powder for further characterization.

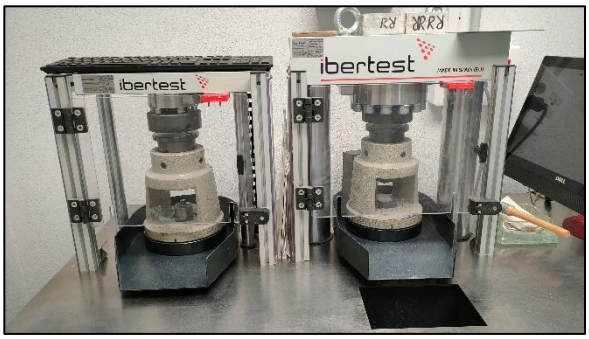

Figure 6.6. Machine Ibertest Autotest 200-10.

6.2.8. X-ray diffraction (XRD)

X-ray diffraction (XRD) is a non-destructive technique used to examine the structural of raw and geopolymer materials. It relies on the constructive interference of monochromatic X-rays with a crystalline sample. In XRD, the emission angles of soft electromagnetic X-rays are altered as they interact with the sample's electron clouds, leading to the re-emission of electromagnetic waves of the same frequency. The directions in space where the intensity of the X-rays is highest determine the directions of X-ray diffraction. The variation of the angles of incidence is governed by the characteristics of the crystal lattice and the incident radiation, following Bragg's law ($2d_{hkl}.\sin\theta = n.\lambda$), where d is the spacing between crystal lattice planes, hkl is the Miller indices of the crystal plane, θ is the angle of incidence, n is the order of reflection, and λ is the wavelength of the incident X-rays.

The X-ray diffractograms of the powder samples were recorded on a Bruker D8 Advance X-ray diffractometer fitted with a high voltage, 3 kW generator and Cu Kα Cu Kα radiation with a tube operating at 40 kV and 30 mA, using the following settings: divergence slit 6 mm; step time 0.5 s; step size 0.019746°; 2 θ angle range, 5–60°.

Table 6.8. Information on XRD analysis of the samples.

Diffractometer	D8 ADVANCE BRIKERAXS
High voltage generator ray tube	3 KW
Tube operating	40 kV and 30 mA
Radiation	CuKα 1,2
Settings	divergence slit: 6mm 2 theta: 5-60° ; step time: 0.5 s step size: 0.02°

6.2.9. Fourier Transform Infrared Spectroscopy (FTIR)

For the FTIR analysis, we used Thermo Scientifc Nicolet 6700 FTIR spectrometers and OMNIC software. The spectra were collected in transmission mode on 13 mm discs prepared by mixing the powder with KBr from approximately 0.2 g of sample powders to record optimal spectra in the regions of 4000-400 cm^{-1}. The nominal resolution was set to 4 cm^{-1}, and 64 scans over the range of 400-4000 cm^{-1} were averaged for each sample.

6.2.10. Thermal analysis (TG/DTG/DSC)

This analysis provides insights into the physico-chemical transformations (oxidation, reduction, decomposition) of hydrated geopolymers pastes. The aim is to measure the change in sample weight with respect to temperature and/or time under controlled conditions (temperature and gas atmosphere). Differential Scanning Calorimetry (DSC) also helps identify temperatures corresponding to phase changes.

Thermogravimetric analysis was performed by heating the grounded samples in a nitrogen atmosphere from room temperature to 1000 °C with a heating rate of 10 °C/min using an SDT-Q600 thermogravimetric analyzer (TA Instruments).

6.2.11. Scanning electron microscopy (SEM)

Morphological analysis of the geopolymers and hybrid geopolymer was conducted after 28 days on an *SEM/EDX* JEOL JSM scanning electron microscope fitted with a solid-state back-scattered electron (BSE) detector and a LINK-ISIS EDX. The samples used in this analysis were polished; they were examined in their fractured state to analyze the natural break surfaces. Prior to SEM analysis, the samples were gold-sputtered with a 5 nm layer to improve conductivity.

6.2.12. Mercury intrusion porosimetry (MIP)

MIP was employed to determine the pore volume and the size distribution of the selected geopolymer using Micromeritics Autopore IV at pressures ranging from 0 MPa to 227 MPa, contact angle of 141.3°, and surface tension of 485.10-1 N/m.

6.2.13. Water absorption (WA)

To determine *water absorption (WA)*, cubic samples (4×4×4 cm^3) were dried at 65 °C until a constant weight was reached to remove moisture from the pores. The chosen temperature for drying the specimens is the same as the curing temperature as higher temperatures can cause disruptions in the microstructure of geopolymer specimens, which can affect the accuracy of the water absorption results. After drying, they were then immersed in distilled water at room temperature of 20 ± 2°C for 30 minutes. The pipe was fixed to the test surface using sealing material (3 replicates, Figure 6.7). The test was carried out at room temperature after 28 days according to BS EN 16302:2013. The amount of water absorbed (W_i) by the test area (Q_i) [ml/cm^2] at the time (t_i) is calculated as follows: $W_i = \frac{Q_i}{A}$

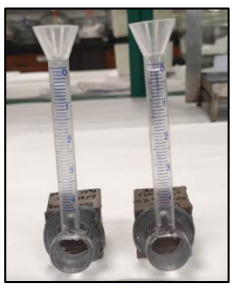

Figure 6.7. Image of the front surface of the sample used for water absorption test.

6.2.14. Wettability analysis

Contact angle measurement (CA) was used at the university of Messina (Polimeri, biopolimeri e composti) to characterize the wettability of the geopolymer and hybrid geopolymer through a DMs-401 measuring instrument (Kyowa Interface Science Co., Ltd. Japan). The contact angles were measured at least 10 times at different positions of the same surface using a 2 μL droplet of distilled water at ambient temperature and the average value of tests was taken.

La borsa di dottorato è stata cofinanziata con risorse del
Programma Operativo Nazionale Ricerca e Innovazione 2014-2020 (CCI 2014IT16M2OP005),
Fondo Sociale Europeo, Azione I.1 “Dottorati Innovativi con caratterizzazione Industriale”

UNIONE EUROPEA
Fondo Sociale Europeo